

Air Force Institute of Technology

AFIT Scholar

Theses and Dissertations

Student Graduate Works

1-14-2002

The Horizontal Extent of Cloud-to-Ground Lightning over the Kennedy Space Center

Todd M. McNamara

Follow this and additional works at: <https://scholar.afit.edu/etd>



Part of the [Meteorology Commons](#)

Recommended Citation

McNamara, Todd M., "The Horizontal Extent of Cloud-to-Ground Lightning over the Kennedy Space Center" (2002). *Theses and Dissertations*. 4497.

<https://scholar.afit.edu/etd/4497>

This Thesis is brought to you for free and open access by the Student Graduate Works at AFIT Scholar. It has been accepted for inclusion in Theses and Dissertations by an authorized administrator of AFIT Scholar. For more information, please contact AFIT.ENWL.Repository@us.af.mil.



**THE HORIZONTAL EXTENT OF CLOUD-
TO-GROUND LIGHTNING OVER THE
KENNEDY SPACE CENTER**

THESIS

Todd M. McNamara, Captain, USAF

AFIT/GM/ENP/02M-06

**DEPARTMENT OF THE AIR FORCE
AIR UNIVERSITY**

AIR FORCE INSTITUTE OF TECHNOLOGY

Wright-Patterson Air Force Base, Ohio

i

APPROVED FOR PUBLIC RELEASE; DISTRIBUTION UNLIMITED.

Report Documentation Page

Report Date 14 Jan 02	Report Type Final	Dates Covered (from... to) Jun 01 - Mar 02
Title and Subtitle The Horizontal Extent of Cloud-to-Ground Lightning over the Kennedy Space Center	Contract Number	
	Grant Number	
	Program Element Number	
Author(s) Captain Todd M. McNamara, USAF	Project Number	
	Task Number	
	Work Unit Number	
Performing Organization Name(s) and Address(es) Air Force Institute of Technology Graduate School of Engineering and Management (AFIT/EN) 2950 P Street, Bldg 640 WPAFB OH 45433-7765	Performing Organization Report Number AFIT/GM/ENP/02M-06	
Sponsoring/Monitoring Agency Name(s) and Address(es) ASC/YCA Attn: Lt Col Robert S. Baerst 2590 Loop Road West WPAFB, OH 45433	Sponsor/Monitor's Acronym(s)	
	Sponsor/Monitor's Report Number(s)	
Distribution/Availability Statement Approved for public release, distribution unlimited		
Supplementary Notes The original document contains color images.		
Abstract Military base weather stations are required to issue lightning warnings to protect military equipment and personnel. The issuance of warnings is based on a 5 nautical mile (n mi) distance criterion. This criterion appears to have evolved over time as a balance between safety and mission impact. The goal of this thesis is to challenge the 5 n mi lightning warning criteria by quantifying the distance that CG lightning travels. A secondary goal is to examine the characteristics of the peak current of CG lightning strokes to determine if a relationship exists between peak current, the distance a stroke travels, and the altitude of the origin point of the lightning stroke. This study found 28.6% of lightning flashes traveled further than 5 n mi from the point of origin. The study used approximately 4 years of data and found that the spring and winter seasons had the highest seasonal frequencies of occurrence of distances greater than 5 n mi. Peak current analysis indicated that higher peak currents are associated with shorter distances that lightning strokes traveled and higher peak currents were found to be associated with strokes that originated at lower altitudes		

Subject Terms

Lightning, Cloud-to-Ground, Lightning Detection and Ranging, LDAR, National Lightning Detection Network, NLDN, Peak Current, Origin Point

Report Classification

unclassified

Classification of this page

unclassified

Classification of Abstract

unclassified

Limitation of Abstract

UU

Number of Pages

114

The views expressed in this thesis are those of the author and do not reflect the official policy or position of the United States Air Force, Department of Defense, or the U. S. Government.

AFIT/GM/ENP/02M-06

THE HORIZONTAL EXTENT OF CLOUD-TO-GROUND LIGHTNING
OVER THE KENNEDY SPACE CENTER

THESIS

Presented to the Faculty

Department of Engineering Physics

Graduate School of Engineering and Management

Air Force Institute of Technology

Air University

Air Education and Training Command

In Partial Fulfillment of the Requirements for the
Degree of Masters of Science in Meteorology

Todd M. McNamara, BS

Captain, USAF

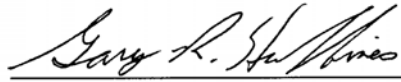
March 2002

APPROVED FOR PUBLIC RELEASE; DISTRIBUTION UNLIMITED

THE HORIZONTAL EXTENT OF CLOUD-TO-GROUND LIGHTNING
OVER THE KENNEDY SPACE CENTER

Todd M. McNamara, BS
Captain, USAF

Approved:



Gary R. Huffines (Chairperson)

15 Mar 2002

date



Ronald P. Lowther (Member)

15 MAR 02

date



Michael K. Walters (Member)

15 MAR 02

date



Daniel E. Reynolds (Member)

15 Mar 02

date

Acknowledgements

The preparation of this thesis was a significant emotional event in my life. Without the support of friends, family, and the AFIT faculty, my research and this thesis would never have been completed.

I would like to start by thanking my professors and committee members for their guidance and knowledge. Their interests in my education truly made my AFIT assignment a positive experience. I would especially like to thank my advisor, Major Gary Huffines, for getting me involved in lightning research. I found atmospheric electricity to be an exciting and extremely fascinating field of study. I would also like to thank him for his guidance and patience. I'm sure my lack of programming skills and continual badgering challenged his teaching skills and truly tested his patience. Additionally, I would like to thank Mr. Jeff Sitler for keeping the computers in the weather lab up and running. Without his assistance, I would still be sitting at the computers in the weather lab wondering why I couldn't access my data on the hard drive.

I'm also grateful to my classmates for their help and sense of humor. Their ability to laugh and keep the mood light during the most stressful times was a huge help. Finally, I would like to thank my family for their continual support through the last 18 months as well as the past 19 years of my military career. Their love and unwavering faith in my abilities made me believe that I could accomplish anything I set my mind to.

Todd M. McNamara

Table of Contents

	Page
Acknowledgements	v
Table of Contents	vi
List of Figures	ix
List of Tables.....	x
Abstract	xi
1. Introduction	1
1.1 Background	1
1.2 Problem Statement	3
1.3 Thesis Organization.....	5
2. Literature Review	6
2.1 The Lightning Flash	6
2.1.1 The Electrification Process.....	6
2.1.2 Categorization of Cloud-To-Ground Lightning	8
2.1.3 The Negative Cloud-To-Ground Lightning Process.	10
2.2 Lightning Detection and Ranging (LDAR) System.....	12
2.3 National Lightning and Detection Network	15
2.4 Previous Research in Determining Horizontal CG Distances.....	17
2.4.1 WSR-88D Storm Centroid Method.....	18
2.4.2 Distance Between Successive Flash Method	19
2.4.3 Distances Computed Using LDAR Data.....	21
2.4.4 Summation of Past Research.....	21
3. Methodology	23

3.1 Objectives.....	23
3.2 Scope	24
3.3 Grouping LDAR Data Points into Flashes	25
3.4 Matching NLDN Ground Strokes to LDAR Lightning Flashes.....	29
3.5 Example of Matching NLDN Ground Strokes with LDAR Lightning Flashes	32
3.6 Data Analysis Methodology.....	34
4. Results and Analysis	37
4.1 Association of Ground Strokes with LDAR Flashes.....	37
4.2 Characteristics of the Distance Lightning Travels	40
4.3 Association Between Distance and Peak Current	44
4.4 Relationship Between Altitude of Stroke Origin Point and Peak Current	49
5. Conclusions	56
5.1 Conclusions	56
5.2 Future research recommendations.....	58
Appendix A. Example NLDN and LDAR Data Files and Program Output Files.....	60
Appendix B. IDL Program	65
Appendix C. Seasonal Frequency Distributions.....	78
Appendix D. Seasonal Scatter Plots and Distance Versus Peak Currents Diagrams	80
Appendix E. Seasonal Scatter Plots and Peak Current Versus Altitude of CG Lightning Stroke Origin Point Diagrams.....	88
Appendix F. List of Acronyms.....	96

Bibliography..... 97

Vita..... 101

List of Figures

Figure	Page
1. Tripole with Screening Layer Charge Structure in a Thunderstorm	8
2. Categories of CG Lightning	9
3. Map of Cape Canaveral Area Showing LDAR Sensor Sites	13
4. NLDN Sensor Locations	17
5. Methodology for Grouping LDAR Data Points into a Flash	27
6. Schematic of the Matching of NLDN Ground Stroke with an LDAR Flash	33
7. Lightning Flash from 2 January 1999	39
8. Lightning Stroke Frequency Distribution for March 1997 through December 2000.....	43
9. Scatter Plot of Distance and Peak Current for March 1999 through December 2000	45
10. Positive Peak Current as a Function of Distance for March 1999 through December 2000.....	46
11. Negative Peak Current as a Function of Distance for March 1999 through December 2000.....	47
12. Scatter Plot of Peak Current and Altitude of the Stroke Origin Point for March 1999 through December 2000.....	50
13. Positive Peak Current as a Function of Altitude for March 1999 through December 2000.....	52
14. Negative Peak Current as a Function of Altitude for March 1999 through December 2000.....	53

List of Tables

Table	Page
1. Past Research on Determining the Distance CG Lightning Travels	22
2. Example of Running Average Computation	35
3. NLDN Ground Stroke and LDAR Flash.....	38
4. Distance Statistics Summary by Season and for the Entire Data Period.....	42
5. Change in Peak Current Versus the Distance a Lightning Stroke Traveled.....	48
6. Change in Peak Current Versus Increasing Altitude of Lightning Stroke's Origin Location.....	54

Abstract

Cloud-to-ground (CG) lightning hampers air operations whether it is at a civilian airport or military installation. Military base weather stations are required to issue lightning warnings to protect military equipment and personnel. The issuance of warnings is based on a 5 nautical mile (n mi) distance criterion. This criterion appears to have evolved over time as a balance between safety and mission impact. The goal of this thesis is to challenge the 5 n mi lightning warning criteria by quantifying the distance that CG lightning travels. A secondary goal is to examine the characteristics of the peak current of CG lightning strokes to determine if a relationship exists between peak current, the distance a stroke travels, and the altitude of the origin point of the lightning stroke.

The method used in this research utilized data from the Lightning Detection and Ranging (LDAR) system and the National Lightning Detection Network (NLDN). LDAR data, representing individual electromagnetic pulses emitted by lightning, are grouped into flashes. Lightning strokes detected by the NLDN are then matched to the flash that produced the stroke using temporal and spatial criteria. Using the origin and ground strike location for each stroke, an algorithm computed the distance each lightning stroke traveled. In addition, research analyzed the association between the stroke's peak current and origin height.

Using 1,585,275 lightning strokes, this study found 28.6% of lightning flashes traveled further than 5 n mi from the point of origin. The study used approximately 4 years of data and found that the spring and winter seasons had the highest seasonal frequencies of occurrence of distances greater than 5 n mi. Peak current analysis indicated

that higher peak currents are associated with shorter distances that lightning strokes traveled and higher peak currents were found to be associated with strokes that originated at lower altitudes. It is highly encouraged that this information be used to make science-based decisions on the issuance criterion for military lightning warnings.

HORIZONTAL EXTENT OF CLOUD-TO-GROUND LIGHTNING OVER THE KENNEDY SPACE CENTER

1. Introduction

1.1 Background

Cloud-to-ground (CG) lightning poses a serious threat to outdoor activities. The National Oceanic and Atmospheric Administration (NOAA) publication, *Storm Data*, reports that lightning strikes cause over \$32 million dollars of damage, 340 injuries, and 51 deaths per year (Holle et al. 1999). However, other publications indicate that these reports underestimate the true impact of lightning strikes. According to Kithil (1999), a more reasonable estimate is \$4-5 billion in costs and over 100 deaths per year in the United States. As for the Air Force, damage to equipment or injury to personnel not only increases cost but also directly affects mission capability and potentially jeopardizes national security. Over the past six years, the possible loss of Air Force assets has moved to the forefront of concerns due to the potential damage lightning can cause to airframes and a lightning strike incident that occurred at a military installation in Florida.

The potential damage to an Air Force aircraft due to a lightning strike is of considerable concern. If an aircraft is sitting in a parking spot or taxiing to a runway and is struck by CG lightning, the most extreme outcome is a “catastrophic” or total loss of the airframe. With the rising cost of airplanes such as the B-2 Spirit with an original price tag of \$1.3 billion per airframe, the financial loss of such an event would be devastating to both the Air Force and taxpayers (USAF Fact Sheet 1999). On the other end of the

damage spectrum, an aircraft struck by lightning may only experience minor structural damage such as pitting in the skin of the aircraft. In this case, the damage may be minor in comparison to the total loss of an airframe; however, the damage still results in an increase in repair costs for the Air Force and an increase in operations tempo for logistics and maintenance organizations. Today, even minor damage such as pitting in the skin of an aircraft can be an expensive repair, especially when the aircraft is built with unique composite materials such as those airframes with stealth technology. In between these two extremes, a lightning strike can damage highly sophisticated and technologically advanced navigational, communications, and weapons systems, resulting in expensive repair costs and rendering the aircraft unusable. All of these potential damages, from the most minor to the most extreme, lead to one fact - wing commanders have one less airframe in their inventory and their capability to complete their mission is impaired. As a result of these concerns, the C-17 Globemaster III System Program Offices (SPO) requested an in-depth examination on the distance that CG lightning travels.

In addition to protecting their equipment from lightning strikes, the Air Force is also concerned with protecting personnel. During inclement weather conditions, personnel working outdoors are at risk from lightning strikes. A lightning occurrence on 29 April 1996 emphasized this risk and brought Air Force safety procedures under question. At 0930 CDT, the Base Weather Station at Hurlburt Field, Florida cancelled a "lightning within three nautical mile" weather advisory since no lightning had been observed for one hour and twenty minutes (Bauman 1998). Minutes later, four crew chiefs and a seven-person training class were dispatched to an aircraft to perform training on an AC-130H aircraft. At 0938 CDT, lightning struck the aircraft resulting in one death, 10 injured

personnel, and damage to the aircraft. Air traffic controllers reported that the lightning strike came from a thunderstorm located 5 – 7 nautical miles (n mi) away from the airfield.

Both the potential damage to aircraft and the lightning strike incident in Florida raise question to whether current severe weather procedures are adequate. Current procedures for alerting base personnel and ensuring the safety of military assets during dangerous lightning conditions are outlined in Air Force Occupational Safety and Health Standards (AFOSH) 91-100 (Department of the Air Force 1998). This publication mandates that Base Weather Stations (BWS) issue a “lightning watch” 30 minutes prior to a thunderstorm being within 5 n mi of a predetermined location such as the middle of the airfield. When a thunderstorm is within 5 n mi, a “lightning warning” must be issued and remain in effect until the thunderstorm moves outside the 5 n mi radius of the predetermined location. During the period when a lightning warning is in effect, all outdoor activities such as aircraft refueling, flight line maintenance, and civil engineering operations cease in an effort to ensure the protection of Air Force assets and personnel. The question then becomes, “Does the 5 n mi criteria ensure the safety of military equipment and lives?” In light of the rising replacement or repair costs in advanced aircraft and the fatal lightning strike event that occurred in Florida, this parameter may fall short in properly protecting military assets.

1.2 Problem Statement

The 5 n mi criterion for issuance of a lightning warning evolved over time with no conclusive research supporting this criterion. The primary purpose of this research is to substantiate whether this criteria for the issuance of lightning watches and warnings is an

appropriate threshold to ensure the safety of Air Force equipment such as aircraft on the ground and Air Force personnel working outdoors.

In the past, three Air Force Institute of Technology (AFIT) students researched this problem; however, their findings were not entirely conclusive and their methodology in conducting their research was different than that used in this study. The process used in this research includes the use of two lightning detection systems. The first is the Lightning Detection and Ranging (LDAR) system, which provides three-dimensional positions of electromagnetic pulses emitted by a lightning flash. The data from this system was used to identify lightning flashes and pinpoint the origin point of each flash. The second system utilized is the National Lightning Detection Network (NLDN). The NLDN provides the location where lightning strokes hit the ground. Using each stroke's point of origin and the location where they hit the ground, the horizontal distance that CG lightning travels is computed. The approach used in this research will provide a more accurate measure of the distance lightning travels in comparison to past research methods.

This research also attempts to correlate several CG lightning features associated with a lightning flash. Specifically, a comparison between the distances CG lightning strokes travel and their peak currents are studied to determine if strokes with a higher peak currents tend to travel further distances from their origin. If peak current is proportional to the distance a lightning stroke travels, longer strokes will produce higher peak currents. Finally, a correlation is made between a lightning stroke's origin height and the peak current of the stroke. To find this correlation, an assumption is made that the amplitude of the peak current is proportional to the strength of the charge region where the flash

originates. With this assumption, results should produce higher peak current values at altitudes where maximum charge regions were measured in past research.

1.3 Thesis Organization

A review of the relevant background information is presented in Chapter 2. A comprehensive explanation of the methodology used in this research is contained in Chapter 3. Chapter 4 discusses the analysis and results, while Chapter 5 provides conclusions of this research.

2. Literature Review

In order to properly conduct research or thoroughly understand the complexities of determining the distance of CG lightning, a basic understanding of the lightning process is required. Along with this, a basic review of the Lightning Detection and Ranging system, National Lightning Detection Network, and past research completed in this area is necessary. The following will provide this information.

2.1 The Lightning Flash

2.1.1 The Electrification Process. Lightning is a transient, high-current electric discharge (Uman 2000). It occurs in thunderstorms when the local electric field is strong enough to accelerate electrons to a velocity sufficient enough to knock other electrons from neutral atoms or molecules when they collide (MacGorman and Rust 1998). This process, known as electron avalanche, significantly increases the number of charged carriers in the atmosphere to the point where air is forced to become a good conductor (preliminary breakdown). There are several mechanisms theorized for producing an electrical field strong enough to cause lightning. These processes can be grouped into two general categories (Uman 2000). The first and most widely accepted group of theories for thunderstorm electrification is the precipitation processes in which heavy precipitation particles collide with lighter particles. As a result, heavy particles become negatively charged while lighter particles become positively charged. The second group of theories includes convection theories, which are based on air motions of thunderstorms moving preexisting pockets of charge to observed locations. It should be understood that there are

many factors in the cloud electrification process and they are poorly understood. Research continues in this area.

As stated, the lightning flash is a result of strong localized electric fields of opposite charge. The charge distribution, which produces these electric fields in a thunderstorm, is very complex. However, basic charge characteristics are evident (MacGorman and Rust 1998). A negatively charged area is usually in the lower region roughly around the -25°C temperature level. A positively charged area exists on top of this negative layer towards the top of the storm. This positively charged region induces a negative charge along the top boundaries of the cloud known as the screening layer. At times, thunderstorms also possess a small positively charged area at the bottom of the cloud. These broad characteristics lead to a general conceptual model known as a dipole/tripole structure with screening layer. Figure 1 depicts a general tripole with screening layer charge structure. This structure is based on measurements and theory (Krehbiel 1986). Actual electric field profiles measured by Stolzenburg et al. (1998) depict the charge structure to be more complex than the simple dipole/tripole model. Vertical motions in the thunderstorm move charge regions resulting in as many as six charge regions vertically stacked in thunderstorm downdrafts. Updrafts and downdrafts also cause oppositely charged regions to exist side-by-side. More recent information from the 2000 Severe Thunderstorm Electrification and Precipitation Project (STEPS 2000), which was conducted in the Kansas and Colorado area, indicated that charge regions frequently appear in an inverted tripole structure (Krehbiel 2001). In this configuration, there are three main charge regions as shown in Figure 1. However, there is a main positive charge region in the middle with

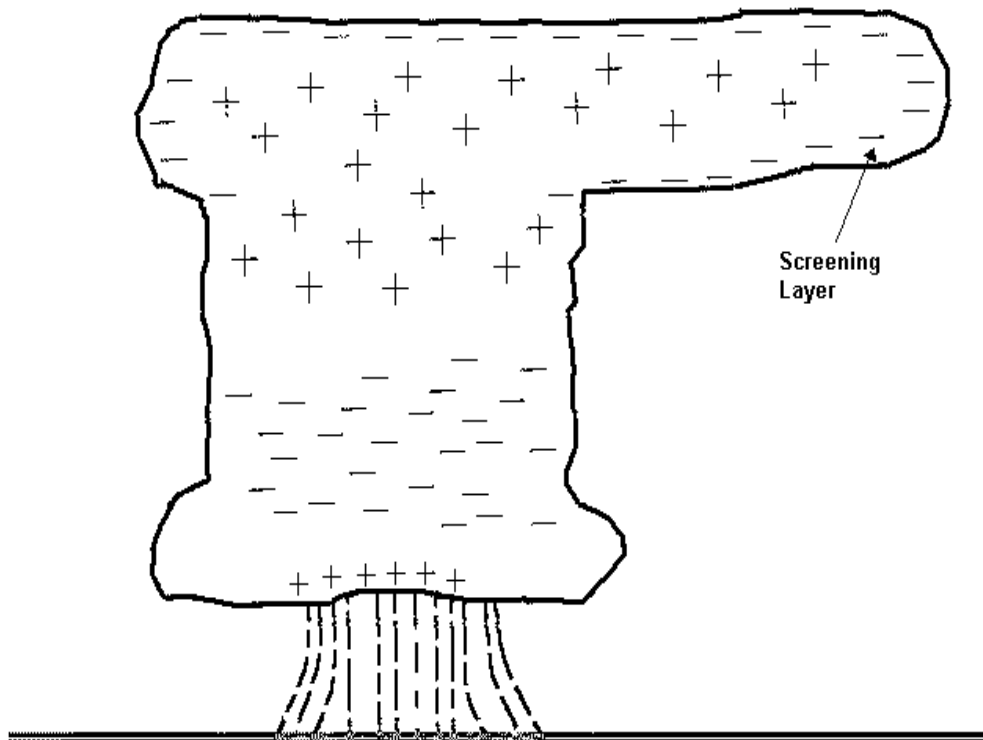


Figure 1. Tripole with Screening Layer Charge Structure in a Thunderstorm.
(Adapted from Krehbiel 1986)

a weak, lower negative charge region below and a stronger, upper negative charge region above. Although it is impossible to comprehensively measure the charge structures within an entire thunderstorm, it is apparent that the charge structure in a thunderstorm is a very complex and dynamic.

2.1.2 Categorization of Cloud-To-Ground Lightning. A lightning flash is an entire lightning event and may last up to one second (Uman 2000). Flashes that do not strike the ground are considered cloud discharges or cloud flashes while cloud-to-ground flashes are those that strike the ground. Cloud-to-ground flashes are further categorized by the direction of the leader initiating the strike and its polarity (Uman 2000). The four

categories of CG lightning are depicted in Figure 2. In Figure 2a, strikes develop as downward propagating, negatively charged leaders and move from the cloud to the ground. The overall effect is for the strike to lower negative charge from a cloud to the ground. This category of lightning is the most frequent type and accounts for ninety percent of flashes (Uman 2000). Figure 2c displays a lightning strike that is also initiated in the cloud and moves to the ground, however, the leader is positively charged. The result is an overall lowering of positive charge to the ground. The remaining two categories of flashes

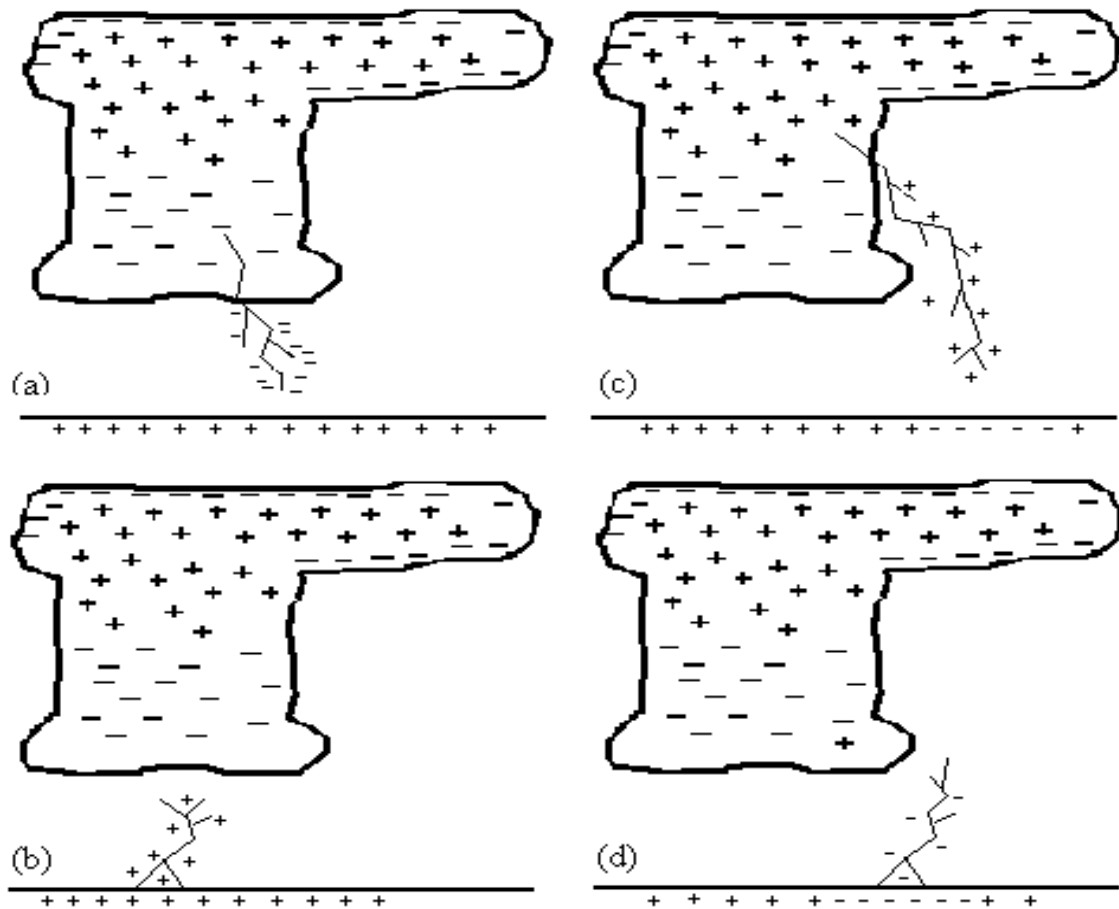


Figure 2. Categories of CG Lightning. a) Negative CG flash with downward moving leader. b) Positive CG flash with upward moving leader. c) Positive CG flash with downward moving leader. d) Negative CG flash with upward moving leader. (Adapted from Uman 2000)

are depicted in Figures 2b and 2d. They both initiate from the ground and the leaders move up to the cloud. The leader in category 2b is a positive leader and the lightning process leads to the lowering of negative charge while the leader in 2d is a negative leader and positive charge is lowered to the ground. These strikes are rare and considered artificially initiated since the upward initiated leader normally originates from a tall man-made structure (Berger 1977).

2.1.3 The Negative Cloud-To-Ground Lightning Process. The initiation of the actual lightning flash is due to electrical charge separation. As the electric field between oppositely charge regions strengthen beyond the breakdown potential, the preliminary breakdown process occurs. This process is verified by electric field changes and photographic evidence. Data indicate that preliminary breakdown typically lasts 90 msec, with a median value of 42 msec (Beasley et al. 1982). Using three different methods, the location of preliminary breakdown was determined in thunderstorms located in South Africa and New Mexico to be from 3.0 km to 8.0 km above sea level (Proctor 1983 and Krehbiel et al. 1979). A train of relatively large bipolar pulses is indicative of the end of this process or the beginning of the stepped leader. Detection systems operating from VLF to VHF frequencies can detect this process.

The stepped leader is a series of short, detached streaks of light that move in steps in a downward direction and branch out towards the ground (MacGorman and Rust 1998). The stepped leader moves towards the ground with an average speed of 2×10^5 m sec⁻¹ (Uman 2000). A typical stepped leader lasts approximately 1 µsec, has a length of tens of meters, and a pause time between steps of about 50 µsec.

As the negatively charged stepped leader approaches the ground, one or more upward moving discharges are induced from sharp objects or irregularities of the ground itself (Uman 2000). This is the beginning of the attachment process. At this point in the CG lightning process, the object to be struck by the lightning flash is determined. The attachment process concludes when one of the upward moving discharges joins with the stepped leader. This connection typically occurs at heights of tens of meters (Orville and Idone 1982). Streak photography reveals a sharp kink at the connection point and, at times, upward branching off the upward moving leader channel.

Once the connection is complete, the return stroke moves up the ionized stepped leader channel and drains negative charge to the ground. The return stroke moves rapidly to the top of the channel at speeds typically from 1×10^8 m sec⁻¹ to 2×10^8 m sec⁻¹ (Orville and Idone 1982). A return stroke typically occurs in a time span of 100 μsec. The return stroke produces a peak current of 30 kA on average and heats the leader channel to temperatures near 30,000 K, which leads to the generation of thunder (Uman 2000). For a single-stroke flash, the process ends.

There are two other situations that may occur after the first return stroke ends. The first is that the channel remains ionized sufficiently to allow a dart leader to move back down the channel and initiate another return stroke (MacGorman and Rust 1998). Negative CG lightning strikes average three to four strokes per flash and multiple strokes are often detectable by the human eye (Uman 2000).

The second condition that can occur just after a return stroke is that current continues to flow from the cloud to the ground. This process is called continuing current and, as the name implies, current flows for a much longer time than that for a normal return stroke.

The continuing current process can last for hundreds of milliseconds (Brook et al. 1962). Between one-quarter and one-half of all CG flashes contain continuing currents and they carry from ten to a few hundred amperes of current, which is comparable to an electric arc welder (Krehbiel et al. 1979). Due to the longer duration of electrical charge transfer in the continuing current process, rapid heating takes place in a very short time period. As a result, continuing current is directly responsible for starting forest and grassland fires (MacGorman and Rust 1998).

2.2 Lightning Detection and Ranging (LDAR) System.

The LDAR system is a long-baseline, Time-of Arrival (TOA) lightning detection system developed by the National Aeronautics and Space Administration (NASA) and located at the Kennedy Space Center, Florida (Britt et al. 1998). The network has six stations arranged in a hexagonal fashion, each being 6 - 10 km away from an additional central controlling station located in the middle (Figure 3). With this architecture, the network can produce three-dimensional lightning data for research and operational use.

The LDAR system is a passive system that senses both cloud discharges and CG lightning discharges (Maier et al. 1995). In a CG lightning flash, the flash emits electromagnetic energy in the VHF range. The LDAR system operating at 66 MHz (VHF) and a bandwidth of 6 MHz senses electromagnetic pulses produced by a lightning flash. LDAR uses the speed of light, the difference in signal arrival times, and the known positions of the stations to compute three-dimensional locations in Cartesian coordinates and the time of electromagnetic pulses within distances of tens of kilometers (Britt et al.

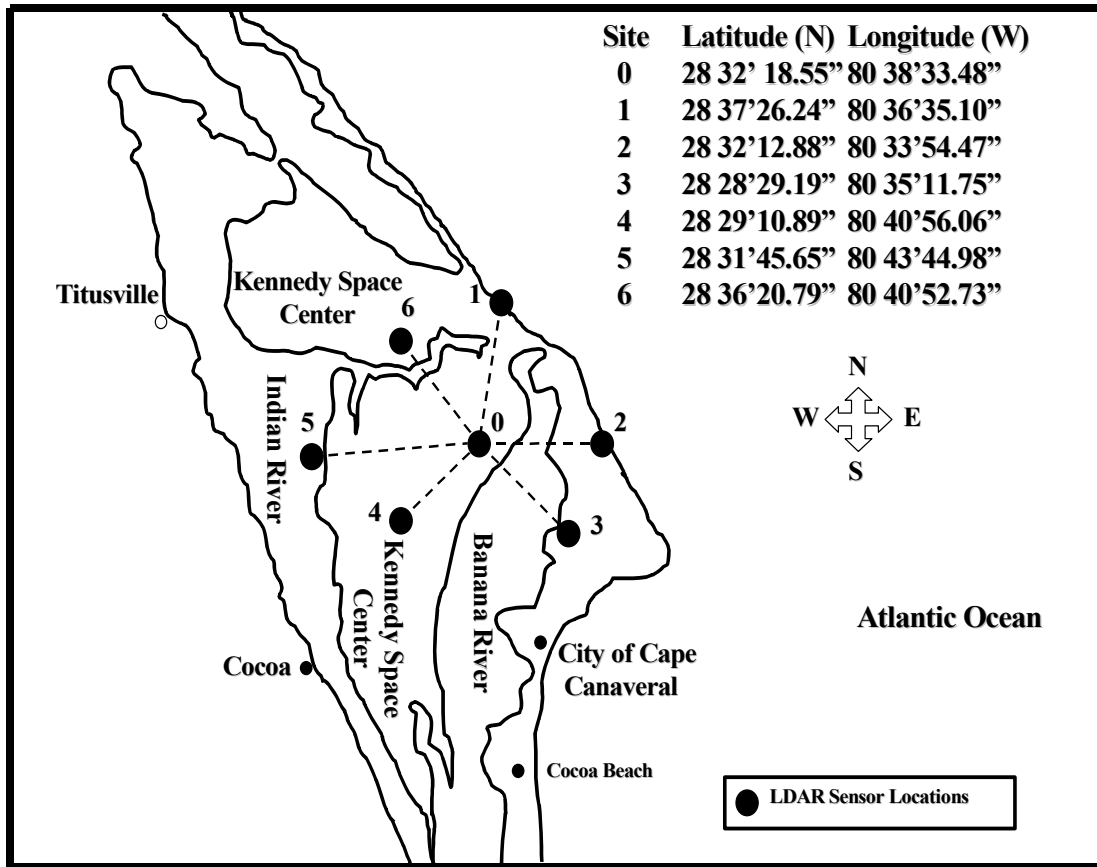


Figure 3. Map of Cape Canaveral Area Showing LDAR Central Processing Site (0) and Sensor Sites (1 - 6) (Adapted from Poehler and Lennon 1979)

1998). When the central site detects a pulse, the system opens a 100 μ sec window in which the peak amplitude and time of the peak amplitude is recorded (Maier et al. 1995). Since LDAR is a TOA sensor, time accuracy is crucial. LDAR uses the Global Positioning Satellite (GPS) system to provide timing accuracy with timing resolution to 10 nsec. Once the remote sites collect the information, the data are sent to the central processing site for location calculations. LDAR processes a maximum of 1000 pulses per second near the center of the LDAR system (Britt et al. 1998).

To provide information on a flash, LDAR requires that at least four of the seven remote stations receive the signal (Maier et al. 1995). For each lightning flash, there are two optimal combinations of four sensors that provide the minimum location error. If each distance from both optimal site combinations agrees within 5 percent or 350 m, whichever is greater, then the average of the two locations is accepted. If they are not within an acceptable distance, data from all possible combinations of all the sensors are averaged through a weighted process.

Maier et al. (1995) conducted location accuracy testing of the LDAR system using an aircraft that transmitted VHF signals. With 300,000 transmitted events per flight and a total of three flights, the median location error was 100 m within 10 km and 1 km or less within 40 km. These figures were computed with aircraft altitudes between 5 and 8 km. For altitudes from the surface to 2.5 km, the median error was less than 250 m within 10 km and less than 1 km within 40 km. Maier et al. (1995) also found the detection efficiency of LDAR to be 99% within 25 km of the central site. Murphy et al. (2000) also reported horizontal location errors for LDAR similar to those of Maier's results.

The Global Hydrology and Climate Center (GHCC) archives LDAR data and produces visualizations for operational use. Products are located on the Internet at http://thunder.msfc.nasa.gov/lightning-cgi-bin/ldar/ldar_browse.pl. Archived data is available through GHCC web site at <http://ghrc.msfc.nasa.gov/uso/readme/ldar.html>. Archive files are compressed and contain both time and three-dimensional location information.

The LDAR system offers several advantages (Britt et al. 1998). For operational forecasters, it is capable of detecting both CG and cloud flashes whereas most lightning

detection systems only provide CG strike information. This LDAR capability provides forecasters with an indication of lightning 10 to 20 minutes earlier than other systems resulting in longer warning lead times. For research, LDAR provides numerous data points for one lightning flash in a three-dimensional view in comparison to other systems that provide one point per flash. LDAR information provides greater insight into lightning flash origin and propagation characteristics.

2.3 National Lightning and Detection Network

The NLDN is a network of lightning sensors positioned around the continental United States that provide real-time lightning data over a total land area of approximately four million square miles. The system provides time, location, polarity, and peak current information for each individual return stroke (Cummins et al. 1998). The NLDN location algorithm uses a least-squares optimization procedure to determine strike locations. The algorithm also groups strokes into flashes using spatial and temporal criteria. Strokes are added to a flash as long as they are within one second and 10 km of the initial stroke and each stroke must be within 500 microseconds of the previous stroke. If a stroke meets the criteria for two separate flashes, it is assigned to the nearest flash. The location algorithm limits the flash multiplicity to 15 strokes.

The motivation for a nation-wide network stemmed from electrical companies realizing the operational benefits of knowing where CG lightning strikes occur (Cummins et al. 1998). In 1987, three regional networks merged providing the capability for lightning coverage on a national scale. In 1989, the network became fully operational.

Currently, the NLDN is owned and operated by Global Atmospheric, Inc. (GAI) in Tucson, Arizona (Idone et al. 1998a).

The NLDN originally consisted of Time of Arrival (TOA) and Magnetic Detection Finder (MDF) sensors (Cummins et al. 1998). The network was upgraded in 1995 with GPS timing and a new location method that combined both the TOA and MDF methods in a single sensor. The new sensors are known as the IMPROVED Accuracy from Combined Technology (IMPACT) sensors. Upgrades to the NLDN also included an increase in the standard gain of the IMPACT sensors, a reduction in the sensor trigger threshold, and a waveform acceptance criterion, which allowed the detection of lightning beyond 500 km. Currently, the NLDN consists of 47 IMPACT sensors and 59 of the original TOA sensors. An adaptation of Huffines' (1999) illustration of NLDN sensor locations is depicted in Figure 4.

The upgrade to the network proved to be very beneficial. Idone et al. (1998a) performed a study on the network to determine the new location accuracy and detection efficiency of the network. The test was conducted in eastern New York and was based on comparisons between video observations and NLDN data. They found the network's location accuracy to be 0.5 km for first strokes with peak currents greater than 5 kA (Idone et al. 1998b). The study also concluded that the overall flash detection efficiency is 72 percent while the stroke detection efficiency is 47%. If strokes with less than 5 kA are discarded from the dataset, a flash detection efficiency of 84 percent and stroke detection efficiency of 69% is achieved (Idone et al. 1998a). Cummins et al. (1998) also reports that GPS timing in the NLDN sensors result in a timing accuracy of approximately five

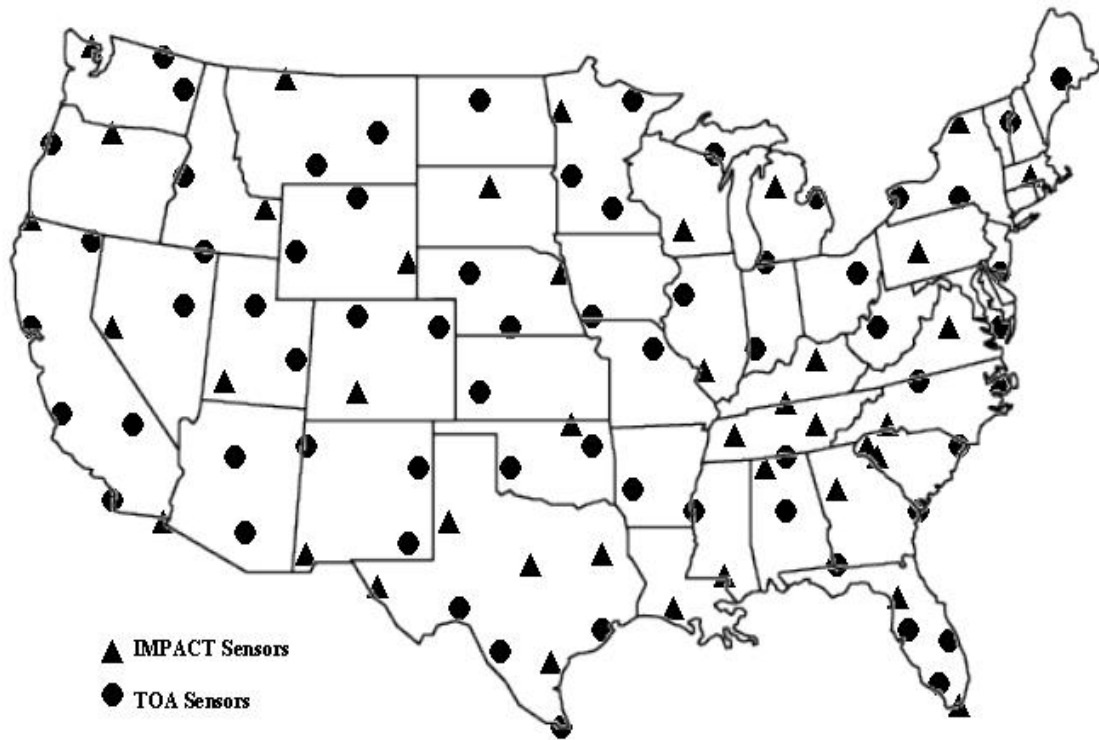


Figure 4. NLDN Sensor Locations (Adapted from Huffines 1999)

microseconds for each individual stroke. The timing accuracy allows for adequate resolution between strokes.

2.4 Previous Research in Determining Horizontal CG Distances

Past research methods used for determining the distance CG lightning travels are the Weather Surveillance Radar – 88 Delta (WSR-88D) storm centroid, Distance Between Successive Flash (DBSF), and Lightning Detection and Ranging (LDAR) system based methods. This section will briefly discuss these methods and summarize results from past research.

2.4.1 WSR-88D Storm Centroid Method. The WSR-88D storm centroid method utilizes the National Severe Storms Laboratory (NSSL) Storm Cell Identification and Tracking (SCIT) algorithm and the WSR-88D storm series algorithm (Parsons 2000). From these algorithms, the centroid of the storm is located. This data is then overlaid with lightning data and the horizontal distance between the storm centroid and the strike on the ground is computed. A drawback to this method is that there is no way to positively identify and associate which thunderstorm or echo return produced a ground strike.

Renner (1998) used this method and found that it was extremely time-consuming and requires a large amount of disk space. In his research, Renner focused on a region in the Gulf coast and one in the Southern Plains. Data used in the research were from four reporting stations within the region and it was limited to four months from April through July of 1996. His research concluded that both regions had a high majority of lightning strikes that traveled from the storm centroid to the ground strike location with distances of 2 and 6 n mi. Cumulative distributions showed 75% of all lightning flashes were within 10 n mi for April, and 85% to 90% were within 10 n mi for July using this method (Renner 1998).

Cox (1999) also used this method to determine strike distances in an effort to verify the 5 n mi criteria for issuing lightning warnings to Air Force installations. In contrast to Renner who used Build 9.0 of WSR-88D Algorithm Testing and Display System (WATADS), Cox used Build 10.0 of WATADS to run the algorithms from the radar data. He concluded that 39% of April flashes and 32% of July flashes occurred at distances greater than 5 n mi (Cox 1999).

2.4.2 Distance Between Successive Flash (DBSF) Method. Another method used for determining lightning strike distances is the DBSF method. This technique groups lightning flashes into clusters based on temporal and spatial criteria. Researchers have used several time and spatial variations to group flashes into clusters. After grouping the lightning clusters, CG lightning flash distances are computed between the individual flashes in the cluster and the lightning cluster center. To a certain degree, the distribution of these distances can be used to forecast when and where the next strike will occur. It is important to note that this method does not measure the path from the lightning origin point to the ground strike location, but assumes the lightning cluster center is the origin point of all lightning flashes within the cluster.

Lopez and Holle (1999) used an algorithm that grouped flashes that were within 5 minutes and 15 km radius of each other. The algorithm used time-ordered data files. Using the first flash that occurred in time, the program checks the next flash that occurs and groups it with the first flash as long as the time and distance criteria are met. The algorithm then continues to the next flash in the data file and tests the time and distance criteria. If the flash is within 5 minutes and 15 km of the previous flash, the flash is grouped into the cluster. Each successive flash in the data file is checked until the criterion is not met. When a flash does not meet the criteria with respect to the successive flash, it is designated as an outlier. Each outlier begins another cluster unless time and distance criteria are not met again. This method continues until each flash is assigned a cluster or it is considered an isolated flash. From each cluster, a center point is determined by taking the arithmetic mean of the latitude and longitude of all flashes in the cluster. The distance of each flash from the cluster's center is then computed. Lopez and Holle (1999)

concluded that for data obtained in Florida and Colorado, fifty percent of all successive flashes were less than 4 to 5 km from the previous flash, twenty five percent were separated by 5 to 8 km, and five percent were separated by 13 km or more.

Krider (1988) conducted a study in Florida on three thunderstorms in the Kennedy Space Center area using the DBSF method. His clustering algorithm used temporal criterion of 5 minutes. He found the average distance between successive flashes to be between 3 (1.9 n mi) and 4 km (2.5 n mi) with the most probable distances between 1 and 4 km.

Along with the WSR-88D storm centroid method, Cox (1999) also used the DBSF method. In his calculations, he used a 15 km distance and a 6-minute time criteria. However, Cox's clustering technique begins the 6-minute time criteria from the first flash of each cluster and not at each flash within the cluster. Thus, his clusters include only those flashes that occur in a 6-minute window from the first flash. He also applied a further limitation in that the lightning data had to correlate with storm centroids. Consistent with his WSR-88D storm centroid method, Cox (1999) found that 30% of lightning flashes occur beyond 5 n mi.

Finally, Parsons (2000) also applied the DBSF method. In an attempt to reduce the number of isolated flashes, she used criteria of 17 kilometers and 15 minutes. Like Cox, Parsons' method applied the time constraint from the initial flash in a cluster. Parsons used over 90 million flashes from 1995 to 1999 covering nearly the entire United States. She broke the area into six regions. In general, Parsons found that some of the regions had as low as 65% of the strike distances within 9 km or approximately 5 n mi. This leaves as many as 35% of lightning strikes that traveled beyond 9 km. In her study, Parsons did not

discard the isolated flashes. Using the isolated flash information, she concluded that these flashes had a much higher tendency to be outside the 9.26 km (5 n mi) distance. In one region, 76% to 80% of the isolated flashes struck outside the 5 n mi distance indicating that a high number of isolated flashes travel long distances and these isolated flashes can be considered more dangerous.

2.4.3 Distances Computed Using LDAR Data. Very little research has utilized LDAR in computing the horizontal distance CG lightning travels. Poehler (1978) conducted the only published study using this method. Using airborne field strength, ground-based field strength, LDAR data, weather radar returns and ground strike locations, he studied the complete life cycle of a thunderstorm that occurred on September 6, 1977. While using an early version of the LDAR system, he computed the horizontal distances by measuring from the center of LDAR signals to ground strike locations of 13 CG flashes. Poehler concluded that 50% of ground strikes fell within 2.1 km (1.3 n mi) of the center of LDAR discharge points, 90% fell within 5.5 km (3.4 n mi), and 100% fell within 7.8 km (4.8 n mi). He also found that 100% of ground strikes fell within 2.7 km (1.7 n mi) of the edge of precipitation echoes.

2.4.4 Summation of Past Research. Overall, previous research, which is summarized in Table 1, indicates that there is conflicting information on the distance CG lightning travels. Studies by Renner, Lopez and Holle, Krider, and Poehler did not focus on 5 n mi specifically. However, findings from their research both support and oppose the fact that lightning travels further than 5 n mi. Studies by Cox and Parsons focused on the 5

Table 1. Past Research on Determining the Distance CG Lightning Travels

Method	Researcher	Location	Scope	Results
WSR-88D Storm Centroid Method	Renner	Gulf Coast Southern Plains	April - July	75% < 10 mi
	Cox	Southeast Coast	April - July	32-39% > 5 n mi
Distance Between Successive Flash Method	Krider	Florida	3 Storms	Avg 1.9 – 2.5 n mi
	Lopez Holle	Florida, Oklahoma Colorado	1995 1 Storm 1996	75% < 4.9 n mi
	Cox	Southeast Coast	April - July	30% > 5 n mi
	Parsons	Continental US	1995-1999	65% < 5 n mi
LDAR Based Method	Poehler	Florida	1 Storm 13 CG Flashes	100% < 4.8 n mi

n mi criteria and both found that as many as 30 % of CG lightning strikes traveled further than 5 n mi.

3. Methodology

This chapter will outline the process used in this research. It will reiterate research objectives, discuss the scope of research data utilized, the grouping of LDAR data points into flashes, the matching of NLDN ground strike locations with LDAR flashes, and the statistical analysis method utilized to obtain research results.

3.1 Objectives

The primary research objective is to compute the distance that CG lightning travels and aid decision makers in determining if the 5 n mi lightning warning criteria is adequate to ensure the protection of military assets from lightning strikes. Lightning strike distances are computed by using the origin of the flash as detected by LDAR and the corresponding ground stroke locations as detected by NLDN sensors. Once distances are computed, a statistical analysis is performed revealing the distribution of distance values.

As discussed in Section 2.4, there are basically three methodologies that could be utilized to compute CG lightning distances. Each method assumes a flash origin location and uses the origin point along with a ground strike location to compute horizontal distances traveled. In both the WSR-88D storm centroid and DBSF methods, the assumption of a flash's origin affects the distances computed. For the WSR-88D storm centroid method, it is assumed that the origin of the flash is the center of the echo return or a particular reflectivity value while the DBSF method assumes the origin is the center of the ground lightning strike clusters. Both of these assumptions introduce possible errors into the results.

The LDAR system provides a unique capability in that lightning discharges are located three-dimensionally for both intra-cloud and CG flashes. These locations map out the entire lightning flash and indicate the path the flash traveled. Using the first detected signal for a flash and the respective NLDN ground strike location, the horizontal distance a CG flash travels can be computed with less error than other methods leading to a more accurate distance analysis. As such, the LDAR method for obtaining the flash origin is utilized in this research for computing CG flash distances.

A secondary objective of this research involves finding correlations between the distance CG lightning travels with certain flash characteristics. Research will find the relationship involving the distance traveled, peak current, and origin height of lightning strokes.

3.2 Scope

The data used in this research are limited by both time and space constraints. Although stroke information from the NLDN is available for several years, the period of LDAR data available through Global Hydrology and Climate Center is limited to only the months from January 1997 through June 2001. The first two months of this data set contains very limited data. As such, data extending from March 1997 through December 2000 is used in this research.

As for spatial constraints, the LDAR system is more restrictive than the NLDN system. Both horizontal and vertical range errors along with detection efficiency increase significantly as the distance from LDAR increases. Per Boccippio (2000), LDAR's effective usable distance for scientific use is approximately 100 km. This effective

distance is a result of LDAR's decrease in detection accuracy and efficiency. Due to the system's limitations, only NLDN detected ground stroke locations within 100 km of the LDAR central site are used in this study.

3.3 Grouping LDAR Data Points into Flashes

The first procedure necessary in conducting this research is to group the individual LDAR data points into lightning flashes. Grouping data points into flashes is accomplished using a program developed by First Lieutenant (1st Lt) Lee Nelson, a graduate student at the Air Force Institute of Technology. The program, written in Interactive Data Language (IDL), is based on a "flash-grouping" program utilized by NASA (NASA 2001).

The flash-grouping program performs four basic functions. It filters out system calibration data from the dataset, groups LDAR data points into flashes, clusters data points within all flashes into branches, and produces an output file which includes the original LDAR data along with flash and branch grouping information.

Calibration data is included in the raw dataset and is virtually indistinguishable from data points produced by actual lightning flashes. To prevent the calibration data from being grouped into flashes, all pulses within a region around the transmitter were prevented from being grouped into flashes. This region is centered at 1,318 meters south and 1,609 meters west of the central LDAR site. The region extends 200 meters in the north-south and east-west directions from this point and extends vertically from the surface of the earth up to 900 meters. The exclusion of data in this region not only eliminates calibration data, but also data points from actual lightning flashes. The overall affect of

this is minimal since the area is small in comparison to the total area covered by LDAR and the large volume of data collected outside of the calibration region.

After removal of calibration data, the program grouped data points into flashes using temporal and spatial constraints. For data points to be included in a flash, the points must fall within a 3 second window beginning from the time of the first data point in the flash. An additional time constraint requires each data point in a flash to be within 0.5 seconds of the previous data point in the flash. Along with these temporal constraints, a data point must also occur within a certain distance from the last point already included in the flash. Since the LDAR location error increases with range from the LDAR site, the distance criteria used to group data points into a flash must also increase with range. This is accomplished by computing an ellipse based on the distance the data point is from the LDAR site. The major axis of the ellipse corresponds to the range error associated with LDAR and equals 5000 m plus a factor that is a function of range error. The minor axis represents LDAR's azimuthal error and equals 5000 m plus the quantity of an angle error times the distance from the LDAR site. Using this method, the further the data point is away from the LDAR site, the larger the major and minor axis of the ellipse and the larger the distance allowed between data points of a flash. Once the ellipse is computed, it is centered over the data point being considered as part of the flash. If the previous data point included in the flash is within the ellipse, the data point under consideration is included in the current flash.

To further illustrate the grouping method, refer to Figure 5 as a visual aid. The program begins by considering the first data point in the file (P1). This data point is the origin of the first flash. Based on the time that this data point occurred, all data

points within three seconds are selected and considered as “possible members” of the first flash. In the example shown in Figure 5, P2 and P3 meet this criterion and become “possible members” of the flash. All “possible members” of the first flash are then tested against temporal and spatial constraints. Beginning with P2, the time P2 occurred is checked to see if it is within 0.5 seconds of P1. In this example, P2 meets the time constraint and is then tested to find whether it is within spatial constraints of P1. An ellipse is calculated for P2 using the method described in the above paragraph and then centered on P2. P1 is then checked to see if it falls within the ellipse around

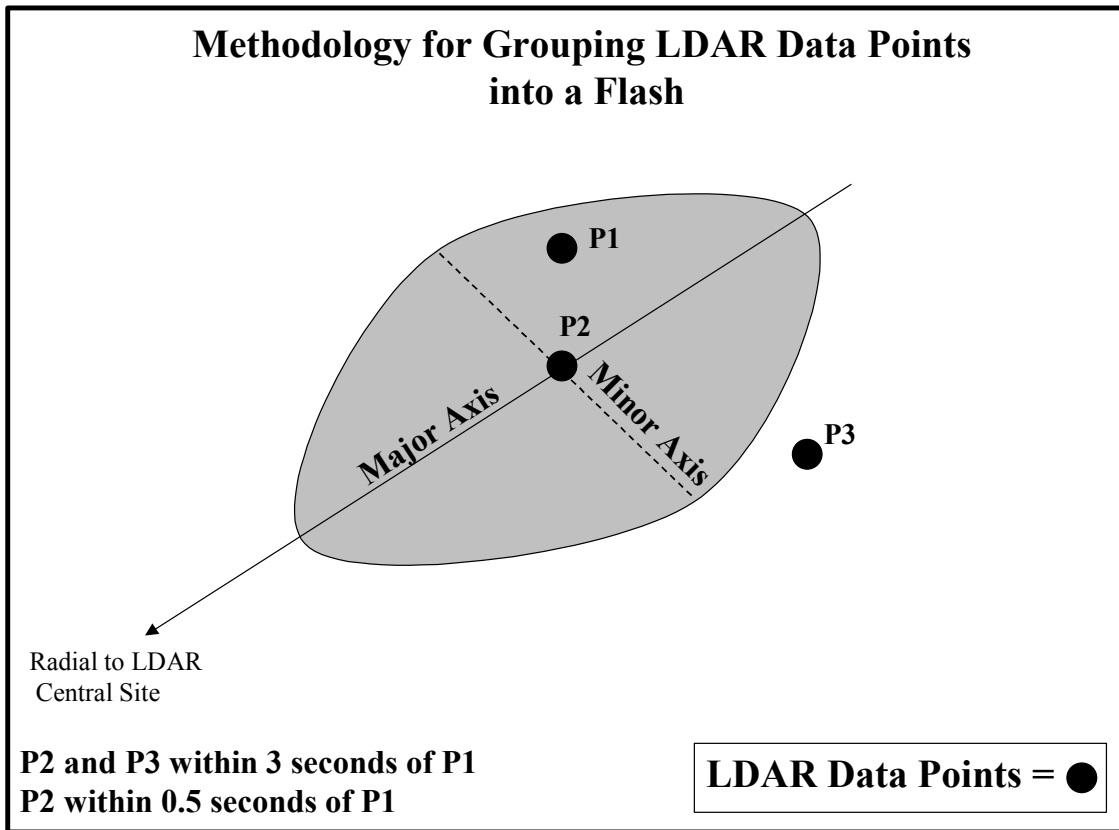


Figure 5. Methodology for Grouping LDAR Data Points into a Flash. P1 is the last LDAR data point included in a flash. P2 meets all temporal and spatial constraints and is included as a data point in the flash.

P2. If it does, as in this example, the data point (P2) is included in the first flash. If it falls outside the ellipse, it is not included in the first flash and becomes a candidate for the beginning of a new flash. The program then continues on to the next “possible member” (P3 in Figure 5). The same time and spatial criterion is applied to determine if P3 is part of the current flash. This process continues until all “possible members” are checked for inclusion in the first flash. Once the first flash is grouped, the first point in the dataset that is not included in a flash is selected as the origin point in a new flash and the grouping process is repeated. If there are no data points within three seconds of an origin point, the point is considered to be an isolated data point and not grouped into a flash. The program continues in this manner until all data points are designated as part of a flash or an isolated data point.

After data points are grouped into flashes, each data point within a flash is grouped into branches based on a second set of temporal and spatial constraints. To be part of a branch, a data point must be within 0.03 s of the previous data point. The spatial constraint is again a function of the data point’s distance from the LDAR central site. If a data point is within 40 km, the point must be within 1 km of the previous branch point to be included in the branch. If the data point is beyond 40 km, the point must be within the distance (in meters) the data point is from the central LDAR site divided by 40. The criteria used for constructing branches within a lightning flash as well as the criteria used for grouping data points into lightning flashes were taken directly from the program used by NASA.

Once all data points were grouped into flashes and branches, the results were written to an output file. Each output file contains a single day of data. The output file includes each line of the original LDAR data (day, time, and three dimensional location), the flash

number of each data point, the branch number, an index indicating the sequential number of that data point within that branch, the line number corresponding to the data point (parent) of the flash where the branch originates (for the first data point in a branch only) and finally, the line number of that data point within the entire output file. An example output file is included in Appendix A.

3.4 Matching NLDN Ground Strokes to LDAR Lightning Flashes

Although LDAR data points provide a good picture of the path of a lightning flash, the LDAR system is unable to detect the location where CG flashes strike the ground. The system's inability to sense ground stroke locations is due to a decrease in location accuracy as pulses approach the ground and the effect of the earth's curvature at greater distances from the LDAR system. As a result of this limitation, NLDN detected ground strike locations are necessary to determine where the flash struck the ground. An example of NLDN data is included in Appendix A. Using both datasets, the origin point and ground strike location of each lightning stroke produced by a flash are available for computing the distance CG lightning travels.

To determine which flash is associated with a ground stroke, a program written in IDL is used. This program is included in Appendix B. The process begins by extracting one month of NLDN data from archived files. This subset of data is then limited to only those ground strokes that occurred within 100 km of the LDAR central site. This limitation is accomplished because of the increasing LDAR inaccuracies past 100 km (Boccippio 2000).

From this “pared down” dataset, the algorithm cycles through each day of the month checking whether there were ground strokes for that day. If so, LDAR data from the corresponding day are extracted from archived, binary formatted files and converted to ASCII format. If there are no ground strokes for a day, the algorithm simply moves on to the next day. After a day with strokes is identified and the LDAR file is converted to ASCII format and opened, the algorithm loops through each ground stroke checking whether there is an LDAR flash that resulted in a ground stroke. The determination of whether a flash produced a ground stroke is based on temporal and spatial constraints. For a flash to be considered as the “creator” of the ground stroke, the flash must have an LDAR detected data point that occurred within 1 second and 50 km of the ground stroke. The use of one second as the time criteria was determined by using the approximate time that a flash lasts (Uman 2000). As for the spatial criteria, the 50 km criterion was determined by computing the distance a flash would travel if it moved at the average downward propagation speed of a stepped leader as discussed in Section 2.1.3. The result was a spatial constraint of 50 km.

Depending on the frequency of lightning activity during a one second time period, there may be only one flash meeting the above mention criteria. If so, this flash is considered the one that produced the ground stroke. However, during periods of frequent lightning, there could be more than one flash that meets the criteria for producing the stroke. In this case, the algorithm extracts all data points for each flash under consideration and determines the distance from the ground stroke to each LDAR data point. The flash with the closest LDAR detected signal to the ground stroke is then chosen as the flash that created the ground stroke. An example of the flash selection process is

displayed in Section 3.5. It should be noted that this method could produce conservative distances for those situations where the closest flash is not the flash that produced the ground stroke.

Once the flash that produced the stroke is identified, the program computes the horizontal distance from the first point of the flash or origin to the location where the flash struck the ground. The quadrant that the NLDN ground stroke occurred with respect to the origin point of the associated flash is also computed.

Three output files are created from this program. The main output file contains information on each ground stroke and the flash that created it. Output files are named using the configuration “**dist**yyyyymm” where “yyyy” is the year and “mm” the month of the data. Each line within in this file contains the month, day, year, hour, minute, second, nanosecond, latitude, longitude, and peak current from the NLDN dataset. Each line of output also includes the flash number, x, y, and z locations of the origin point from the LDAR dataset, horizontal distance from the origin point to ground stroke location, the quadrant in which ground stroke location occurred with respect to the origin, and finally the total number of branches of the LDAR flash. The content of this output is the primary information for this research, and a sample can be found in Appendix A.

A second output file is generated which contains the distances from the ground stroke location to the closest point in the flash that produced the ground stroke. This output was used to determine if the 1 second and 50 km criteria is too lenient. If the criteria are too lenient, the distribution of these distances would be strongly negatively skewed and have a large median value. The distribution of these distances for randomly selected months in 1999 showed positively skewed distributions and median values near 2 to 3 n mi. These

findings indicate that the criteria used for matching ground strokes with flashes are reasonable.

The final output file generated by the “matching” program contains statistical information. This file contains data on the number of NLDN ground strokes within 100 km of the central LDAR site, number of NLDN strokes matched to LDAR flashes, percentage of NLDN strokes matched to LDAR flashes, and the number of ground strokes that were not matched to LDAR flashes. The distances of those strokes not matched to a flash are tracked to determine whether a large number of unmatched strokes occurred further away from the LDAR system than closer in. cursory review of this output revealed that the majority of unmatched strokes occurred greater than 60 n mi away from the central site. This is a logical result since LDAR’s detection accuracy decreases with distance from the system.

3.5 Example of Matching NLDN Ground Strokes with LDAR Lightning Flashes

For this example, the reader should refer to Figure 6 as a visual aid. The triangles, squares, and circles represent LDAR data points that comprise three different flashes. Data points are oriented in the horizontal plane. Those filled with black occurred within 1 second of the ground stroke time and those filled with gray occurred more than one second after the ground strike time.

The matching process begins by extracting all data points equal to or within 1 second and 50 km of the ground stroke, which is indicated by an asterisk. Flash 1, represented by triangles, occurred within the time constraints but is outside of 50 km. Flash 2, symbolized

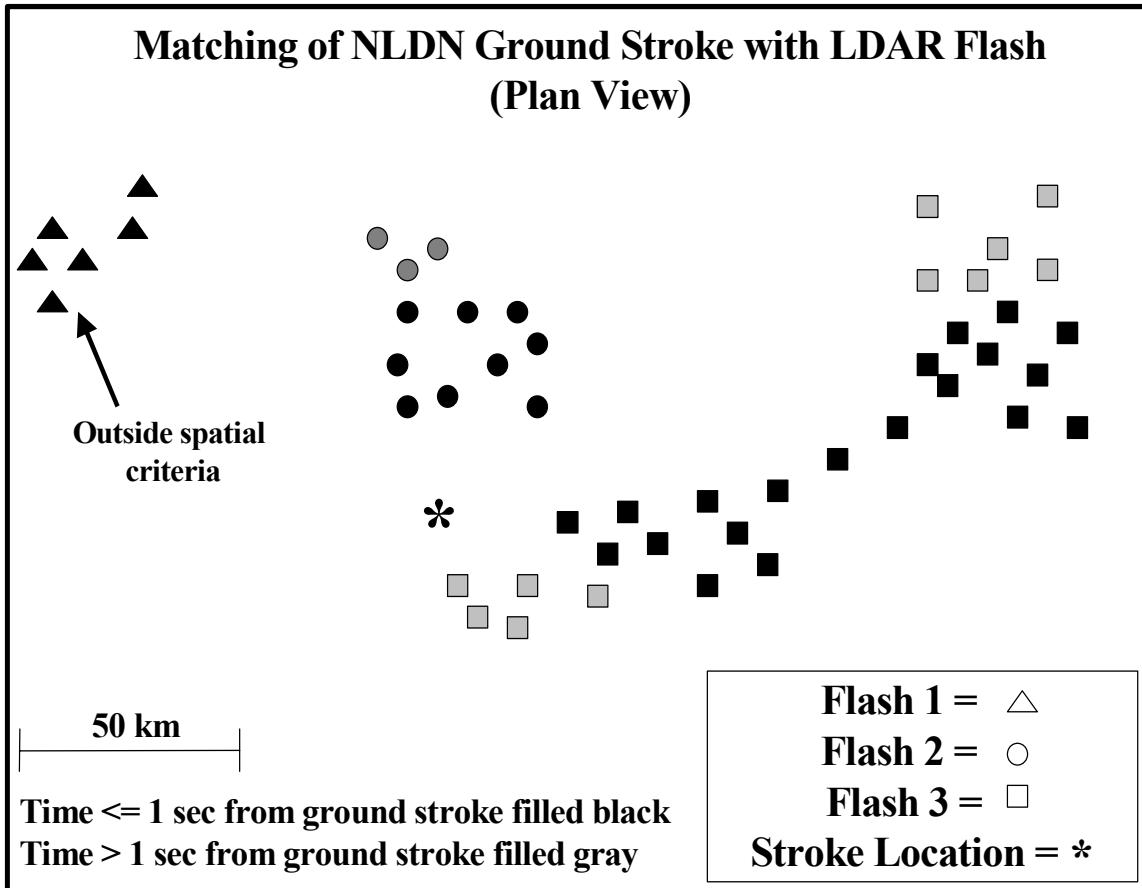


Figure 6. Schematic of the Matching of NLDN Ground Stroke with an LDAR Flash. Flash 3 meets all temporal and spatial constraints while having the closest data point to the stroke location. Thus, it is chosen as the flash that created the ground stroke.

by circles, and flash 3, characterized by squares, have data points within both time and distance criteria. The program tags these flashes as the possible initiator of the stroke and discards flash 1. All LDAR points making up flash 2 and 3 are pulled out of the dataset and the distance from each data point to the stroke is computed. The flash with the closest LDAR data point, which is flash 3 in the example, is then designated as the flash that caused the ground stroke.

3.6 Data Analysis Methodology

To analyze the distance information obtained from the matching program, an algorithm was created that combined all “**distyyymm**” files into one file that includes all data for the entire period and four other files that specifically contain seasonal data. Another algorithm calculates median and percentile values. A third algorithm creates a frequency distribution of the horizontal distances for each bin. Each bin corresponded to a range of distances that lightning traveled away from its origin point, and the frequency distribution displays the number of all the flashes that occurred in each bin. The bins used in this routine span from 0.0 to 15.0 n mi in the following manner. The first bin extends from equal to or greater than 0.0 to less than 1.0 km while the second bin ranges from equal to or greater than 1.0 km to less than 2.0 km. The bins continue in this manner out to 15.0 n mi, which is at the maximum extent of interest in this research. The frequency information is then manipulated in Microsoft Excel to display the histograms for the entire dataset along with those for each season.

To relate the horizontal distance with the peak current value of each ground stroke, an IDL program wrote the distances and peak currents from the “**distyyymm**” into one data file for the entire period and also produced files with only seasonal information. From these files, another IDL routine produced scatter plots of each these files. A third program then calculates the 95th percentile peak current value for each 0.1 n mi distance from 0.0 through 15.0 n mi. The top three outlying peak currents in each 0.1 n mi bin are discarded during this process to eliminate extreme outliers. Peak current values are manipulated further in Microsoft Excel to determine a trend with distance values. New peak current values are computed for each 0.1 n mi bin by computing a running average. The running

Table 2. Example of Running Average Computation.

Bin	5	6	7	8	9	10	11	12	13	14	15	16
Distance (n mi)	0.5	0.6	0.7	0.8	0.9	1.0	1.1	1.2	1.3	1.4	1.5	1.6
Peak Current (kA)	46.2	39.5	33.1	36.7	40.9	44.7	47.7	51.9	39.8	44.6	42.8	39.8
Running Average Peak Current (kA)						42.5	42.2	42.2	38.9	35.2	31.1	26.7

average is calculated by taking the average of the peak values for 10 of the 0.1 n mi bins around the bin being calculated. Table 2 is an example of this method. The peak current value at 1 n mi or bin 10 is computed by taking the average of the peak current values ranging from 0.5 to 1.4 n mi. This value becomes 42.5 kA. Bin 11 or the running average peak current for 1.1 n mi is then computed by averaging the values from 0.6 to 1.5 n mi. The running average peak current values for the original dataset used in this research are computed in this manner from the 0.6 n mi bin to the 14.6 n mi bin. This manipulation provided representative peak current values for each 0.1 n mi bin and reduced the extreme fluctuations or variance in peak currents from bin to bin. This smoothing procedure also slightly dampened the peak current values; however, this is not critical in this research since the goal is to determine the overall trend in peak current as the distance increases. Values are then plotted for each distance bin and a line was fit to the data to find the change in peak current with distance.

To show the relationship between peak current and the altitude of the origin point of the lightning stroke, a similar process to the peak current versus distance method described in the above paragraph is used. A program written in IDL determines the 95th percentile peak current value for each 1,000 ft in the atmosphere. During this computation, the top

three outliers in each bin are discarded. The peak current values for each bin are then manipulated in Microsoft Excel to determine a running average and then plotted versus height to indicate the trend.

4. Results and Analysis

This chapter summarizes the results found in this research. The outcome from the matching of ground strokes with LDAR flashes, analysis of the distance CG lightning flashes travel, association between the distance and peak current, and finally, the relationship between the altitude that flashes originate with their respective peak current is presented.

4.1 Association of Ground Strokes with LDAR Flashes

As stated in Chapter 3, LDAR detected data points are grouped into lightning flashes. NLDN identified strokes are then matched to the flash that produced the stroke. Table 3 summarizes the number of strokes, flashes, and percentage of strokes associated with flashes. For the months of March 1997 through December 2000, there were a total of 5,570,090 LDAR detected flashes. As expected, the summer months of June through August possessed the highest number of flashes with August containing 23.7% of the total number of flashes. December had the fewest lightning flashes with only 2.1% of the total flashes. A total of 2,622,824 NLDN lightning strokes occurred within 100 km of the LDAR site. Of these strokes, 1,585,725 were matched with an LDAR flash resulting in 60.44% of the total NLDN strokes. The percentage of NLDN strokes matched to LDAR flashes is somewhat misleading. Breaking down the rate for individual years showed that the rate for 2000 is extremely low (27.24%) while 1997 through 1999 is between 77.62% and 93.79%. The reason for such a low match rate in 2000 is unknown at this time since there were no apparent changes to the lightning detection systems or the matching algorithm.

Table 3. NLDN Ground Stroke and LDAR Flash Summary. Total number of NLDN ground strokes, total number of LDAR flashes, the number of NDLN ground strokes matched with the LDAR flash that created the stroke, and the percentage of ground strokes matched to flashes.

Month	Total Number of NLDN Ground Strokes	Total Number of LDAR Flashes	NLDN Ground Strokes Matched to LDAR Flashes	Percentage of Ground Strokes Matched
Jan	15,563	66,550	11,786	75.73
Feb	22,019	145,442	20,296	92.17
Mar	33,743	136,350	29,718	88.07
Apr	30,561	340,255	26,403	86.39
May	159,777	769,300	142,622	89.26
Jun	287,761	836,360	219,019	76.11
Jul	990,765	1,272,932	513,824	51.86
Aug	646,213	1,322,790	430,607	66.64
Sep	398,970	495,706	158,424	39.71
Oct	21,658	108,968	19,738	91.13
Nov	13,461	63,751	11,612	86.26
Dec	2,333	11,686	1,226	52.55
Total	2,622,824	5,570,090	1,585,275	60.44

Even with a low match rate for the 2000 data, the overall percentage of strokes matched to flashes is reasonable indicating that the criterion used in the matching algorithm is appropriate for this research.

Once NLDN ground stroke locations are associated with a flash, it is possible to look at an entire CG lightning flash three-dimensionally. Figure 7 is an example of a complete CG flash that occurred on 2 January 1999 at 1604 UTC. The flash consists of over 350 electromagnetic pulses detected by the LDAR system. Each pulse is depicted as a gray

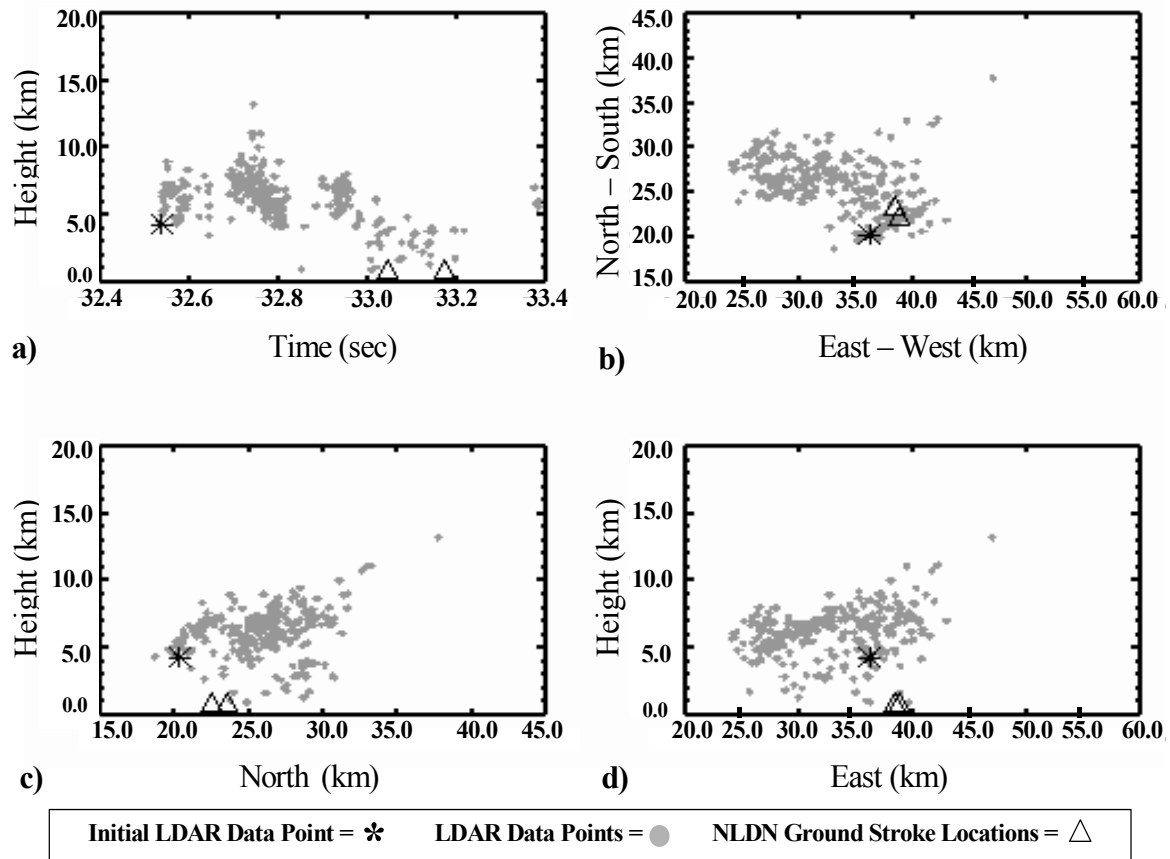


Figure 7. Lightning Flash from 2 January 1999. a) Time versus Height. b) Plan view (North-South versus East-West). c) North versus height. d) East versus height. (Asterisks indicate origin location while triangles represent ground stroke locations)

circle. Figure 7a is a time versus height depiction of the flash. The first pulse of the flash, designated by the asterisk, occurred at 32.5 seconds and at a height of approximately four kilometers. The flash continued for just under one second and produced two ground strokes which are shown as triangles. The altitude of the flash varied from as high as 14 km to as low as 1 km. It is interesting to note the electromagnetic pulses decreasing in altitude just prior to the strokes hitting the ground at approximately 33.05 and 33.15 seconds. In these instances, electromagnetic pulses decrease from 5.0 km to altitudes as

low as 0.5 km. Between the time periods of 32.8 and 32.9 seconds in Figure 7a, it appears a lightning branch drops towards the ground to as low as 1.0 km; however, there is no indication of a ground strike. There are four possible situations that could explain this lone data point. First, a branch did come close to the ground without actually hitting the ground and LDAR was only able to detect one data point in the branch. Second, there was actually a ground strike but the NLDN did not sense the event. Third, a lightning flash did not produce the data point and the signal came from a source other than a lightning flash. Finally, LDAR sensed a pulse emitted by lightning but computed the location of the pulse much lower than the true level it occurred.

Figure 7b is a plan view of this lightning event. It provides a good look of both the total horizontal extent of the flash and the horizontal distance from the flash's origin point to each ground stroke location. Figure 7c is a North-South representation of the flash. It displays the flash's movement in the North-South plane from the LDAR central site while Figure 7d provides a look at the flash's movement in the East-West direction. The flash extends from 18 to 38 km north of LDAR and 24 to 48 km east. It is also apparent that the ground strokes occurred approximately one to two kilometers in the North-South direction from each other and at approximately the same East-West location. The combination of all four depictions provides a unique view of the characteristics of this lightning flash.

4.2 Characteristics of the Distance Lightning Travels

The issuance of lightning warnings is critical to safe military operations. The goal of this research is to compute the distance CG lightning travels in hopes of aiding decision makers determine whether the 5 n mi criterion is adequate for issuing lightning warnings.

However, this criteria is not the only limiting factor in the lightning warning process. Currently, operational meteorologists only have tools available that provide information on where CG lightning has occurred or where a thunderstorm is currently located. They do not have a tool that indicates where lightning may originate so they can apply the distance a CG lightning flash travels and issue a lightning warning at the earliest moment. An AFIT research objective is to provide the distance a CG lightning stroke travels and to describe the areas where lightning originates. This research will determine the distance portion of this objective. The second piece is the focus of research being conducted by 1st Lt Lee Nelson. He is using the LDAR system and the WSR-88D to determine where lightning originates with respect to composite reflectivity values. This will provide insight into the preferred locations where lightning originates. With this information, meteorologist can locate the reflectivity values for an approaching thunderstorm via the WSR-88D, apply the distance a CG flash travels, and determine if a lightning warning is necessary. With this tool, meteorologist will be able to issue lightning warnings before a CG lightning detection system would ever detect the first CG lightning flash. This obviously decreases the risk of damage to military assets and increases the forecaster's ability to provide better resource protection.

The results presented in this section refer to the distance the CG stroke traveled from the point of origin to the location the stroke hit the ground. Distance information is presented for the entire data period and then broke into seasons. Since military lightning warning criterion is described in units of nautical miles, all distances in this study are presented in nautical miles.

Table 4 displays summary information for the entire period of data and also seasonal subcategories. The mean distance that CG lightning strokes travel for seasonal subcategories range from 3.5 n mi to 5.8 n mi, while median distances range from 2.0 to 3.6 n mi. It is interesting to note that the extreme minimum and maximum distance values occur during the spring and fall seasons. For data from March 1997 through December 2000, the mean distance is 4.7 n mi and the median distance is 2.7 n mi. Each mean distance is slightly larger than the median distance due to the sensitivity of the mean to extreme values. Median values are less sensitive to outliers in the data.

The percentile that lightning strokes traveled 5 n mi or less occurs at ranges between 61.5% in the spring and 81.3% in the fall. The seasonal range of lightning strikes occurring beyond 5 n mi is from 18.7% to 38.5%. The spring season has the maximum frequency of lightning strikes further than the current lightning warning criteria. Fall possesses the lowest frequency outside this range with only 18.7%. For the entire period, 28.4% of the strokes occurred further than the criteria used for issuing a lightning warning.

Table 4. Distance Statistics Summary by Season and for the Entire Data Period. Number of strokes, mean distance from origin to ground stroke location, median distance, percentile at 5 n mi, distance of the 90th percentile, distance of the 95th percentile, and distance of the 99th percentile.

Season	Number of Strokes	Mean Distance (n mi)	Median Distance (n mi)	Percentile at 5 n mi (%)	Distance at 90 th Percentile (n mi)	Distance at 95 th Percentile (n mi)	Distance at 99 th Percentile (n mi)
Spring	198,743	5.8	3.6	61.5	13.6	19.2	31.0
Summer	1,163,450	4.6	2.7	71.8	10.8	16.3	28.3
Fall	189,774	3.5	2.0	81.3	7.6	11.7	25.2
Winter	33,308	5.2	3.1	65.4	12.0	17.5	29.1
Period	1,585,275	4.7	2.7	71.6	10.9	16.4	28.4

Seasonal results indicating the distance at which 90% of the strokes occurred is consistent with results described above. Spring has the furthest distance at 13.6 n mi while fall has the shortest at 7.6 n mi. Figure 8 provides a graphical representation of the number of strokes per nautical mile for the entire data period. Individual seasonal distributions are available in Appendix C. The distance bins are limited to those from 0 to 15 n mi since the focus of this research is the distribution with respect to 5 n mi. All frequency distributions are positively skewed with the mode occurring at the 1.0 to less than 2.0 n mi bin.

The lightning information contained in Table 4 and Figure 8 provides a basis for determining a safe distance for issuing lightning warnings. Most lightning flashes travel between 1 and 2 n mi. However, only 71.6% of the lightning strokes travel distances

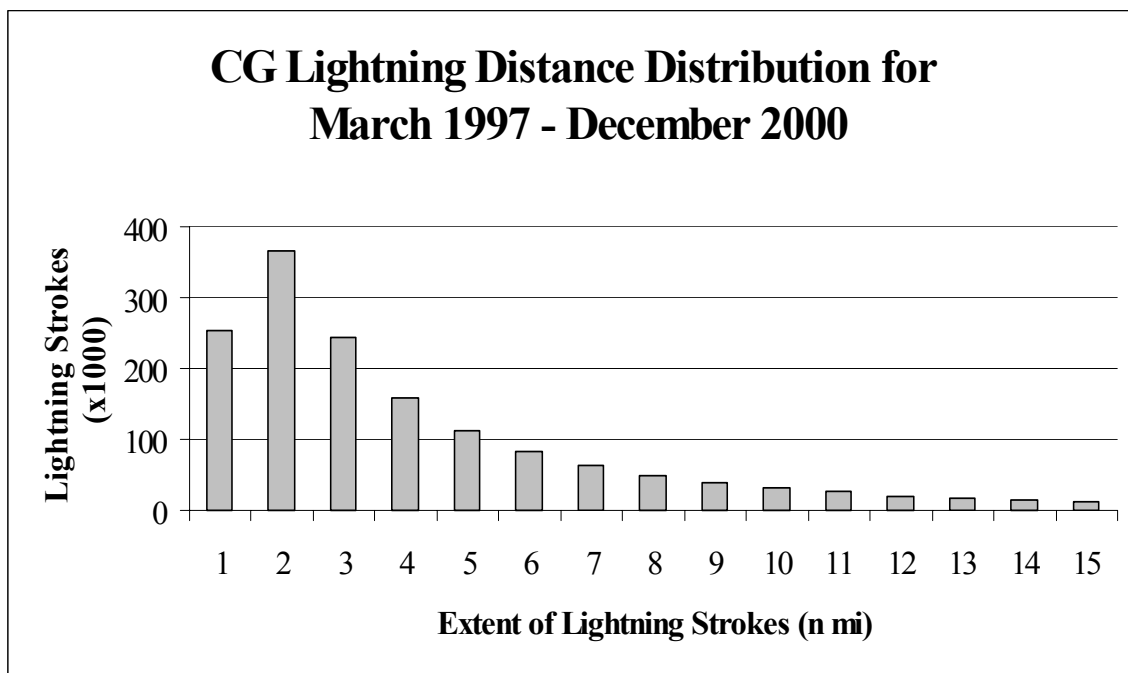


Figure 8. Lightning Stroke Frequency Distribution for March 1997 through December 2000.

less than the current 5 n mi lightning warning criterion. This leaves 28.4% of the flashes traveling further than 5 n mi and indicates that a is associated with the warning criteria. If this risk were to be minimized, a higher distance criterion must be instituted based on results found in this research. If the criteria were set so that 90% of CG lightning strike would be within a particular distance, then the safety criteria would need to be increased to 11.0 n mi for operational use.

4.3 Association Between Distance and Peak Current

As described by Huffines (1999), variations in the peak current of lightning flashes are evident in past research. Peak currents tend to vary with altitude, latitude, and time of year. Also, higher positive peak currents are likely to occur over the Great Plains. Two possible theories explaining these variations are as follows. First, the variations in peak current are a function of the length of the lightning channel as charge is deposited on or along the channel itself. Hence, the longer the channel, the more charge deposited on the channel and a higher peak current. Second, peak current variations occur as a result of the amount of charge in the cloud that is eventually transferred to the ground. With the methodology used in this research, it is possible to test these theories and determine if a relationship exists between the length of the lightning flash and the peak current.

The distance lightning strokes travel and their associated peak currents for March 1999 through December 2000 are shown in Figure 9. Positive peak currents are displayed in black while negative peak currents are in gray. It is important to note that the peak current for every stroke is displayed and used in all calculations in this section versus using the peak current for only the first stroke of a flash. Due to large number of data points,

points plot over the top of each other and the frequency of occurrence in each 1 n mi bin is difficult to interpret. To alleviate this problem, a solid black line displays the frequency of occurrence for both positive and negative currents. The frequency of occurrence is computed by dividing the total number of occurrences in each 0.1 n mi bin by the total number of lightning strike events. Frequencies for both positive and negative polarities are computed. In Figure 9, it is evident that the mode occurs between 1 and 2 n mi. The most noticeable relationship between peak current and distance is that the variation of the peak current decreases as the length of the lightning stroke increases.

To isolate and quantify this decreasing peak current variability, peak currents are

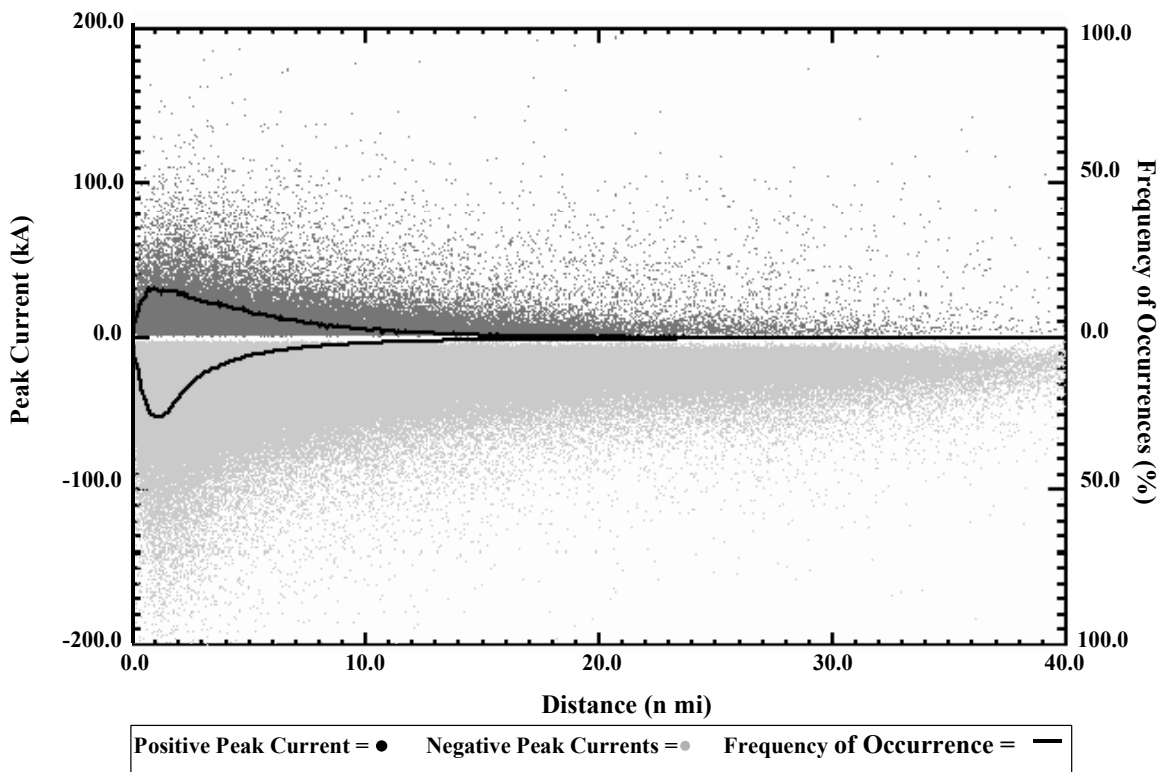


Figure 9. Scatter Plot of Distance and Peak Current for March 1999 through December 2000.

placed into 0.1 n mi bins. The top three outliers in each bin are discarded and the 95th percentile value is computed. To remove large fluctuations in 95th percentile peak current values, a running average is calculated from 2 to 14 n mi as described in Section 3.5.

Figure 10 displays the decrease in positive peak current values as the distance lightning strokes travel increases. Figure 11 illustrates this trend for the negative peak currents.

Positive peak currents decline more rapid than negative peak currents. A line was fit to the data using the least squares technique. Positive peak currents drop off approximately 7.3 kA from 2 n mi to 10 n mi while negative peak currents decrease by

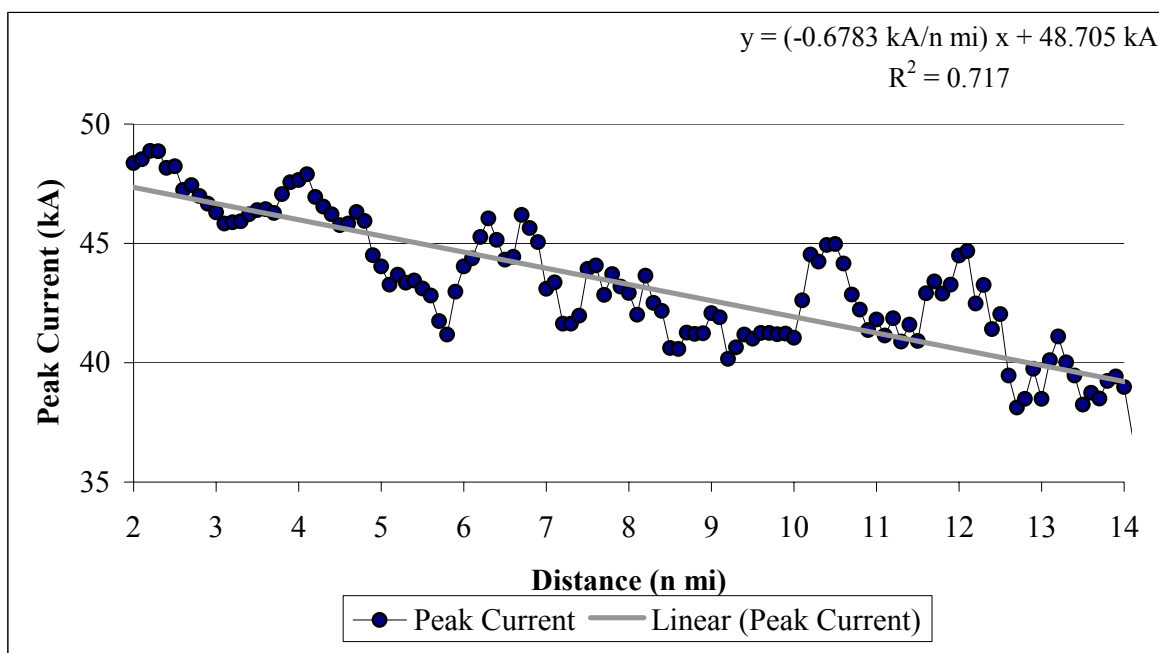


Figure 10. Positive Peak Current as a Function of Distance for March 1999 through December 2000. Data points indicate the running average of the 95th percentile positive peak current values and the solid line displays the regression line fitted using the least squares technique.

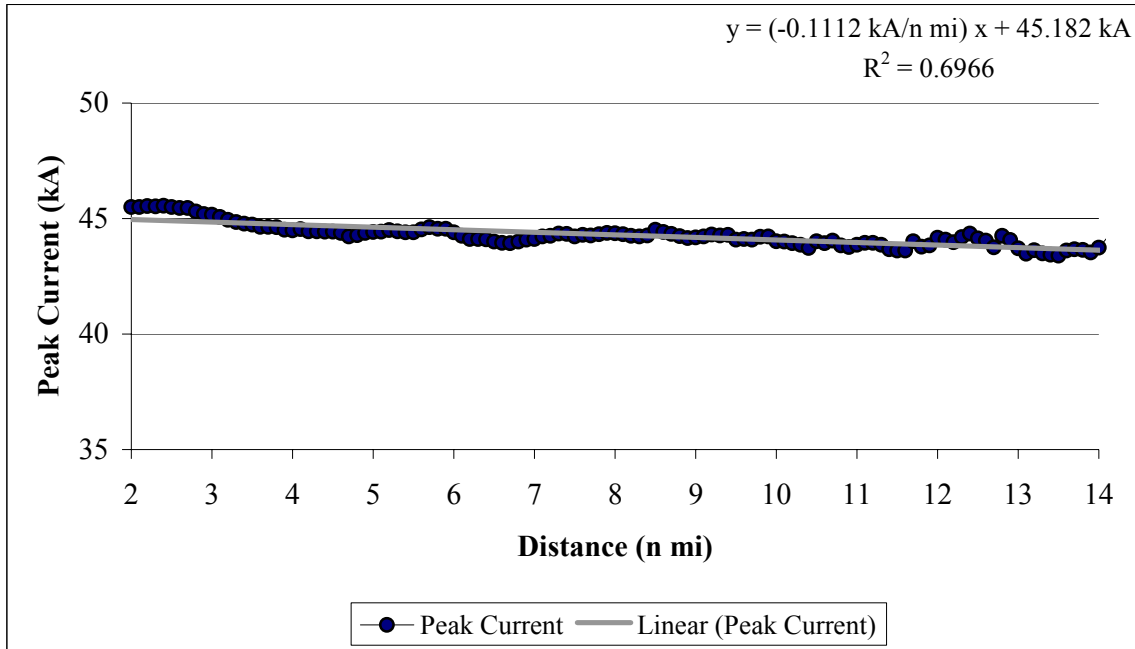


Figure 11. Negative Peak Current as a Function of Distance for March 1999 through December 2000. Data points indicate the running average of the 95th percentile negative peak current values and the solid line displays the regression line fitted using the least squares technique.

only 1.5 kA over the same distance. Coefficients of determination (R²) values measuring the goodness of fit for each line are approximately 0.70 indicating a relatively good fit for both positive and negative currents.

Seasonal peak current values as a function of distance were also computed. Scatter plots and trend diagrams similar to Figures 9, 10, and 11 are displayed in Appendix D for each season. Seasonal scatter plots show only minor differences from the scatter plot for the entire period shown in Figure 9. The most frequent distance for lightning to travel is between 1 and 2 n mi and the variations in peak current decrease with distance in all scatter plots. Seasonal trend diagrams show that the peak current decreases with increasing

Table 5. Change in Peak Current Versus the Distance a Lightning Stroke Traveled. Peak current is the difference in peak current values for strokes that traveled 2 n mi and those that traveled 10 n mi.

Current Polarity	Spring	Summer	Fall	Winter	Period
Positive (kA/n mi)	-17.8	-4.1	-27.3	-40.5	-7.3
Negative (kA/n mi)	-0.7	-1.7	-3.2	-1.7	-1.5

lightning channel distances. The winter months have the overall highest positive peak current values at 2 n mi. The largest decrease over distance is clear from the slope of the linear, best-fit line. The winter season has the steepest decrease in positive peak current with distance with a slope of $-3.69 \text{ kA n mi}^{-1}$. The coefficient of determination for this line is 0.91, which is the highest coefficient of determination for all seasons. The lowest decrease in positive peak current with distance occurs in the summer months. For negative peak currents, the amplitudes also decrease with height but not as drastically as the positive peak current trends. The steepest slope for negative peak currents is only $-0.6980 \text{ kA n mi}^{-1}$ in the summer while the slope for spring is $-0.1291 \text{ kA n mi}^{-1}$. Table 5 summarizes the decrease in peak current with distance for each season and for the complete data set.

In general, it was found that the peak current of a lightning stroke decreases with increasing distance the stroke travels. The decrease is more pronounced for positive peak currents while negative peak currents taper off gradually with lightning stroke channel distance. Although the amount of decrease varies from one to the other, each season also displayed this general decrease in peak current values.

4.4 Relationship Between Altitude of Stroke Origin Point and Peak Current

The second theory explaining the variation in amplitude of the peak current in a lightning flash is that the peak current is a function of the amount of charge in the region the flash originated. To test this theory, we will make two assumptions. First, we will assume that the polarity of a CG lightning stroke is the same as the charge region in which the stroke originated. With this, we would expect to see negative and positive polarity lightning strokes originating from regions with the same respective charge. Past research summarized in MacGorman and Rust (1998) indicates that the measured altitude of the main charge negative region extends from 9,800 ft (3 km) to 19,600 ft (6 km) and the main upper positive region is between 19,600 ft (6 km) and 32,800 ft (10 km). With this in mind, we should see a high number of negative and positive strokes originating from these heights.

The second assumption is that the peak current of a stroke is directly proportional to the amount of charge in the region where the flash originated. Under this assumption, we could expect to see higher peak current strokes beginning from altitudes where the highest charge regions exist in a thunderstorm. These values are mentioned in the above paragraph.

Figure 12 is a scatter plot of the peak current of the stroke versus the altitude at which a flash began. Positive peak currents are displayed in black while negative peak currents are in gray. The solid black line (one for positive and one for negative peak currents) represents the frequency of occurrence for each 1,000 ft height increment. The frequency of occurrence is computed by dividing the total number of occurrences in each bin by the total number of positive or negative strokes.

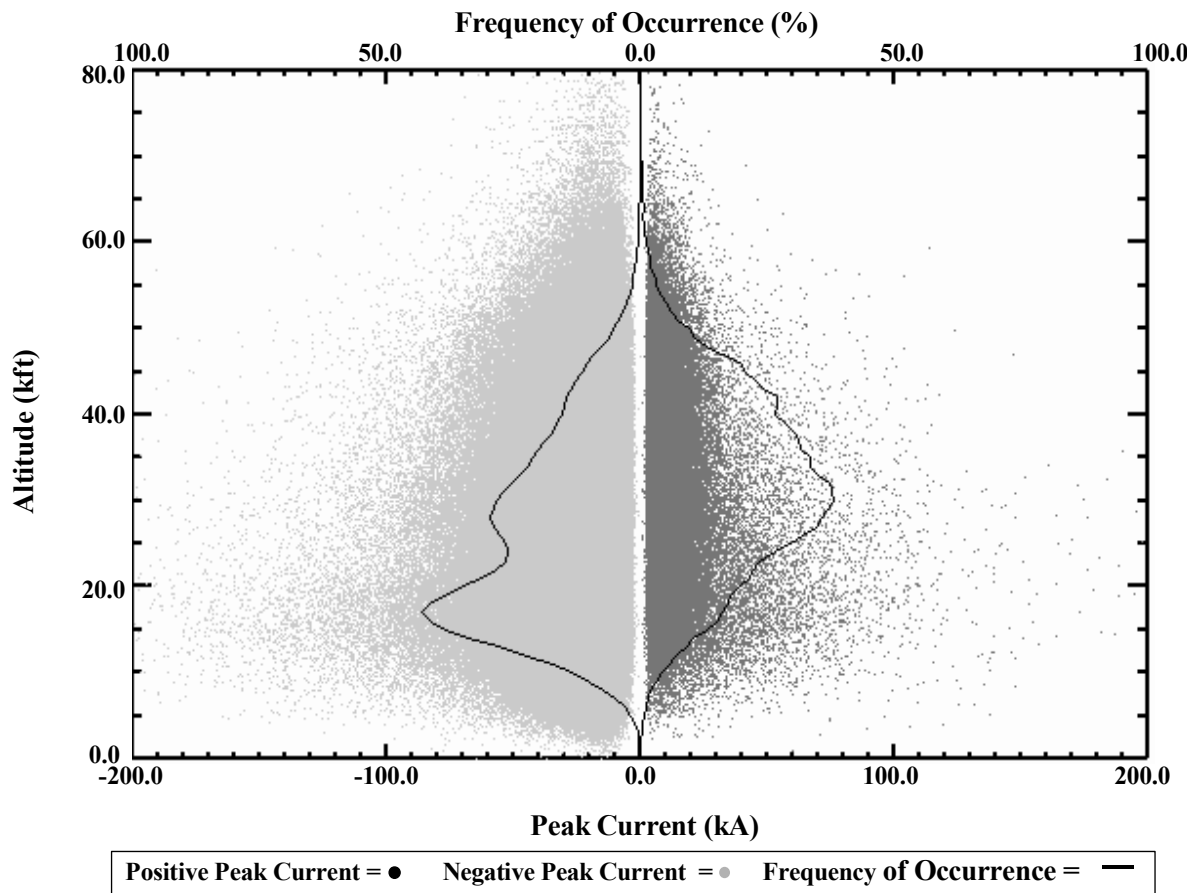


Figure 12. Scatter Plot of Peak Current and Altitude of the Stroke Origin Point for March 1999 through December 2000.

Figure 12 shows that lightning stroke origin points for both positive and negative lightning strokes occur throughout the atmosphere from just above the surface to 80,000 ft. Overall, there is a decrease in the variation of peak current values as origin heights increase. In other words, the lightning strokes with lower origin altitudes tend to produce higher amplitude peak currents than those that begin at higher altitudes. At altitudes displayed above 60,000 ft in Figure 12, this trend should be ignored since these data points are few and they exist above the average, summer tropical tropopause.

The frequency of occurrence line for negative peak current strokes depicted in Figure 12 displays two maximums. The lowest peak, which is also the overall maximum, occurs in the 17-kft bin indicating that most negative CG lightning strokes began between 17,000 and 17,900 ft (approximately 5.3 km). This height agrees well with measured heights of main the negative charge region from the tripole structure discussed in Chapter 2. The interesting portion of the negative peak current frequency plot is the second or upper peak. The upper peak occurs between 27,000 and 27,900 ft (approximately 8.4 km). This region is located where normally the upper positive charge region is located. This peak may be a result of the complex charge structures as described by Stolzenburg et al. (1998) where vertical motions in a thunderstorm affect the height of the charge regions. This second peak may also be a reflection of the upper negative charge region in an inverted tripole structure thunderstorm as reported by Krehbiel (2001).

The positive peak current frequency line in Figure 12 shows one maximum located between 30,000 and 30,900 ft or approximately 9.2 km. Again, assuming the polarity of the CG stroke is representative of the charge region at the origin, this height is indicative of the upper positive charge region shown in Figure 1. The altitude of this maximum is comparable to measured altitudes of the upper positive charge regions as summarized by MacGorman and Rust (1998).

To take a more quantitative look at the decrease in peak current with increasing altitude, Figures 13 and 14 are presented. These diagrams are graphs of positive and negative peak current values versus the altitude of the lightning stroke origin points for data from March 1999 through December 2000. Data points are calculated by placing peak current values in 1,000 ft bins. In each bin, the top three outliers are discarded and

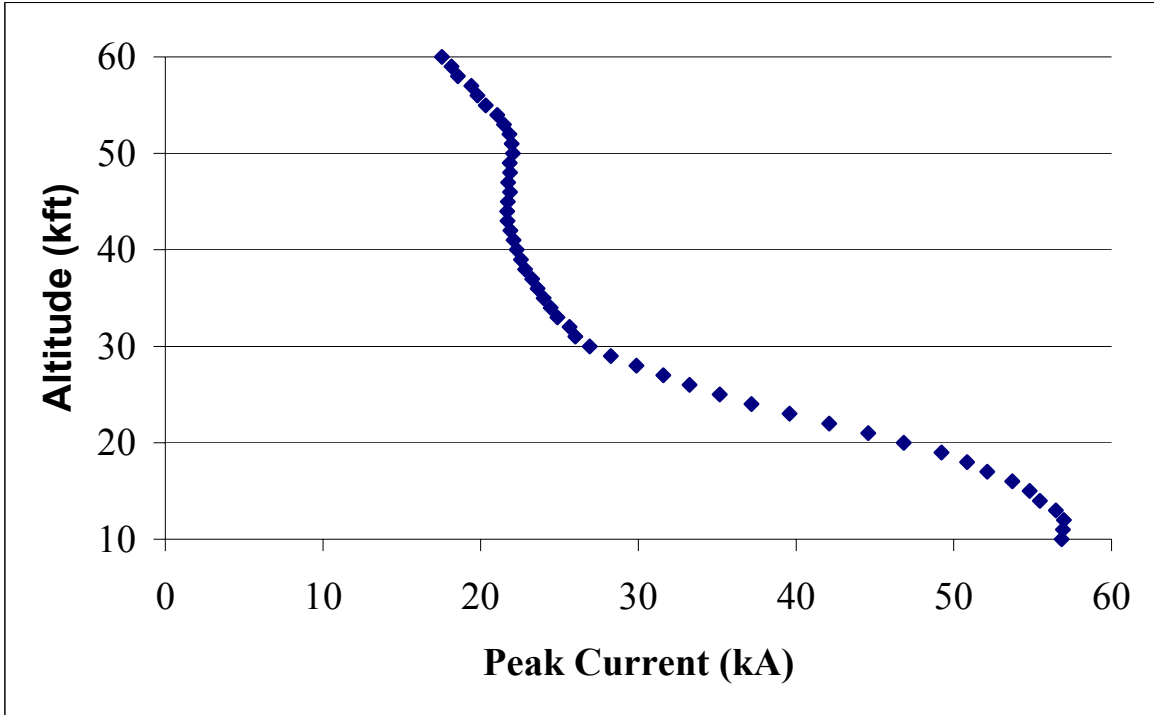


Figure 13. Positive Peak Current Values as a Function of Altitude for March 1999 through December 2000. Data points indicate the running average of the 95th percentile positive peak current values.

the 95th percentile value is found. To reduce fluctuations, a running average of the peak current values are computed as described in Section 3.5. The x-axis values for the negative peak current graphs range from 30 to 60 kA while the x-axis for the positive peak current graphs range from 0 to 60 kA.

Again, one of the assumptions is that a charge region with a higher charge produces a CG stroke with a larger peak current, than it would seem logical that higher peak currents would be evident around the heights where maximum positive and negative charge regions tend to occur. However, Figures 13 and 14 do not support this. Both diagrams show that the 95th percentile for peak currents for both positive and negative strokes drop with

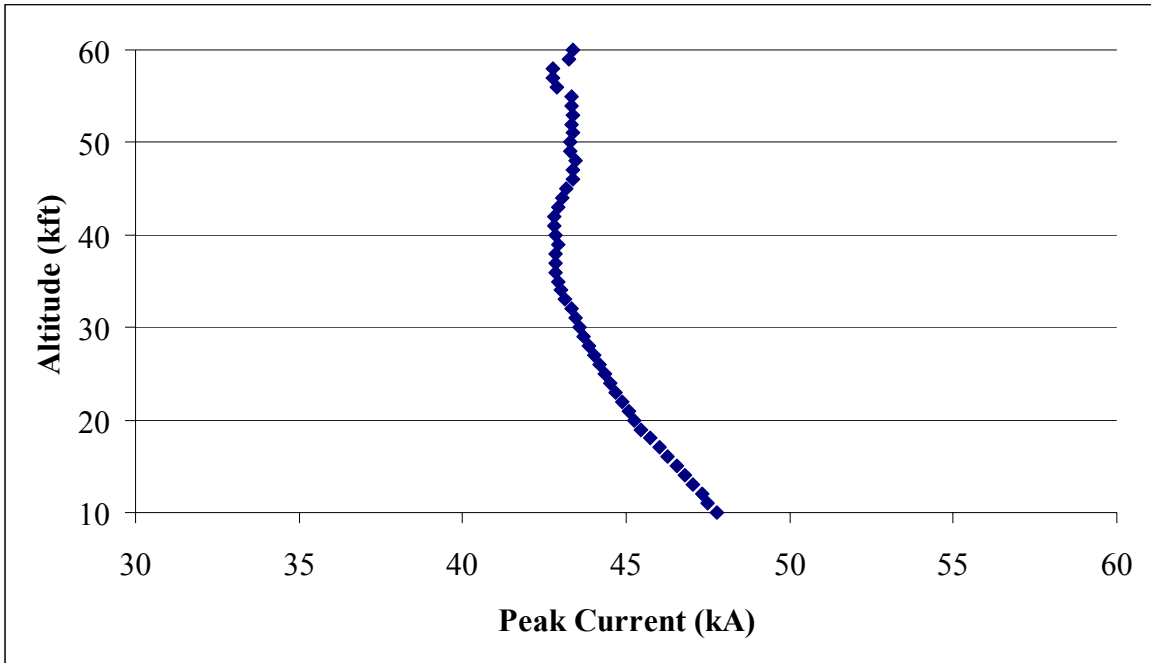


Figure 14. Negative Peak Current Values as a Function of Altitude for March 1999 through December 2000. Data points indicate the running average of the 95th percentile negative peak current values

increasing height of the stroke origin location. The highest positive peak current is approximately 58 kA and occurs at 12,000 ft or 3.7 km. From 10,000 to 40,000 ft, positive peak current values drop 34.6 kA. It appears from these data that strokes with the largest peak currents do not occur from strokes that originate in the more positively charged, upper positive charge region. The larger positive peak current strokes actually originate in the lower portion of the thunderstorm closer to the location of the weaker, lower positive charge region. Negative peak currents also decrease with height but much more gradually. The maximum amplitude of negative peak currents occurs in the lower atmosphere at 10,000 ft with a value of 48 kA. Negative peak currents decrease only 5.0 kA from 10,000 to 40,000 ft. Thus, CG lightning strokes with maximum peak currents originate low in the atmosphere for both positive and negative polarity lightning strokes.

Peak current values as a function of lightning origin point heights are also computed. Scatter plots and trend diagrams similar to Figures 12, 13, and 14 are displayed in Appendix E for each season. Seasonal scatter plots indicate two similar trends as the scatter plot in Figure 12, which is for the entire data period. The first similarity is that peak current variations decrease with height. Table 6 provides a summary of the amount of decrease in peak current. It is clear that winter displays the largest seasonal decrease in peak current values for both positive and negative lightning strokes. The second similarity is that each seasonal scatter plot displays two maximums in the negative peak current frequency line similar to that in Figure 12.

One additional interesting fact is evident in the trend diagrams displayed in Appendix E. Each trend diagram for the positive peak current indicates a maximum in the peak current at altitudes ranging from 10,000 ft (3.0 km) up to 14,000 ft (4.3 km). This height actually corresponds well with measured heights of the lower positive charge region in a thunderstorm. Again, all seasonal trend diagrams show a decreasing trend in peak current with increasing altitude of the stroke origin point similar to that shown in Figures 13 and 14.

Table 6. Change in Peak Current Versus Increasing Altitude of Lightning Stroke's Origin Location. Change in peak current is the difference between peak current values at 10,000 ft and 40,000ft.

Current Polarity	Spring	Summer	Fall	Winter	Period
Positive (kA/n mi)	-31.0	-19.1	-24.0	-45.4	-34.6
Negative (kA/n mi)	-0.6	-5.4	-6.3	-6.4	-5.0

In summary, the analysis of peak current and flash origin altitude resulted in two findings. First, scatter plots show that positive or negative charge regions occur throughout the atmosphere indicating, based on our first assumption, that charge structures of thunderstorms are very complex. The maximum frequency of negative strokes occurs at the altitudes where the main negative charge region exists according to past thunderstorm charge measurements. However, a second maximum occurs near the area that the upper positive charge region has been measured. This may be evidence that updrafts and downdrafts within a thunderstorm displace charge regions in the vertical or inverted tripole structures occur frequently.

Second, the amplitude of the peak current in CG flashes decreases as the origin height of the flashes increases. According to our second assumption that larger amplitude charge regions produce a larger peak current, we expected the higher peak currents to occur at heights where the largest positive or negative charge tend to accumulate. Trend analysis graphs (Figures 13 and 14) contradict this assumption. Large amplitude peak currents occur from CG strokes that originate in the lower atmosphere and peak current values decrease as the stroke origin height increases.

5. Conclusions

5.1 Conclusions

This research is the first to measure a large number of lightning strokes from their point of origin to the location where they struck the ground. This study examined over 1.5 million lightning strokes that occurred in the Kennedy Space Center area during the period of March 1997 through December 2000. The path the lightning flash traveled was constructed by grouping LDAR detected electromagnetic pulses into flashes and then determining which flash caused ground strokes detected by the NLDN system. The grouping of the lightning flashes along with matching them to their respective ground strike locations was accomplished using temporal and spatial criteria. The capability of the NDLN to provide the peak current of a lightning stroke enabled further research into the characteristics of CG lightning. Peak current values were studied along with the distance strokes traveled and the height of the stroke origin point to determine if relationships exist.

This research found that CG lightning in the Central Florida area frequently travels further than 5 n mi from the flash origin point and the distance CG lightning strokes travel varies with season. For the entire period, 71.6% of the lightning strokes traveled 5 n mi or less leaving 28.4% of the strokes extending beyond the AFOSH 91-100 lightning warning criteria. Seasonally, spring and winter had the highest frequencies with 38.5% and 34.6%, respectively, beyond 5 n mi and the lowest frequency occurred in the fall months with 18.7% beyond 5 n mi. It appears that the current lightning warning criteria of 5 n mi puts Air Force assets at risk. However, it is important to keep in mind that the current warning process does not measure the distance lightning is away from an airfield by taking into

account the origin point of a lightning stroke. As shown in Table 4, the lightning warning criterion must be increased to a distance of 11.0 n mi for 90% of lightning strikes to occur within the lightning standard. If the desire were for 95% of the lightning strokes to occur within the criterion, the distance criterion for lightning warnings would need to be set at 17 n mi.

Research delving into the characteristics of the peak current of a CG flash attempted to explain the variations seen in peak current measurements. Trend analysis comparing the peak current and the distance a lightning stroke travels indicated that larger amplitude peak currents were created by lightning strokes with shorter channel lengths. As the distance traveled by a GG lightning stroke increased, the positive peak current values decreased by 5.4 kA from 2 to 10 n mi while the amplitude of negative peak current strokes decreased by 0.8 kA. The decrease in peak current with the distance a lightning stroke travels contradicts the initial postulation that these two variables are directly proportional. Analysis of the change in peak current with increasing altitude of the origin point of a stroke indicated that higher peak currents were produced from strokes that originated lower in the atmosphere. Positive peak current values decreased 30 kA from 10,000 to 40,000 ft and negative peak current values decreased 4.0 kA over the same altitudes. Since higher peak current strokes did not occur where maximum charge regions typically exist, the hypothesis that the peak current of a stroke is proportional to the strength of the charge region where the stroke originates is inaccurate. In summary, the combination of these findings suggests that larger peak current CG strokes begin in the lower portions of thunderstorms. High peak current strokes also travel a short distance from their origin

location. Those with lower peak currents originate at higher altitudes and tend to travel further distances.

The most critical conclusion of this research is that lightning frequently travels further than the current AFOSH 91-100 lightning warning criteria of 5 n mi when the distance of a flash is computed from the flash origin to the ground strike spot. From a strictly scientific standpoint, the warning criteria should be increased. However, if the lightning warning criterion is increased to a distance as to ensure that no CG lightning strike will threaten military assets, military operations would come to a halt and combat readiness would drop to unacceptable levels. At this point in lightning research, there is no one criteria that will unquestionably ensure the safety of military assets. With this in mind, lightning safety comes down to the amount of risk to which one is subjected versus the importance of the mission at hand. For policy makers and military commanders, this is a difficult position. Hopefully, with the information provided in this research, policy makers and commanders will have a better understanding of the lightning process and the threat it presents to military operations. Armed with this knowledge, informed decisions can ensure the proper protection of our fighting men and women while achieving mission requirements.

5.2 Future research recommendations

Further research on the characteristics of CG lightning strikes should continue. In particular, three-dimensional lightning data from a recently installed lightning detection system at Dallas-Fort Worth International Airport could be analyzed in the same manner as in this research. Since most thunderstorms in the Kennedy Space Center area are of the air mass variety and are a result of small scale forcing mechanisms such as sea breeze effects,

data from this system could be used to determine if different synoptic situations that induce thunderstorm activity affect distance and peak current characteristics. Also, the combination of LDAR detected flashes and atmospheric parameters such as temperature and moisture data from upper air soundings may give further insight into the characteristics of lightning, specifically the atmospheric effects on the peak current of a lightning stroke. This could be accomplished using both the LDAR system in Florida and the Texas system.

Since the peak current in subsequent strokes in a lightning flashes decreases with each stroke, another significant research avenue would be to examine the peak current of only the first stroke peak currents in association with the distance a lightning flash travels. This information may prove that the peak current is more dependent on the multiplicity of a lightning stroke versus the distance the flash travels or the altitude the flash originates.

Appendix A. Example NLDN and LDAR Data Files and Program Output Files

Appendix A contains sample NLDN and LDAR data. Examples of two computer program output files as described in Section 3 are also included.

Table A-1. Sample LDAR data

Day	Hour	Minute	Second	Microsecond	X	Y	Z
2	15	27	39	239220	48982	-1285	6711
2	15	27	39	239898	48945	-272	47930
2	15	27	39	240923	49765	91	6890
2	15	27	39	241429	48755	184	4034
2	15	27	39	241912	51436	-268	88192
2	15	27	39	243093	51168	-108	86062
2	15	27	39	243557	47052	448	4698
2	15	27	39	246163	46919	-2400	7797
2	15	27	39	246873	51082	-1217	6793
2	15	27	39	246977	44825	332	2728
2	15	27	39	248473	48533	-840	5648
2	15	27	39	248818	48181	319	6316
2	15	27	39	250696	46680	296	5941
2	15	27	39	250941	58869	-3581	13656
2	15	27	39	252093	52341	-378	6351
2	15	27	39	253769	46964	-30	5378
2	15	27	39	253894	50106	11	5131
2	15	27	39	254106	50454	111	4762
2	15	27	39	254956	50929	-3185	8841
2	15	27	39	255067	50856	-113	7000
2	15	27	39	255654	45475	318	4234
2	15	27	39	255961	51918	365	5723
2	15	27	39	256105	49779	267	5061
2	15	27	39	257357	50113	371	5561
2	15	27	39	257471	48196	453	2555
2	15	27	39	258660	51085	32	4707
2	15	27	39	259724	50069	489	4322

Table A-2. Sample NLDN data

DATE	TIME	LATITUDE	LONGITUDE	PEAK CURRENT
01/02/99	06:22:29.757398771	26.674	-80.195	-17.8
01/02/99	06:23:59.453924764	26.669	-80.176	-31.0
01/02/99	06:26:55.802358800	26.702	-80.199	-24.3
01/02/99	06:31:58.862951890	26.558	-79.970	-20.1
01/02/99	06:34:12.170484283	26.718	-80.195	-25.7
01/02/99	06:36:29.066801242	26.596	-79.995	-15.5
01/02/99	06:37:13.001012715	26.579	-79.968	-15.5
01/02/99	06:37:13.115778525	26.581	-79.967	-18.9
01/02/99	06:38:36.753617733	26.553	-79.975	-27.5
01/02/99	06:38:36.870938097	26.552	-79.952	-32.0
01/02/99	06:52:40.104562559	26.572	-79.720	-121.9
01/02/99	06:59:51.582102398	26.871	-80.229	-33.2
01/02/99	07:02:55.355645566	26.638	-79.799	-68.4
01/02/99	07:02:55.389222292	26.638	-79.767	-27.6
01/02/99	07:02:55.432708210	26.646	-79.783	-29.2
01/02/99	07:02:55.544898718	26.646	-79.784	-34.3
01/02/99	07:09:11.319493432	26.826	-80.042	-139.5
01/02/99	07:09:11.358866250	26.828	-80.050	-32.7
01/02/99	07:13:30.833920200	26.895	-80.166	-28.7
01/02/99	07:13:30.855351544	26.856	-80.169	-20.7
01/02/99	07:13:31.048901000	26.854	-80.162	-19.4
01/02/99	07:15:42.565815913	26.867	-80.150	-79.3
01/02/99	07:16:25.694939300	26.464	-79.992	-97.8
01/02/99	07:16:25.732135737	26.871	-80.174	-18.7
01/02/99	07:17:26.727092446	26.682	-79.810	-18.5
01/02/99	07:22:48.112014259	26.866	-80.190	-130.1
01/02/99	07:22:48.112165100	27.145	-80.164	+40.3
01/02/99	07:23:56.277184037	26.904	-80.152	-68.9
01/02/99	07:23:56.310303644	26.926	-80.094	-16.7
01/02/99	07:25:19.596999774	26.899	-80.201	-97.9
01/02/99	07:25:19.638179850	26.892	-80.202	-32.7
01/02/99	07:25:19.661556839	26.873	-80.218	-11.8
01/02/99	07:29:30.861712603	26.564	-79.767	-29.7
01/02/99	07:29:30.998327844	26.568	-79.762	-22.0
01/02/99	07:29:43.031265076	26.806	-80.059	-153.3
01/02/99	07:32:11.120253847	26.843	-80.083	-31.6
01/02/99	07:32:11.538763500	26.946	-80.014	-69.9
01/02/99	07:45:37.826763664	26.591	-79.695	-62.9
01/02/99	08:10:39.636999700	26.836	-80.068	-31.4
01/02/99	08:13:25.897532968	26.722	-80.187	-20.3
01/02/99	08:18:35.620962616	26.688	-80.241	-18.9

Table A-3. Sample flash grouping output file

Julian Day	Hour	Minute	Second	Microsecond	X	Y	Z	Flash Number	Branch Number	Index Number	Parent Number	Line Number
32	16	46	0	642800	-54489	81647	14029	1	0	0	0	5
32	16	46	0	698140	-48241	79387	12004	1	1	1	5	6
32	16	46	0	707970	-49989	80187	7345	1	1	2	0	7
32	16	46	0	725827	-46354	73375	8442	1	2	1	6	8
32	16	46	0	727112	-49137	77538	9980	1	3	1	6	9
32	16	46	1	381000	-50487	73725	10380	-1	0	0	0	10
32	16	51	0	346185	-52062	77627	9714	-1	0	0	0	11
32	16	51	0	392439	-55576	68629	10299	-1	0	0	0	12
32	16	51	0	401888	-62587	71315	12509	-1	1	1	0	13
32	17	4	0	950589	-26190	82420	10022	-1	0	0	0	14
32	17	6	32	365355	3060	142730	4827	-1	0	0	0	15
32	17	20	1	176017	-18313	78768	9548	-1	0	0	0	16
32	17	20	1	275651	-31536	60737	4206	-1	0	0	0	17
32	17	20	1	297994	-27169	82801	10581	-1	0	0	0	18
32	17	21	23	112163	5369	72	8948	2	0	0	0	19
32	17	21	23	445890	5424	-4	8960	2	1	1	19	20
32	17	21	23	556483	5353	-25	8878	2	2	1	20	21
32	17	21	23	556825	5428	-28	8960	2	2	2	0	22
32	17	21	23	635623	5436	-50	8937	2	3	1	2	23
32	17	21	23	670822	5427	-42	8906	2	4	1	23	24
32	17	21	23	674343	5371	-119	9011	2	4	2	0	25
32	17	21	23	843822	5469	-92	8961	2	5	1	23	26
32	17	21	24	177474	5511	-188	8967	2	6	1	26	27
32	17	21	24	658336	5565	-268	8949	2	7	1	27	28
32	17	21	24	784659	5632	-302	8954	2	8	1	28	29
32	17	21	24	871531	5585	-334	8917	2	9	1	29	30
32	17	21	25	74758	5606	-382	8921	2	10	1	30	31
32	17	21	25	151808	5631	-391	8947	2	11	1	31	32
32	17	21	25	204674	5622	-396	8918	2	12	1	31	33
32	17	21	25	238417	5638	-405	8940	2	13	1	32	34
32	17	21	25	329487	5673	-424	9107	2	14	1	32	35
32	17	21	25	381120	5655	-439	8939	2	15	1	34	36
32	17	21	25	419328	5667	-447	8959	2	16	1	36	37
32	17	21	25	457338	5659	-456	8937	2	17	1	36	38
32	17	21	25	523703	5681	-465	8949	2	18	1	37	39
32	17	21	25	563238	5692	-476	8962	2	19	1	39	40
32	17	21	25	594250	5680	-491	8938	2	20	1	39	41
32	17	21	25	632385	5680	-486	8918	2	21	1	41	42
32	17	21	25	648723	5702	-497	8969	2	21	2	0	43
32	17	21	25	709328	5692	-513	8959	2	22	1	43	44
32	17	21	25	710436	5713	-515	8983	2	22	2	0	45
32	17	21	25	726753	5694	-524	8923	2	22	3	0	46
32	17	21	25	775500	5700	-522	8932	2	23	1	46	47
32	17	21	25	776837	5707	-523	8948	2	23	2	0	48
32	17	21	25	877143	5698	-554	8922	2	24	1	46	49
32	17	21	25	992840	5735	-571	8941	2	25	1	49	50
32	17	21	26	34530	5733	-591	8929	2	26	1	50	51
32	17	21	26	34722	5740	-578	8944	2	26	2	0	52
32	17	21	26	67873	5739	-588	8938	2	27	1	51	53
32	17	21	26	110894	5758	-605	8975	2	28	1	52	54
32	17	21	26	138111	5749	-612	8926	3	0	0	0	55
32	17	21	26	154466	5755	-614	8954	3	1	1	55	56
32	17	21	26	221254	5755	-623	8936	3	2	1	55	57
32	17	21	26	221420	5757	-629	8925	3	2	2	0	58
32	17	21	26	262631	5761	-639	8921	3	3	1	58	59
32	17	21	26	320193	5783	-643	8971	3	4	1	56	60
32	17	21	26	371276	5785	-663	8961	3	5	1	60	61
32	17	21	26	384887	5784	-659	8953	3	5	2	0	62

Table A-4. A portion of the dist199812.txt output file

Month	Day	Year	Hour	Minute	Second	Nanosecond	Latitude	Longitude	Peak Current	IDAR Flash	X	Y	Z	Horizontal Distance	Three Dimensional Distance	Quadrant	Branch Number
12	2	98	0	6	0	82276273	29.01	-80.282	-8.8	2	39553	56586	5435	5873.93	8002.64	3	7
12	2	98	1	47	52	213257231	29.325	-80.457	13.4	6	23179	89897	7008	5514.58	8917.55	3	14
12	2	98	1	51	47	750238338	29.357	-80.45	9.9	8	20296	86300	6639	4829.73	8209.91	2	7
12	13	98	19	48	34	76119636	28.904	-81.536	8.5	180	-75872	41767	8496	11845.95	14577.67	3	45
12	13	98	19	55	49	680866295	28.973	-81.461	-9.7	198	-71101	45112	7071	9723.35	12022.58	2	11
12	13	98	20	6	52	436678351	28.855	-81.442	2.8	216	-67930	38626	7623	11059.78	13432.38	3	90
12	13	98	20	17	39	451128511	28.94	-81.382	-24.7	231	-64054	39207	5586	10058.11	11505.17	2	3
12	13	98	20	29	53	516264343	29.321	-80.931	-22.9	256	-30788	80299	9072	7104.3	11522.68	1	33
12	13	98	20	35	38	344702921	29.278	-80.926	6.7	267	-26392	76650	8137	5682.65	9924.88	2	36
12	13	98	20	39	20	46385705	29.319	-80.886	5.6	277	-19283	69462	9091	17849.35	20031.11	2	63
12	13	98	20	39	20	852972114	29.348	-80.773	-49.5	277	-19283	69462	9091	21494.17	23337.64	1	63
12	13	98	20	39	20	909061259	29.386	-80.733	-16.8	277	-19283	69462	9091	26823.1	28321.81	1	63
12	13	98	20	39	20	955349330	29.387	-80.734	-10.4	277	-19283	69462	9091	26887.44	28382.76	1	63
12	13	98	20	46	36	324061848	29.298	-80.787	-60.9	292	-11433	75014	5320	9750.27	11107.22	2	8
12	13	98	20	46	36	345332265	29.303	-80.773	-19.2	292	-11433	75014	5320	10013.41	11338.91	2	8
12	13	98	20	46	36	395790324	29.293	-80.762	-19.8	292	-11433	75014	5320	8818.02	10298.54	2	8
12	13	98	20	46	36	415838653	29.31	-80.783	-10.7	292	-11433	75014	5320	10948.47	12172.57	2	8
12	13	98	20	49	25	745044025	29.321	-80.816	-15.6	298	-16154	72390	7902	14573.23	16577.71	2	62
12	13	98	20	49	25	868338800	29.317	-80.802	-44.1	298	-16154	72390	7902	14116.5	16177.67	1	62
12	13	98	21	0	32	88172901	29.377	-80.677	-52.6	314	-10001	88935	8093	7899.16	11309	1	62
12	13	98	21	0	32	146904810	29.385	-80.679	-31	314	-10001	88935	8093	8253.67	11559.4	1	62
12	13	98	21	0	32	180463385	29.396	-80.669	-10.9	314	-10001	88935	8093	9788.18	12700.59	1	62
12	13	98	21	1	1	873689471	29.39	-80.742	-7.9	315	-8825	91241	4894	3480.64	6005.51	2	5
12	13	98	21	1	1	929204953	29.404	-80.755	-18.4	315	-8825	91241	4894	5375.47	7269.59	2	5
12	13	98	21	1	2	13941610	29.394	-80.72	-9.1	315	-8825	91241	4894	4018.46	6332.4	1	5
12	13	98	21	2	11	147453331	29.37	-80.665	-25.2	317	-2628	88314	5057	4099.07	6509.66	1	5
12	13	98	21	2	11	229851547	29.354	-80.68	-25.8	317	-2628	88314	5057	2499.71	5641.08	2	5
12	13	98	21	2	11	314901986	29.372	-80.664	-18	317	-2628	88314	5057	4331.7	6658.59	1	5
12	13	98	21	2	11	388901745	29.37	-80.665	-18.5	317	-2628	88314	5057	4099.07	6509.66	1	5
12	13	98	21	2	57	5646957	29.405	-80.648	-41	318	7344	1E+05	9136	12704.86	15648.64	3	89
12	13	98	21	2	57	27069427	29.409	-80.658	-14.1	318	7344	1E+05	9136	13001.32	15890.27	3	89
12	13	98	21	2	57	45724074	29.41	-80.659	-7.9	318	7344	1E+05	9136	12986.92	15878.49	3	89
12	13	98	21	2	57	103939434	29.409	-80.653	-21.3	318	7344	1E+05	9136	12674.13	15623.7	3	89
12	13	98	21	2	57	158300697	29.409	-80.659	-15.4	318	7344	1E+05	9136	13067.98	15944.86	3	89
12	13	98	21	2	57	206196013	29.409	-80.655	-22.8	318	7344	1E+05	9136	12803.75	15729.04	3	89
12	13	98	21	4	1	539614857	29.402	-80.704	-25.2	320	-1304	86703	5941	10353.69	11937.1	2	40
12	13	98	21	4	1	597775058	29.402	-80.701	-22.6	320	-1304	86703	5941	10223.82	11824.63	2	40
12	13	98	21	4	48	753902473	29.386	-80.674	-24.4	321	-2668	85494	6004	8676.69	10551.44	2	6
12	13	98	21	5	47	369486442	29.389	-80.65	-18.7	323	89	91572	3401	3023.21	4550.45	2	29
12	13	98	21	5	47	403437982	29.391	-80.65	-8.8	323	89	91572	3401	3238.77	4696.43	2	29
12	13	98	21	8	22	949125976	29.408	-80.62	-8.4	329	-3340	91671	3060	7470.79	8073.18	1	6
12	13	98	21	8	23	24985222	29.407	-80.624	-16.6	329	-3340	91671	3060	7104.86	7735.8	1	6
12	13	98	21	8	23	210938524	29.407	-80.626	-19.4	329	-3340	91671	3060	6962.1	7604.89	1	6
12	13	98	21	8	23	321918773	29.406	-80.621	-18.4	329	-3340	91671	3060	7250.94	7870.18	1	6
12	13	98	21	9	46	92105769	29.376	-80.51	15.1	331	9068	62027	6722	6562.45	10053.32	1	12
12	13	98	21	10	31	406622208	29.403	-80.592	-69.2	333	8616	90523	7164	6597.65	9739.2	2	2
12	13	98	21	10	31	421306203	29.414	-80.599	-16.1	333	8616	90523	7164	7997.24	10736.8	2	2
12	13	98	21	10	31	443826780	29.418	-80.601	-15.1	333	8616	90523	7164	8477.95	11099.48	2	2
12	13	98	21	10	31	464349709	29.418	-80.603	-15.6	333	8616	90523	7164	8583.33	11180.18	2	2
12	13	98	21	10	31	489398065	29.419	-80.603	-17.5	333	8616	90523	7164	8676.83	11252.12	2	2
12	13	98	21	10	31	563624575	29.412	-80.579	-26.4	333	8616	90523	7164	6930.3	9967.55	2	2
12	13	98	21	10	31	624392802	29.423	-80.598	-14.9	333	8616	90523	7164	8810.76	11355.72	2	2
12	13	98	21	10	31	634750713	29.413	-80.581	-12.1	333	8616	90523	7164	7102.26	10087.86	2	2
12	13	98	21	10	31	704359286	29.412	-80.582	-19.1	333	8616	90523	7164	7034.46	10040.25	2	2
12	13	98	21	10	31	728268717	29.414	-80.588	-10.5	333	8616	90523	7164	7474.12	10353.04	2	2
12	13	98	21	10	31	769311186	29.419	-80.582	-41.9	333	8616	90523	7164	7761.83	10562.62	2	2
12	13	98	21	10	31	887547290	29.422	-80.601	-11.5	333	8616	90523	7164	8858.48	11392.79	2	2
12	13	98	21	12	59	4053903	29.38	-80.522	-13.7	339	10753	89521	8624	4134.12	9563.7	1	23
12	13	98	21	12	59	33160462	29.396	-80.54	-19.2	339	10753	89521	8624	5787.74	10386.11	2	23

Appendix B. IDL Program

Appendix B contains the program used to match NLDN groundstrokes with LDAR detected flashes as described in Section 3.4. The program is written in IDL.

```

; Program match2v4
;
; Version 2.4
;
; Created by Capt Todd McNamara
;
; AFIT ENP/GM-02
;
; This program uses one month of NLDN data. It looks at each NLDN ground stroke
; within a specified distance of the LDAR system and determines which LDAR flash
; created the ground stroke. Possible flashes that produced the ground stroke are extracted
; using time (timedev) and distance (distdev) criteria which can be changed by the user.
; From the flashes that may have caused the ground stroke, the flash with the closest ldar
; point is chosen as the flash that caused the ground stroke. Four output files are
; generated: One with the NLDN strike point data, LDAR flash origin point information,
; the horizontal/three-dimensional distance between the origin point and nldn stroke
; location, the quadrant that the nldn stroke point occurred with respect to LDAR flash
; origin, and the max number of branches within the flash. These files are named as such
; "distyyyymm.txt" where yyyy is the year and mm is the month. The second output file
; provides a list of every NLDN ground stroke that occurred within the specific distance of
; LDAR. This file is used to ensure that the program completed running through the
; entire dataset and provides the total run time for that month. The third output file
; provides statistical information on the total number of NLDN strokes within the
; specified distance of LDAR, the number of NLDN strokes that was matched with an
; LDAR flash, the percentage of NLDN strokes matched with an LDAR flash, and a
; count of the total number of NLDN strokes that were not matched that occurred within
; 20 n mi, 20 - 60 n mi, and greater than 60 n mi from LDAR. The last output file is a list
; of the distances from the ground stroke location to the closest point in the matched
; LDAR flash.

```

```

; To run the program, the user must pass the month of LDAR data only. The program will
; automatically go to the appropriate subdirectory for the LDAR file.
;
;
;

```

```

; Summary of Revisions:
; Version      Date          Changes
; =====
; 2.0          27 Aug 01     Initial program
; 2.1          26 Oct 01     Add max brannum to output
; 2.2          30 Oct 01     Revised to print output in
;              a "track" file
; 2.3          05 Nov 01     Changed to read binary files/
;              print distance of closest LDAR
;              point to grnd stroke
; 2.4          08 Nov 01     Changed to only include NLDN data
;              within a variable named max_dist
; =====
; nldn_struct definition. This structure will hold monthly nldn data files.
; =====

```

```

FUNCTION nldn_struct
    nldnline = {nldnline, month:0, $
                day:0, $
                year:0, $
                hour:0, $
                minute:0, $
                second:0, $
                nanosecond:0L,$
                lat:0.0, $
                long:0.0, $
                current:0.0, $
                multi:0}
    RETURN, nldnline
END

```

```

=====
;
; ldar_struct definition. This structure will hold daily LDAR files.
;
=====

```

```

FUNCTION ldar_struct
    ldarline = {ldarline, day:0, $
                hour:0, $
                minute:0, $
                second:0, $
                microsec:0L, $
                x:0L, $
                y:0L, $
                z:0L, $
                flashnum:0L, $
                branchnum:0L, $
                index:0L, $
                parent:0L, $
                linenum:0L}
    RETURN, ldarline
END

```

pro match2v4, filename

```

close,/all          ; Ensure all files are closed
time = systime(1)   ; Start timer

```

```

=====
;
; Define format statements for reading/printing data.
;
=====

```

```

;format1 is for reading/printing NLDN data in original NLDN data
;format2 is for reading/printing flash group data in original format
;format3 is for printing NLDN/LDAR match to output file
format1='(I2, 1x, I2, 1x, I2, 1x, I2, 1x, I2, 1x, I2, 1x, I9, 1x, F7.3, 1x, F8.3, 1x, F7.1, 1x, I3)'
```

```

format2='(I2, 1x, I2, 1x, I2, 1x, I2, 1x, I6, 1x, I9, 2x, I8, 2x, I8, 1x, I7, 1x, I7, 1x, I7, 1x, I7, 1x, I7)'
```

```
format3=(I2, 1x, I2, 1x, I2, 1x, I2, 1x, I2, 1x, I2, 1x, I9, 1x, F7.4, 1x, F8.4, 1x, F8.1, 1x, I9, 1x, I8,
1x, I8, 1x, I5, 1x, F11.2, 1x, F11.2, 1x, I1)'
format3=(I2, 1x, I2, 1x, I2, 1x, I2, 1x, I2, 1x, I2, 1x, I9, 1x, F7.4, 1x, F8.4, 1x, F8.1, 1x, I9, 1x, I8,
1x, I8, 1x, I5, 1x, F11.2, 1x, F11.2, 1x, I1, 1x, I6)'
```

```
=====
;
; Define constants used in the program.
=====
;
latconv=60.00*1852.0      ;converts degrees latitude to meters
longconv=53.01*1852.0    ;converts degrees longitude to meters
ldarlat=28.5386          ;latitude of ldar central site
ldarlong=-80.6431       ;longitude of ldar central site
timedev1=1000000000     ;time deviation criteria for matching nldn
                        ;Ground strokes to ldar flashes (in nanoseconds)
dusted=50000.0          ;spatial criteria (meters) for matching
                        ;nldn ground strokes to ldar flashes
max_ldar=10000          ;number of ldar lines read at one time
nldn_lines=0            ;variable to hold number of lines in nldn file
m=0                    ;variable to hold number of lines in ldar file
s=' '                  ;string variable for reading in nldn lines
output_check='start'    ;flag for opening output files
prev_leftovers=0        ;initialization of variable that holds the number
                        ;of data points associated with the last chunk
                        ;of ldar data read
leftovers=0            ;initialize variable
Num_of_misses=0D        ;initialization of variable that holds number of
                        ;nldn strokes not matched to ldar flash for each
                        ;pass
Num_of_match=0D         ;initialization of variable that holds number of
                        ;nldn strokes matched with an ldar flash for each
                        ;pass
Tot_misses=0D           ;initialization of variable that holds the total
                        ;number of nldn strokes not matched to ldar flash
Tot_match=0D            ;initialization of variable that holds the total
                        ;number of nldn strokes matched with an ldar flash
close_miss=0D           ;initialization of variable that counts the number
                        ;of nldn strokes not matched with ldar flash and
                        ;occurred within 20 n mi of ldar
Tot_close_miss=0D      ;initialization of variable that has total count
                        ;the number of nldn strokes not matched with ldar
                        ;flash and occurred within 20 n mi of ldar
medium_miss=0D          ;initialization of variable that counts the number
                        ;of nldn strokes not matched with ldar flash and
                        ;occurred within 20 n mi and 60 n mi of ldar
Tot_medium_miss=0D     ;initialization of variable that has total number
                        ;of nldn strokes not matched with ldar flash and
                        ;occurred within 20 n mi and 60 n mi of ldar
far_miss=0D            ;initialization of variable that counts the number
                        ;of nldn strokes not matched with ldar flash and
                        ;occurred within further than 60 n mi of ldar
```

```
Tot_far_miss=0D           ;initialization of variable that has total number
                           ;of nldn strokes not matched with ldar flash and
                           ;occurred further than 60 n mi of ldar
max_dist=100000          ;distance (in meters) of ground strikes to process
                           ;from the ldar site
```

```
=====
;Open NLDN day and count lines
;=====
```

```
;build nldn file to open
path = '/home/fujita7/mcnamara/stroke_data/'
filename1 = path+filename
```

```
;open the file
openr, nldninput, filename1, /get_lun
```

```
;find total number of nldn lines
y=fstat(nldninput)
nldn_lines=y.size/56L
```

```
;echo number of lines to the screen
print, "num of nldn lines", nldn_lines
```

```
;reset pointer
point_lun, nldninput, 0
```

```
;read nldn data
line = nldn_struct()      ;call structure
nldndata = replicate(line, nldn_lines)
readf, nldninput, nldndata, FORMAT=format1
```

```
;close file and free lun
close, nldninput
free_lun, nldninput
```

```
;convert latitudes and longitudes to meters
lat_dist=(nldndata.lat-ldarlat)*latconv
long_dist=(nldndata.long-ldarlong)*longconv
```

```
;compute stroke distances away from ldar
hypot=sqrt((lat_dist)^2+(long_dist)^2)
```

```
;keep those strokes with max_dist
keep3=where(hypot LE max_dist, nldn_flashes)
```

```
;echo number of lines to the screen
print, "num of nldn lines", nldn_flashes
```

```
;continue processing if there are ground strokes within max_dist
if (nldn_flashes GT 0) then begin
```

```

;save ground strokes within max_dist to array
    nldndata=nldndata[keep3]

;save latitude and longitude distances for the ground strokes within max_dist to new arrays
    lat_dist=lat_dist[keep3]
    long_dist=long_dist[keep3]

=====
;
;Loop through all days of nldn data
=====
;
;loop through every day of a month
for nldnloop = 1, 31 do begin    ;NLDN day loop

;get strokes that occur within the day
    keep = where(nldndata.day EQ nldnloop, count)

;continue processing if there are nldn strokes for day "nldnloop" to match with ldar data
    if (count GT 0) then begin

;if there are strokes in that day, save them to array named day_of_NLDN
    day_of_NLDN = nldndata[keep]

;compute time in nanoseconds for each strike
    nldntime=(day_of_NLDN.hour*60LL*60LL*10LL^9LL)+$
        (day_of_NLDN.minute*60LL*10LL^9LL)+(day_of_NLDN.second*10LL^9LL)$
        +(day_of_NLDN.nanosecond)

;construct year and number array used to construct file variables
    year = 2000+nldndata[nldnloop].year-100*(nldndata[nldnloop].year GT 80)
    num = strcompress(sindgen(100), /remove_all)
    num[0:9] = '0'+num[0:9]

;build ldar file name that will hold the ldar file in ascii
    ldarfile = '/home/fujita7/mcnamara/flash_grouping/ldar'+strcompress(string(year)$
        ,/remove_all)+num[day_of_NLDN[0].month]+num[day_of_NLDN[0].day]+' .txt'

;build ldar file name of the ldar file in binary format
    filename = '/home/fujita11/ldar/ldar'+strcompress(string(year), /remove_all)+$
        num[day_of_NLDN[0].month]+num[day_of_NLDN[0].day]+' .bin'

=====
;
;Build and open output files
=====
;
    if (output_check EQ "start" ) then begin

;construct filenames for output files

```

```

close_pt='/home/fujita7/mcnamara/close_pt/2pt_dist'+strcompress(string $
(year),/remove_all)+num[nldndata[0].month]+'.txt'

flashoutput='/home/fujita7/mcnamara/ashes/dist'+strcompress(string $
(year), /remove_all)+num[nldndata[0].month]+'.txt'

trackfile='/home/fujita7/mcnamara/track/'+strcompress(string(year), $
/remove_all)+ num[nldndata[0].month]+'.txt'

statfile='/home/fujita7/mcnamara/track/2stat'+strcompress(string(year), $
/remove_all)+num[nldndata[0].month]+'.txt'

;open output files
openw, output1, flashoutput, /get_lun
openw, output2, close_pt, /get_lun
openw, output3, trackfile, /append, /get_lun
openw, output4, statfile, /get_lun
output_check=string(nldndata[0].month) ;sets flag to not open files on next pass

;close output file for distances (it will be reopened every time a line of data is to be
;appended to it)
close, output1
free_lun, output1

endif

=====
; Open LDAR file and read in file
=====

;Check to see if there are ldar files corresponding to the day and month of NLDN data
result = findfile(filename, count=num_ldar_file)

;if there is a corresponding month of ldar data, continue
if (num_ldar_file GT 0) then begin

;convert binary ldar data file into ascii format
ldar_ascii, filename, path='/home/fujita7/mcnamara/flash_grouping/'

;open appropriate ldar file
openr, ldarinput, ldarfile, /get_lun

;print to output file which ldar file was opened
printf, output3, "opened", ldarfile

;find number of lines of the ldar file
x=fstat(ldarinput)
ldar_lines=x.size/90L

```

```

;find number of passes (based on the number of ldar lines to be read at one time) through ;ldar data
    num_passes=ceil(float(ldar_lines)/float(max_ldar))
    remainder=ldar_lines mod max_ldar

=====
;Loop through LDAR file
=====
;loop through the number of passes until all of the ldar file is read and checked for ground
;stroke matches
    for i = 1L, num_passes do begin ; loop through ldar day

;determine array size for the ldar pass
        if (i LT num_passes) then begin
            ldar_lines_needed=max_ldar

        endif else begin
            ldar_lines_needed=remainder
        endelse

;read ldar data
        lines=ldar_struct() ;call ldar structure
        ldardata = replicate(lines, ldar_lines_needed)
        readf, ldarinput, ldardata

;append the last flash from the previous chunk of ldar data read to the current chunk of
;ldar data read
        if (i GT 1) then ldardata=[keep_last_flash, ldardata]

;extract the last flash from every ldar data chunk read in so that it is appended to the next
;chunk of ldar data read
        if (i LT num_passes) then begin
            last_flash=where(ldardata.flashnum EQ max(ldardata.flashnum), $
            leftovers)
            keep_last_flash=ldardata[last_flash]
        endif

;compute total number of lines in the ldardata array
        if (i GT 1) then begin
            total_ldar_lines=ldar_lines_needed+prev_leftovers
        endif else begin
            total_ldar_lines=ldar_lines_needed
        endelse

;compute time in nanoseconds for all ldar data in ldardata array
        ldartimes=((ldardata.hour*60LL*60LL*10LL^6LL)+ $
        (ldardata.minute*60LL*10LL^6LL)$
        (ldardata.second*10LL^6LL)+(ldardata.microsec))*1000

```

```

;find time of 1st and last line of data in ldardata array
    first_ldar_time=ldartimes[0]
    last_ldar_time=ldartimes[total_ldar_lines-1]

;change variable to append last flash to next ldardata array
    prev_leftovers=leftovers

;extract all nldn points within the ldar data's start and finish time
    keep1 = where((nldntime GE first_ldar_time) AND $
    (nldntime LE last_ldar_time), nldnlines)

;continue processing nldn strokes within the 1st and last times of the ldar data
    if (nldnlines GT 0) then begin

;save these ground strokes into an array named nldn_subset
    nldn_subset=day_of_NLDN[keep1]

;save the corresponding times of these ground strokes into an array named ;nldntime_subset
    nldntime_subset=nldntime[keep1]

;convert nldn ground stroke locations from latitude and longitude into meters from the ;ldar central
site
    latmeters=(nldn_subset.lat-ldarlat)*latconv
    longmeters=(nldn_subset.long-ldarlong)*longconv

;initialize variables and construct array to hold match flags
    close_miss=0
    medium_miss=0
    far_miss=0
    strike_track=intarr(nldnlines)

;=====
;Loop through each nldn stroke in nldn_subset
;=====

;loop through each nldn ground stroke to find the flash that created it
    for j=0L, nldnlines-1 do begin

;Extract all ldar data points within a time and distance criteria set by the user
    keep2 = where((ldartimes GE nldntime_subset[j]- $
    timedev1)AND (ldartimes LE $
    nldntime_subset[j]+timedev2) $ AND (ldardata.x$ LT
    longmeters[j]+distdev) AND $ (ldardata.x GT $
    longmeters[j]-$ distdev) AND $ (ldardata.y LT $
    latmeters[j]+distdev) AND $
    (ldardata.y GT latmeters[j]-distdev) AND $
    (ldardata.flashnum NE -1), num_of_ldar_lines)

;continue to process as long as there are data points within temporal and spatial

```

```

;constraints
                                if (num_of_ldar_lines GT 0) then begin

;open output file for appending the appropriate flash data
                                openw, output1, flashoutput, /append, $
                                /get_lun

;keep all data points meeting criteria in an array named ldar_subset
                                ldar_subset=ldardata[keep2]

;change the flag in the strike_array to a 1 to indicate a match was made
                                strike_track[j]=1

;construct array to hold distances of all the points that met the temporal and spatial ;criteria
                                dist=fltarr(num_of_ldar_lines)
                                dist1=fltarr(num_of_ldar_lines)

;=====
;Find distance from nldn stroke
;=====

;compute all distance from stroke location to ldar data points
                                for k=0L, num_of_ldar_lines-1 do begin
                                    dist[k]=sqrt((ldar_subset[k].x-$
                                        longmeters[j])^2+(ldar_subset[k].y-$
                                        latmeters[j])^2+(ldar_subset[k].z)^2)

                                    dist1[k]=sqrt((ldar_subset[k].x-$
                                        longmeters[j])^2+(ldar_subset[k].y-$
                                        latmeters[j])^2)
                                endfor

;find closest ldar data point to ndln stroke
                                closest_flash=min(where(dist EQ $
                                    min(dist)))

;find flash number of closest ldar data point
                                flash_num=ldar_subset[closest_flash].flashnum

;extract all data points for the flash associated with the ground stroke
                                pt=where((ldardata.flashnum EQ $
                                    flash_num))
                                tot_flash=ldardata[pt]

;find the origin point of the flash associated with the ground stroke

```

```

originpt=where(tot_flash.linenum EQ $
min(tot_flash.linenum

;extract the number of branches of this flash
num_branches=max(tot_flash.branchnum)

;compute horizontal distance from stroke and origin point of the flash
horizontaldist=sqrt((tot_flash[originpt].x- $
longmeters[j])^2+ $
(tot_flash[originpt].y-latmeters[j])^2)

;compute three-dimensional distance from stroke and origin point of the flash
threeddist=sqrt((tot_flash[originpt].x- $
longmeters[j])^2+ (tot_flash[originpt].y- $
latmeters[j])^2+(tot_flash[originpt].z)^2)

;determine the quadrant that the flash occurred
quadrant=1
if (longmeters[j] LT tot_flash[originpt].x) $
and (latmeters[j] GT tot_flash[originpt].y) $
then begin
    quadrant=2
endif
if (longmeters[j] LT tot_flash[originpt].x) $
and (latmeters[j] LT tot_flash[originpt].y) $
then begin
    quadrant=3
endif
if (longmeters[j] GT tot_flash[originpt].x) $
and (latmeters[j] LT tot_flash[originpt].y) $
then begin
    quadrant=4
endif

;print pertinent data to output file

printf, output1, nldn_subset[j].month, $
nldn_subset[j].day, nldn_subset[j].year, $
nldn_subset[j].hour, $
nldn_subset[j].minute, nldn_subset[j].second, $
nldn_subset[j].nanosecond, nldn_subset[j].lat, $
nldn_subset[j].long, nldn_subset[j].current, $
ldar_subset[originpt].flashnum, $
ldar_subset[originpt].x, $
ldar_subset[originpt].y, ldar_subset[originpt].z, $
horizontaldist, threeddist, $
quadrant, num_branches, $
FORMAT=format3

;close output file containing the flash information
close, output1

```

```

                                free_lun, output1
                                endif
                                endfor

;compute statistical information on how many strokes was matched, not matched, and the
;distances of those not matched

;find strokes not matched from strike_array
                                keep4=where(strike_track EQ 0, num_misses)

;compute distances from ldar of those not matched and count them for each distance
;category
                                if (num_misses GT 0) then begin
                                dist_missed=sqrt((latmeters[keep4]^2)+(longmeters[keep4]^2))
                                for m=0L, num_misses-1 do begin
                                if (abs(dist_missed[m]) LE 20000) then begin
                                close_miss=close_miss+1
                                endif
                                if ((abs(dist_missed[m]) GT 20000) AND $
                                (abs(dist_missed[m]) LE 60000)) then begin
                                medium_miss=medium_miss+1
                                endif
                                if (abs(dist_missed[m]) GT 60000) then begin
                                far_miss=far_miss+1
                                endif
                                endif
                                endfor
                                endif

;extract all strokes that were matched to an ldar flash and count them
                                keep5=where(strike_track EQ 1, num_match)
                                Tot_misses=Tot_misses+num_misses
                                Tot_match=Tot_match+num_match
                                Tot_close_miss=Tot_close_miss+close_miss
                                Tot_medium_miss=Tot_medium_miss+medium_miss
                                Tot_far_miss=Tot_far_miss+far_miss

                                endif ; nldn within ldar time

                                endfor ; loop through ldar day
;close ldar file
                                close, ldarinput
                                free_lun, ldarinput

;delete the ldar ascii file
                                ldar_ascii, ldarfile, /delete

                                endif

                                endif

```

```

endifor

endif

;print time information to output file
printf, output3, "The program has completed the run in", (systemtime(1) - time), "seconds!"

;close the output file
close, output3
free _lun, output3

;print statistical information to appropriate file
printf, output4, "There were", Tot_match, "NLDN strokes matched to LDAR flashes", $
    Format='(A10, 1x, I7, 1x, A37)'
printf, output4, "There were", Tot_misses, "NLDN strokes not matched to an LDAR $
flash", Format='(A10, I6, 1x, A41)'
printf, output4, "The total possible NLDN matches for this month is", $
    Tot_misses+Tot_match, Format='(A49, 1x, I7)'
printf, output4, "The percentage of NLDN strokes matched were", $
    (Tot_match/(Tot_misses+Tot_match))*100, Format='(A43, 1x, F6.2)'
printf, output4, "The number of NLDN strokes not matched to an LDAR flash within 20$
km is", Tot_close_miss, Format='(A72, I4)'
printf, output4, "The number of NLDN strokes not matched to an LDAR flash within 60$
km is", Tot_medium_miss, Format='(A72, I6)'
printf, output4, "The number of NLDN strokes not matched to an LDAR flash greater $
than 100 km is", Tot_far_miss, Format='(A79, I6)'

;close the output file
close, output4
free _lun, output4

;echo to the screen that the program has finished
print, "I'm Done!"
end

```

Appendix C. Seasonal Frequency Distributions

Appendix C contains seasonal CG lightning distance frequency distributions. Each distribution represents the number of lightning strokes for each 1 n mi bin.

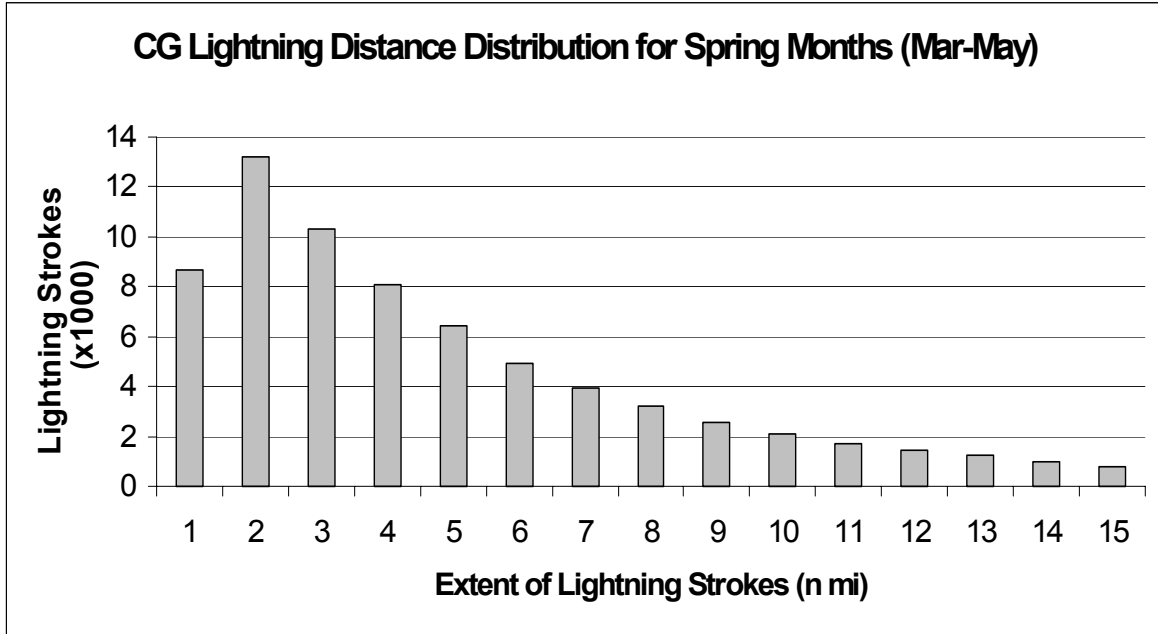


Figure C-1. Spring Lightning Stroke Frequency Distribution.

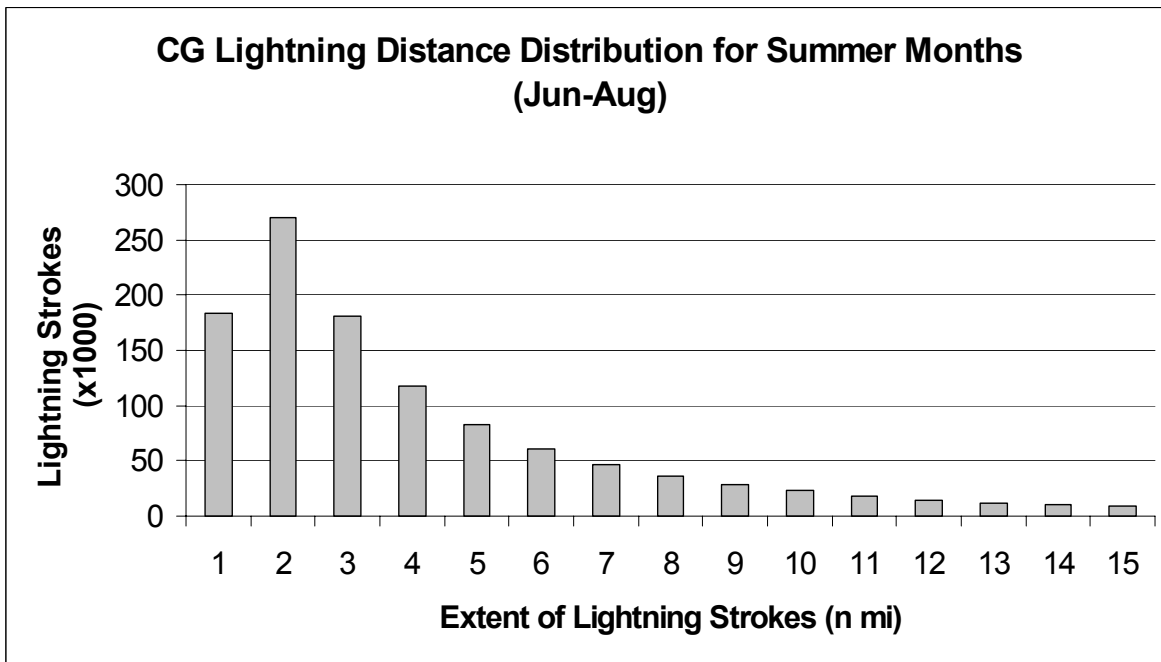


Figure C-2. Summer Lightning Stroke Frequency Distribution.

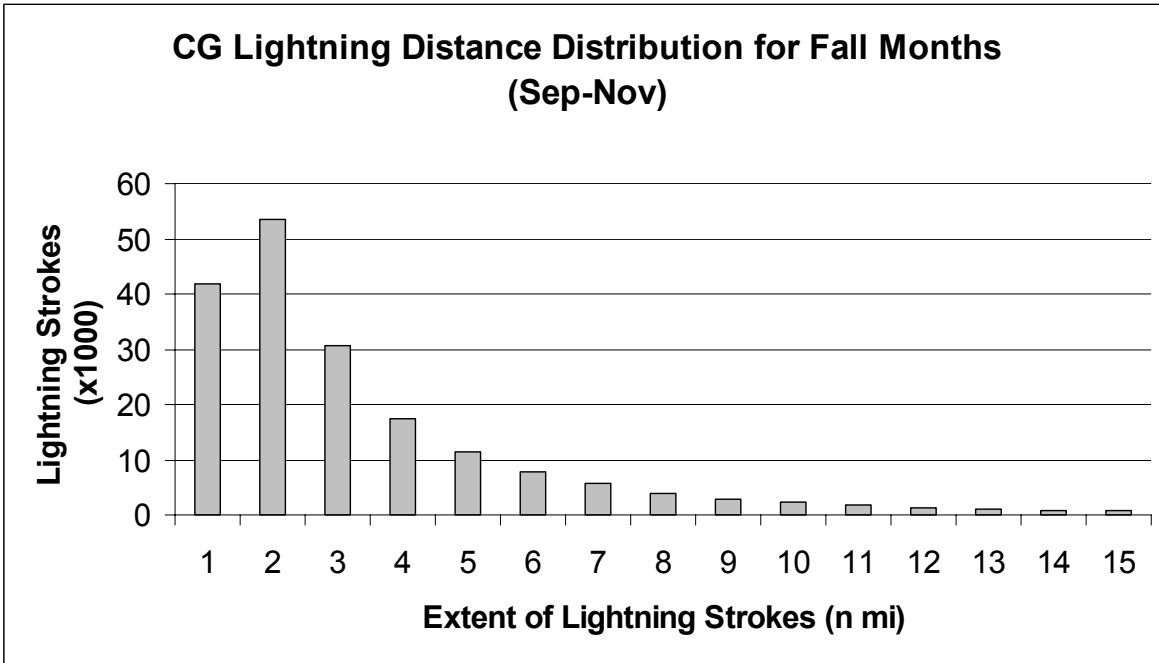


Figure C-3. Fall Lightning Stroke Frequency Distribution.

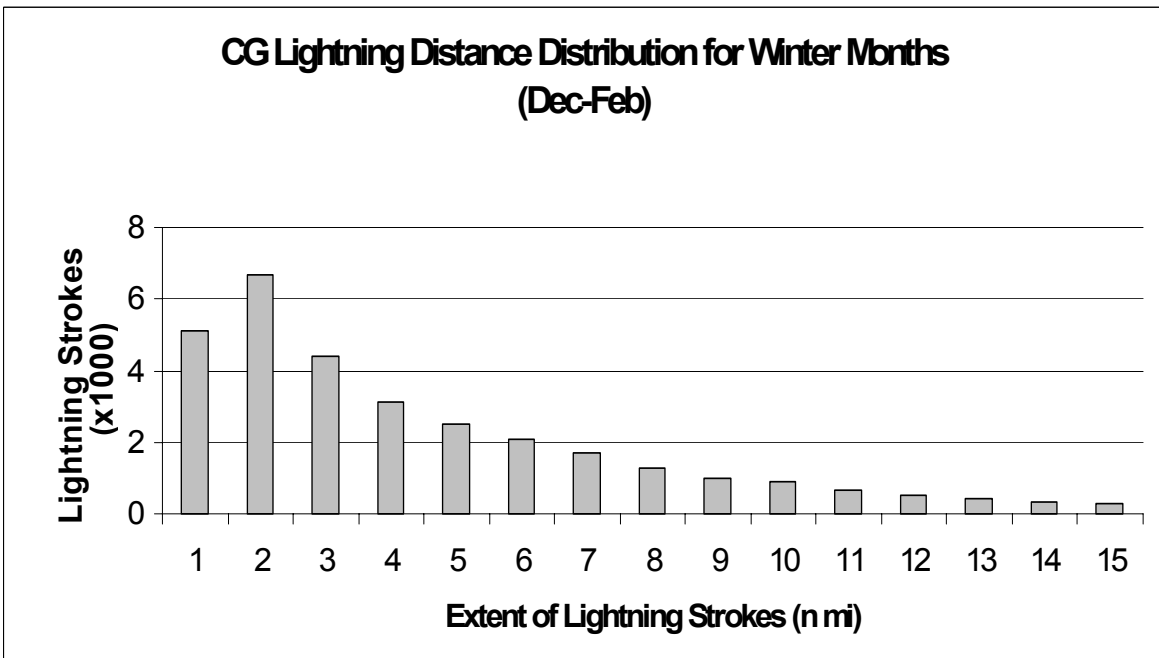


Figure C-4. Winter Lightning Stroke Frequency Distribution.

Appendix D. Seasonal Scatter Plots and Distance Versus Peak Current Diagrams

Appendix D contains seasonal scatter plots of lightning stroke distances against stroke peak currents. Graphs associating the distance a lightning stroke travels with the 95th percentile peak current value for each 0.1 n mi bin are also included.

Spring

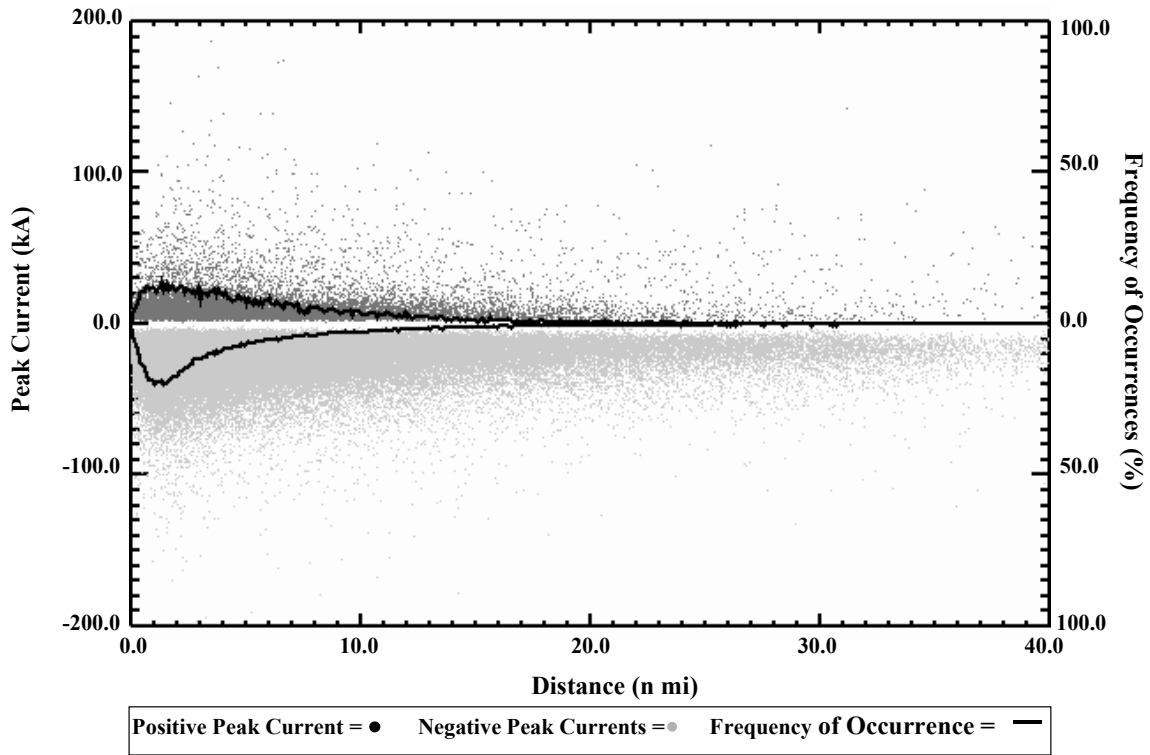


Figure D-1. Spring Scatter Plot of Distance and Peak Current. Positive peak currents are displayed in black while negative peak currents are in gray. The solid black lines (one for positive and one for negative peak currents) display the frequency of occurrence for both positive and negative currents for each 0.1 n mi bin.

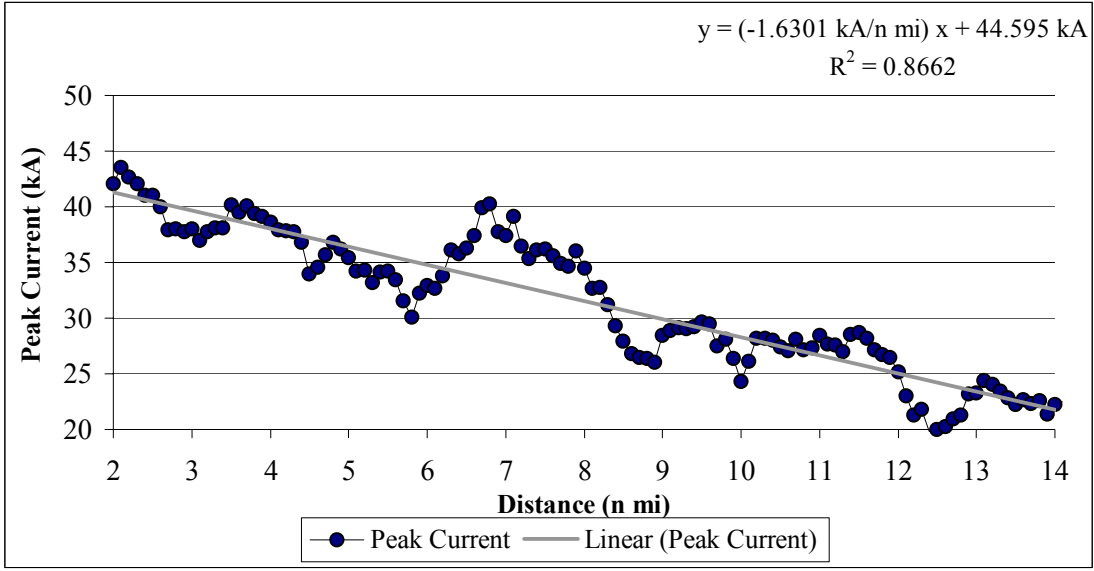


Figure D-2. Positive Peak Current as a Function of Distance for Spring Months. Data points indicate the running average of the 95th percentile positive peak current values and the solid line displays the regression line fitted using the least squares technique.

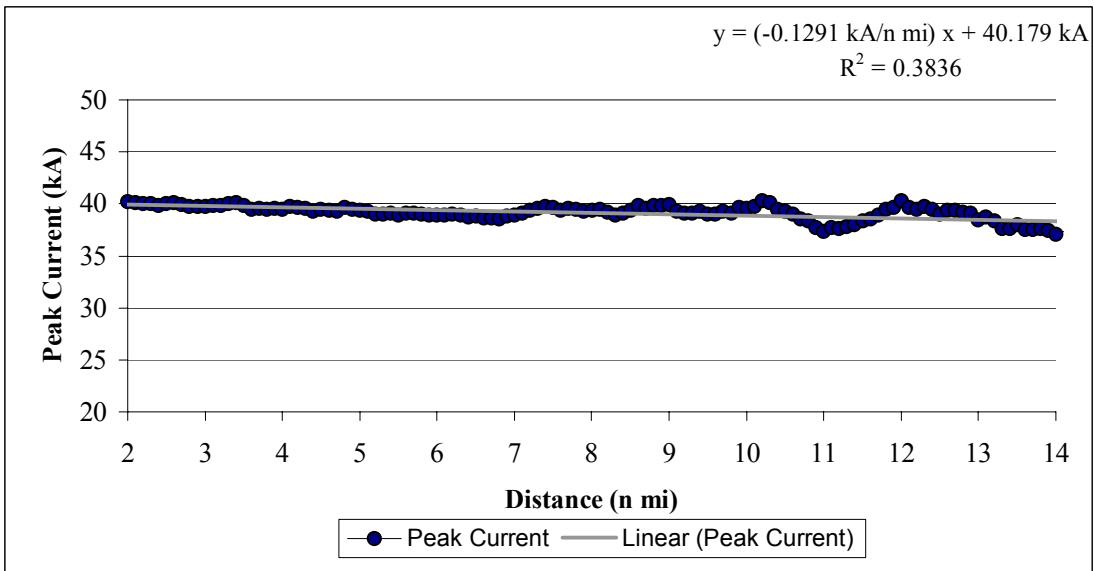


Figure D-3. Negative Peak Current as a Function of Distance for Spring Months. Data points indicate the running average of the 95th percentile negative peak current values the solid line displays the regression line fitted using the least squares technique.

Summer

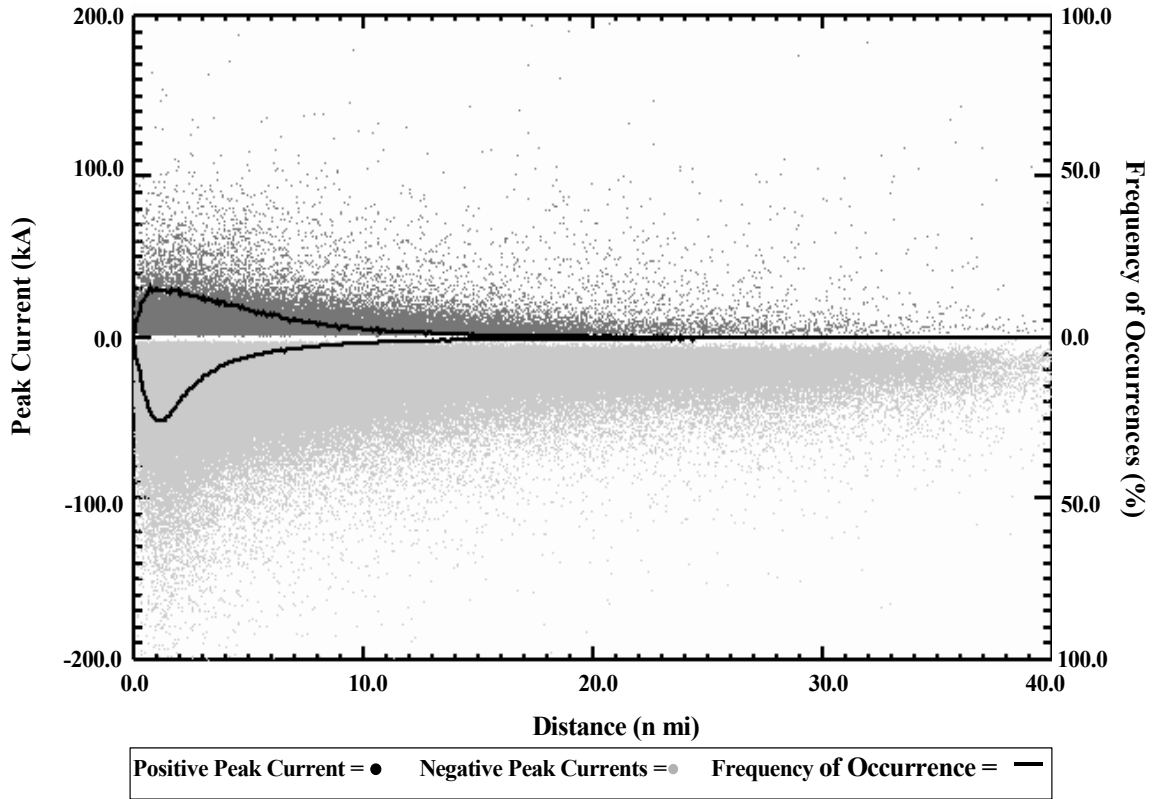


Figure D-4. Summer Scatter Plot of Distance and Peak Current. Positive peak currents are displayed in black while negative peak currents are in gray. The solid black lines (one for positive and one for negative peak currents) display the frequency of occurrence for both positive and negative currents for each 0.1 n mi bin.

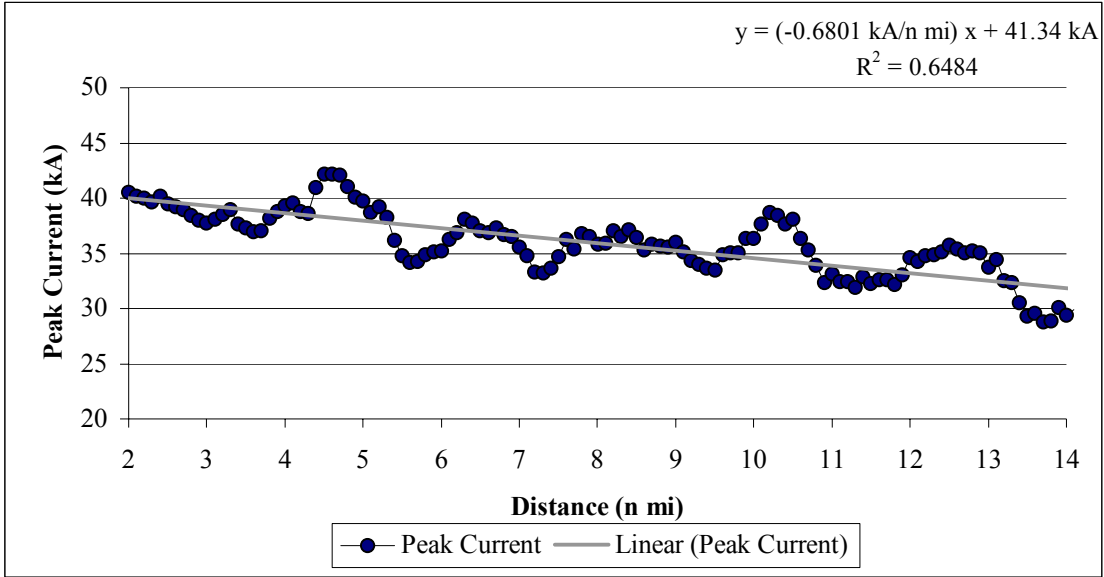


Figure D-5. Positive Peak Current as a Function of Distance for Summer Months. Data points indicate the running average of the 95th percentile positive peak current values and the solid line displays the regression line fitted using the least squares technique.

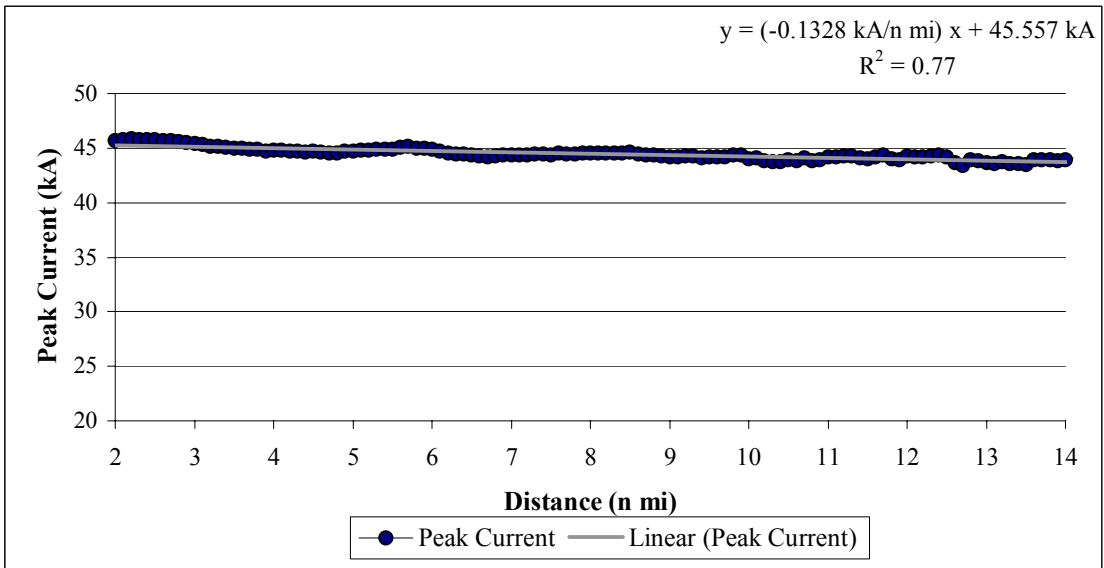


Figure D-6. Negative Peak Current as a Function of Distance for Summer Months. Data points indicate the running average of the 95th percentile negative peak current values and the solid line displays the regression line fitted using the least squares technique.

Fall

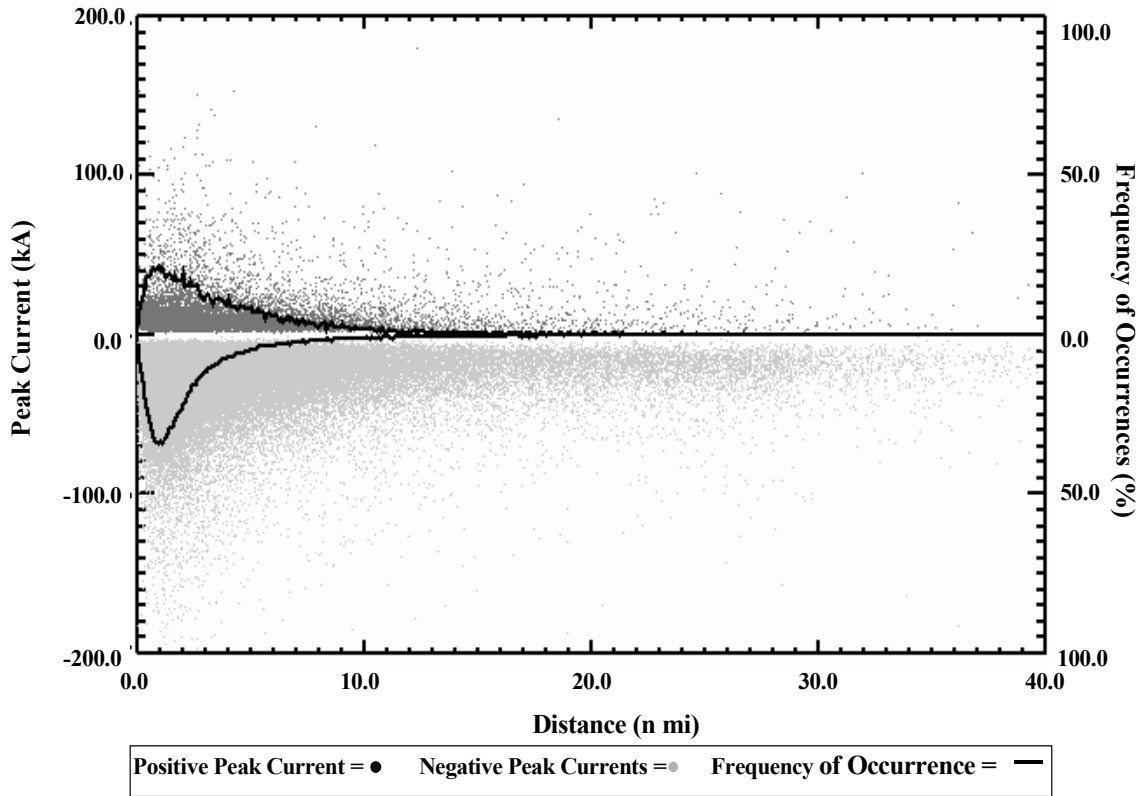


Figure D-7. Fall Scatter Plot of Distance and Peak Current. Positive peak currents are displayed in black while negative peak currents are in gray. The solid black lines (one for positive and one for negative peak currents) display the frequency of occurrence for both positive and negative currents for each 0.1 n mi bin.

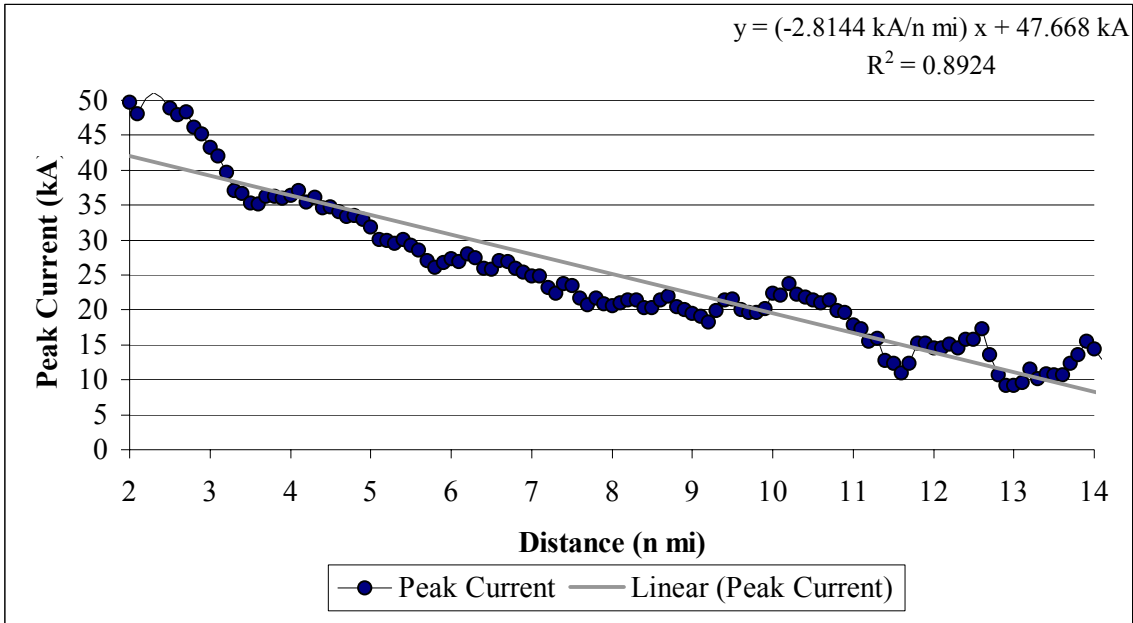


Figure D-8. Positive Peak Current as a Function of Distance for Fall Months. Data points indicate the running average of the 95th percentile positive peak current values and the solid line displays the regression line fitted using the least squares technique.

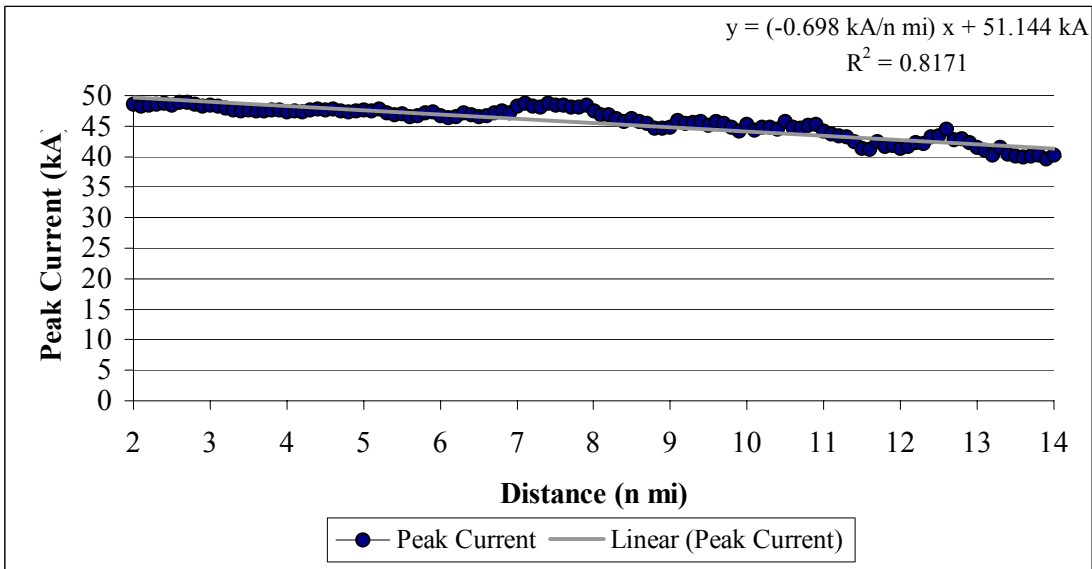


Figure D-9. Negative Peak Current as a Function of Distance for Fall Months. Data points indicate the running average of the 95th percentile negative peak current values and the solid line displays the regression line fitted using the least squares technique.

Winter

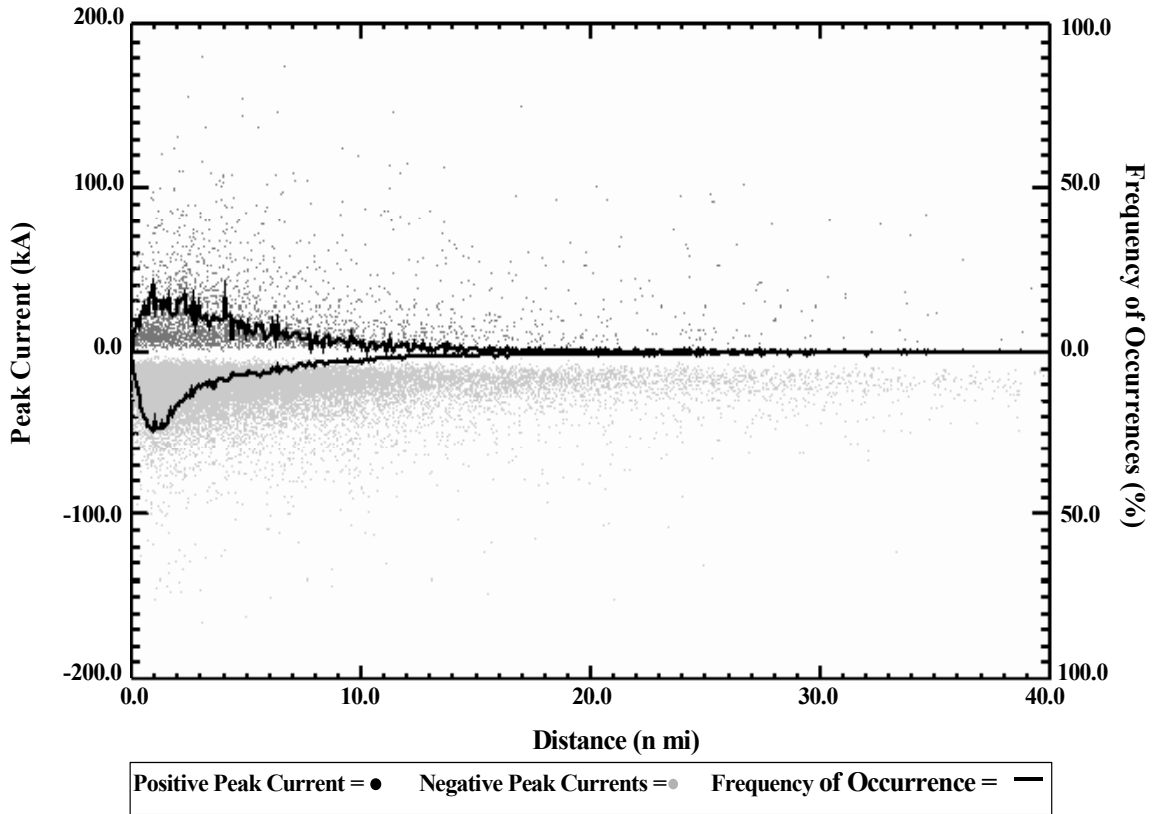


Figure D-10. Winter Scatter Plot of Distance and Peak Current. Positive peak currents are displayed in black while negative peak currents are in gray. The solid black lines (one for positive and one for negative peak currents) display the frequency of occurrence for both positive and negative currents for each 0.1 n mi bin.

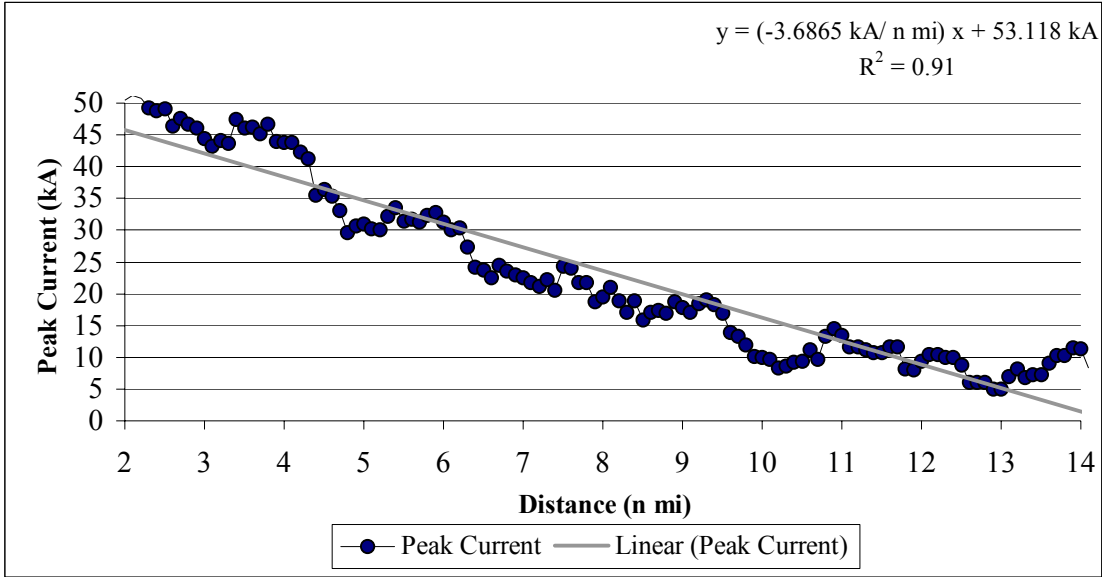


Figure D-11. Positive Peak Current as a Function of Distance for Winter Months. Data points indicate the running average of the 95th percentile positive peak current values and the solid line displays the regression line fitted using the least squares technique.

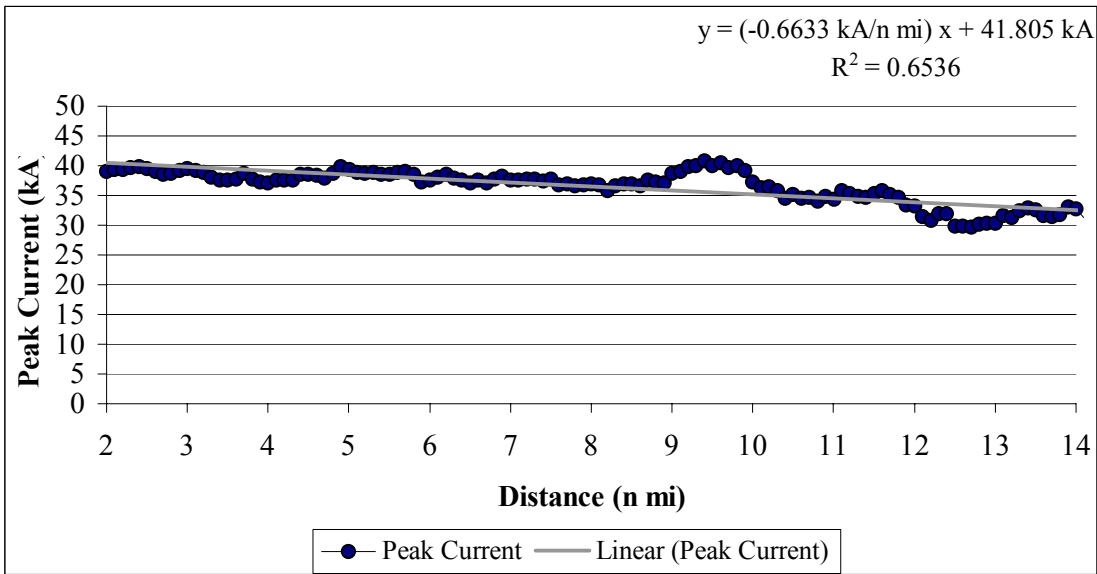


Figure D-12. Negative Positive Peak Current as a Function of Distance for Winter Months. Data points indicate the running average of the 95th percentile negative peak current values and the solid line displays the regression line fitted using the least squares technique.

Appendix E. Seasonal Scatter Plots and Peak Current Versus Altitude of CG Lightning Stroke Origin Point Diagrams

Appendix E contains seasonal scatter plots of lightning stroke peak current values versus the altitude of the lightning stroke origin points. Graphs associating the lightning stroke origin height and the 95th percentile peak current value for each 1,000 ft bin are also included.

Spring

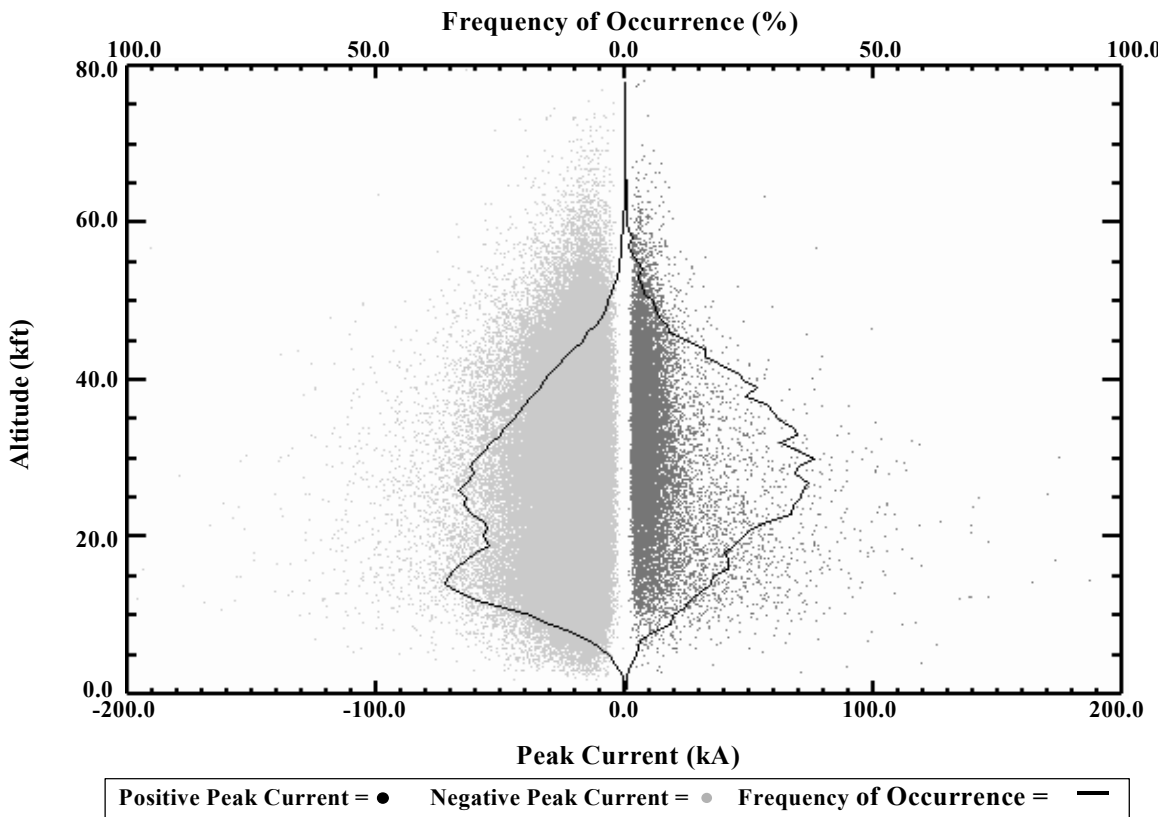


Figure E-1. Spring Scatter Plot of Peak Current Versus Altitude of CG Lightning Stroke Origin Point. Positive peak currents are displayed in black while negative peak currents are in gray. The solid black lines (one for positive and one for negative peak currents) represent the frequency of occurrence for each 1,000 ft height increment.

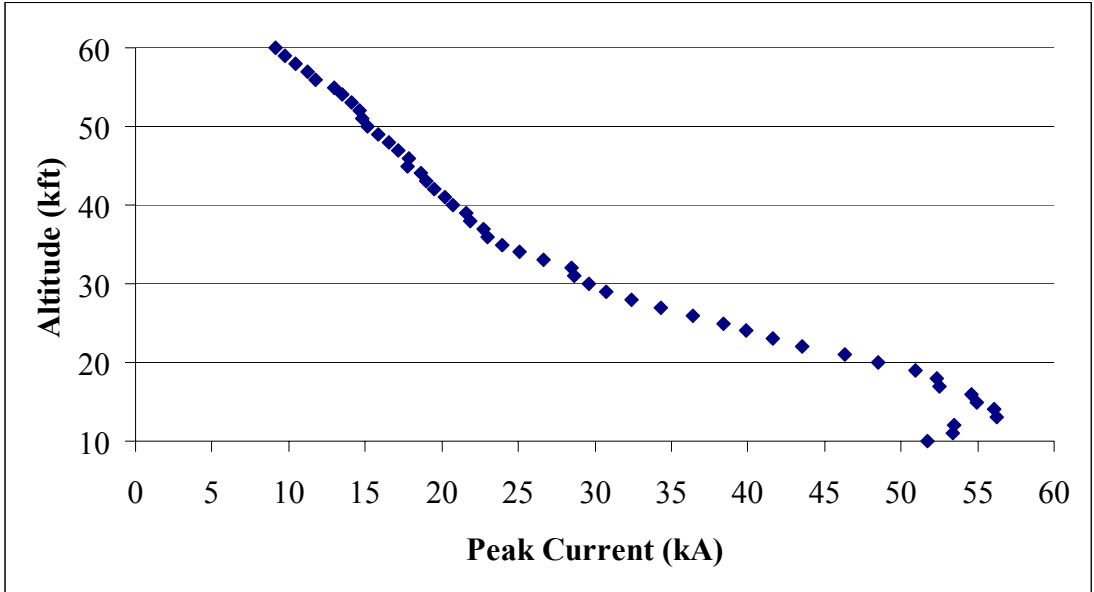


Figure E-2. Positive Peak Current Values as a Function of Altitude for Spring Months. Data points indicate the running average of the 95th percentile positive peak current values.

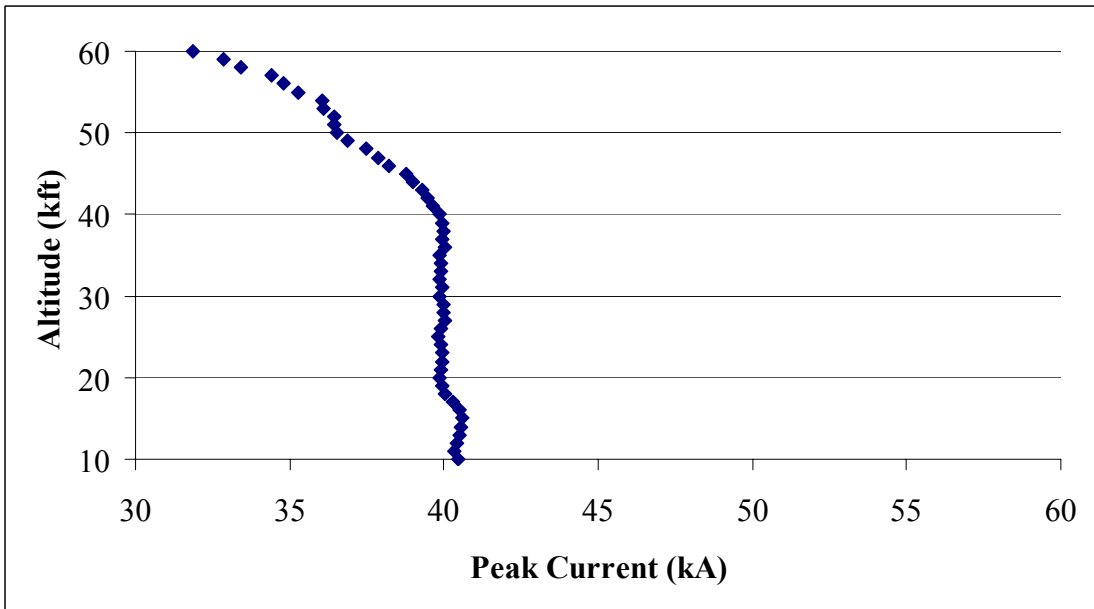


Figure E-3. Negative Peak Current Values as a Function of Altitude for Spring Months. Data points indicate the running average of the 95th percentile negative peak current values.

Summer

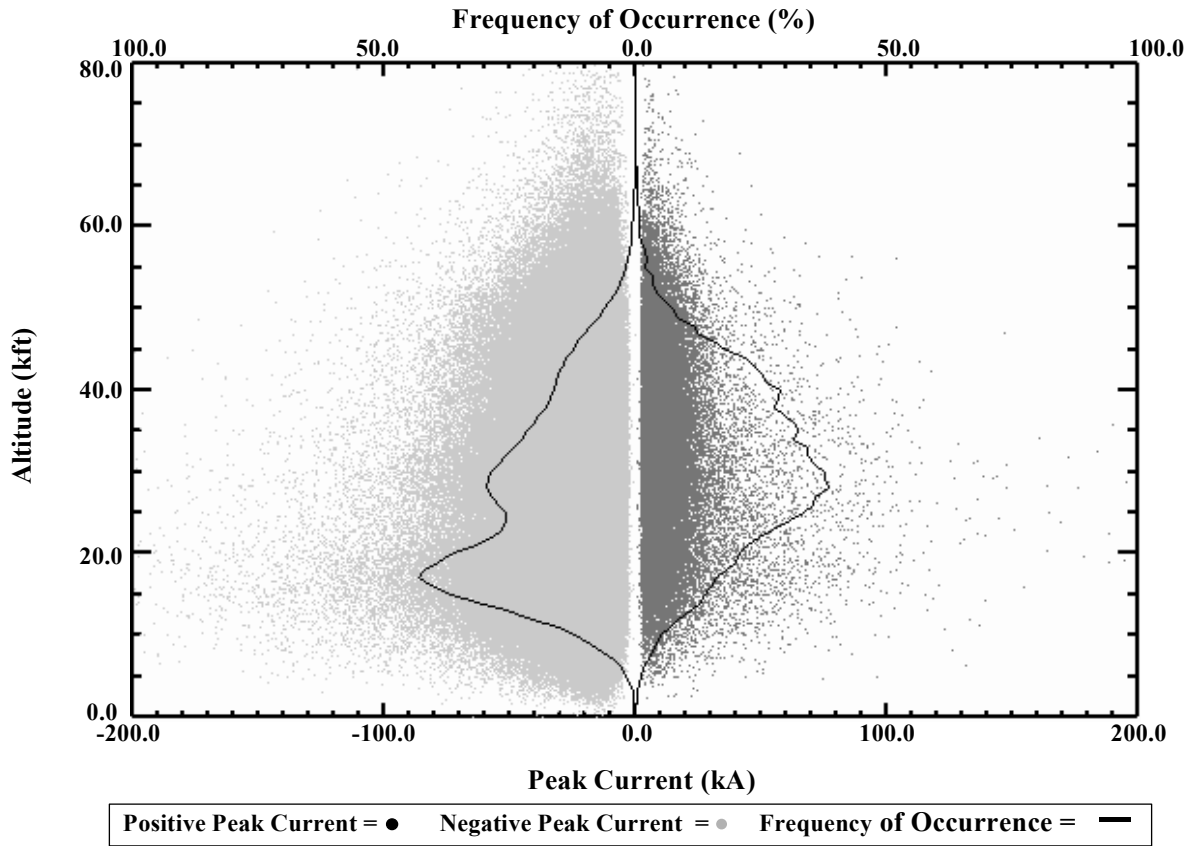


Figure E-4. Summer Scatter Plot of Peak Current Versus Altitude of CG Lightning Stroke Origin Point. Positive peak currents are displayed in black while negative peak currents are in gray. The solid black lines (one for positive and one for negative peak currents) represent the frequency of occurrence for each 1,000 ft height increment.

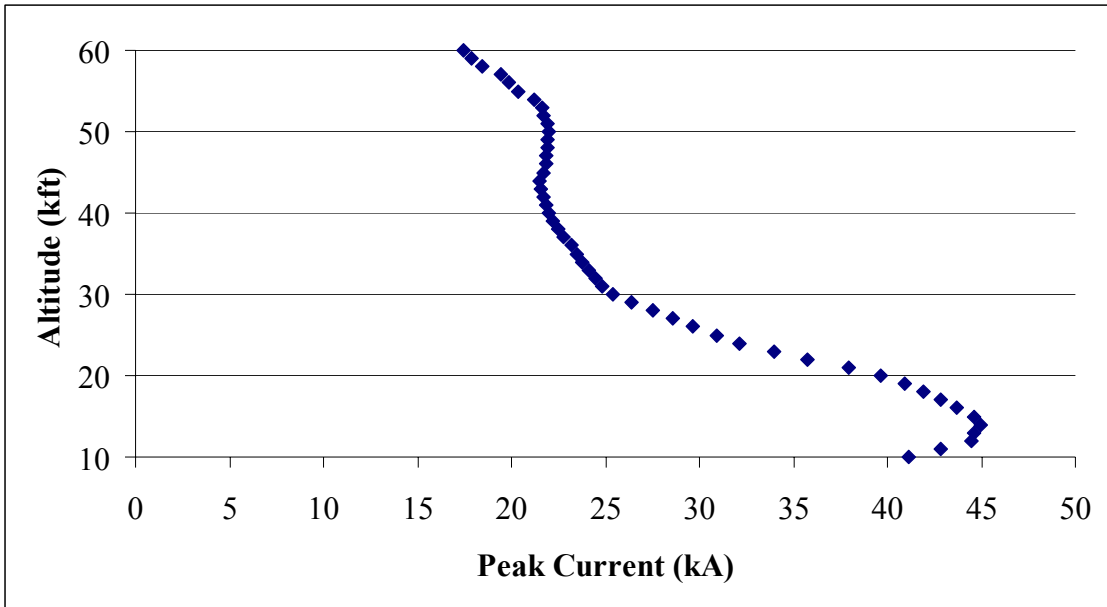


Figure E-5. Positive Peak Current Values as a Function of Altitude for Summer Months. Data points indicate the running average of the 95th percentile positive peak current values.

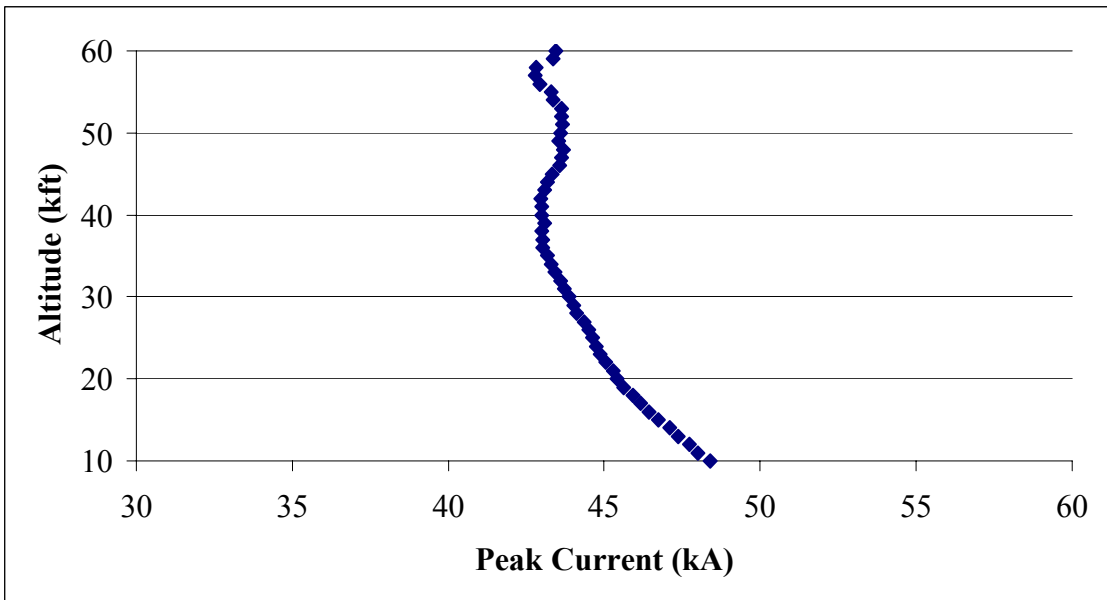


Figure E-6. Negative Peak Current Values as a Function of Altitude for Summer Months. Data points indicate the running average of the 95th percentile negative peak current values.

Fall

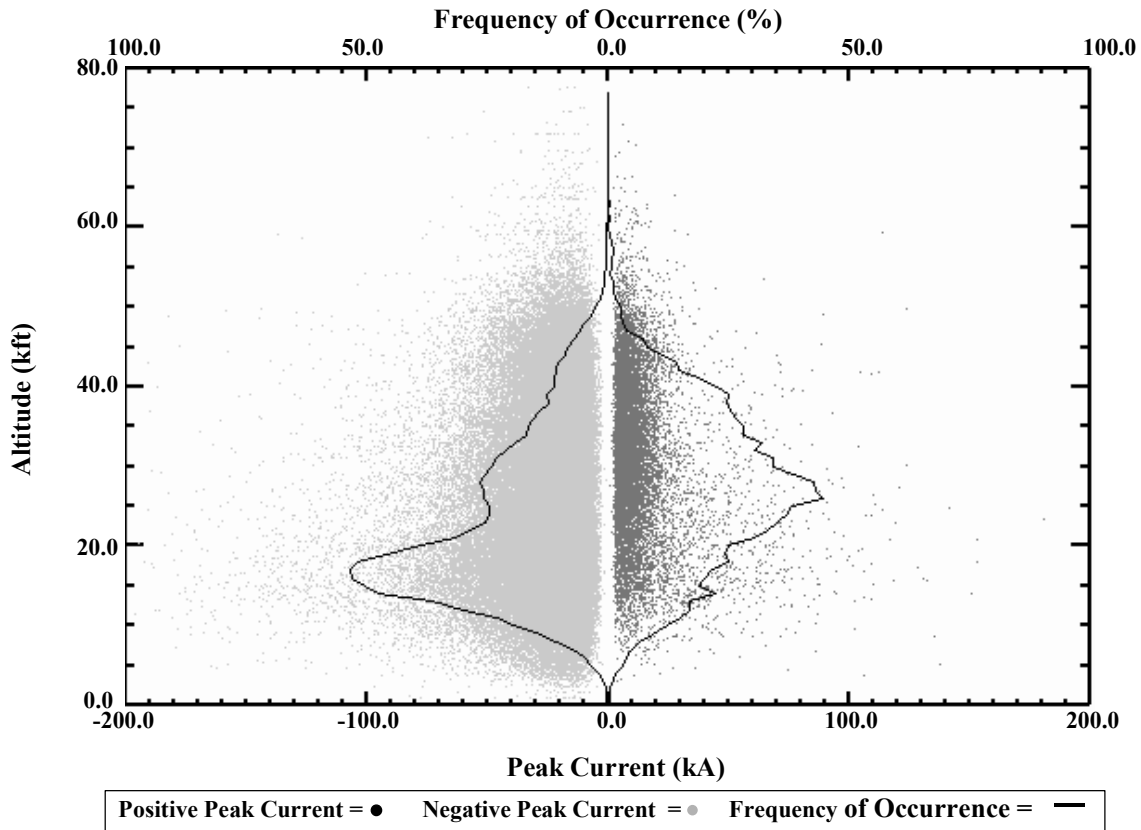


Figure E-7. Fall Scatter Plot of Peak Current Versus Altitude of CG Lightning Stroke Origin Point. Positive peak currents are displayed in black while negative peak currents are in gray. The solid black lines (one for positive and one for negative peak currents) represent the frequency of occurrence for each 1,000 ft height increment.

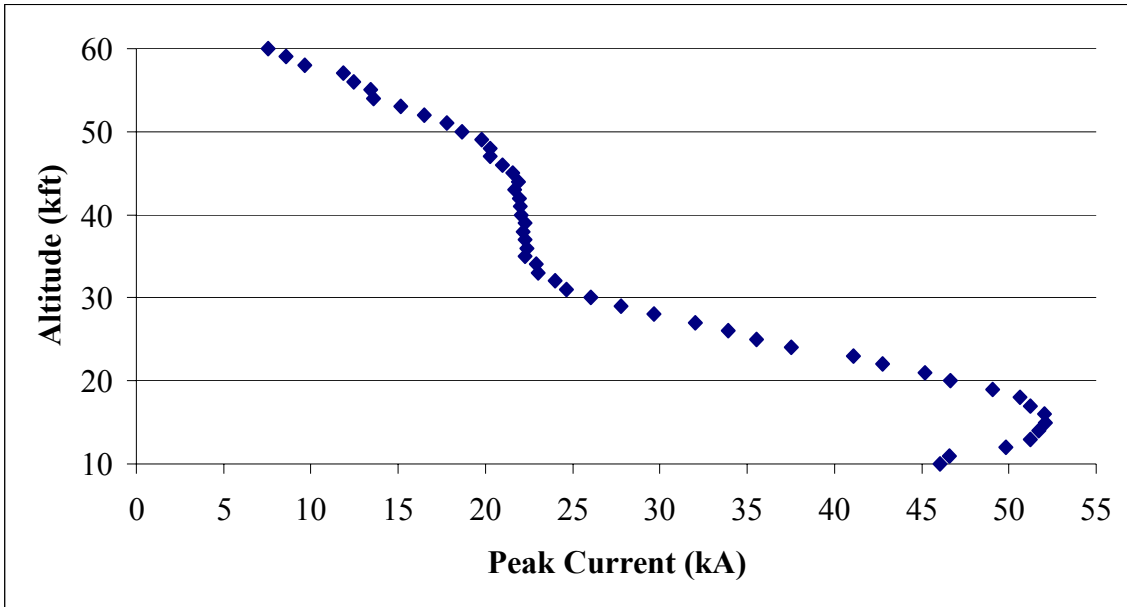


Figure E-8. Positive Peak Current Values as a Function of Altitude for Fall Months. Data points indicate the running average of the 95th percentile positive peak current values.

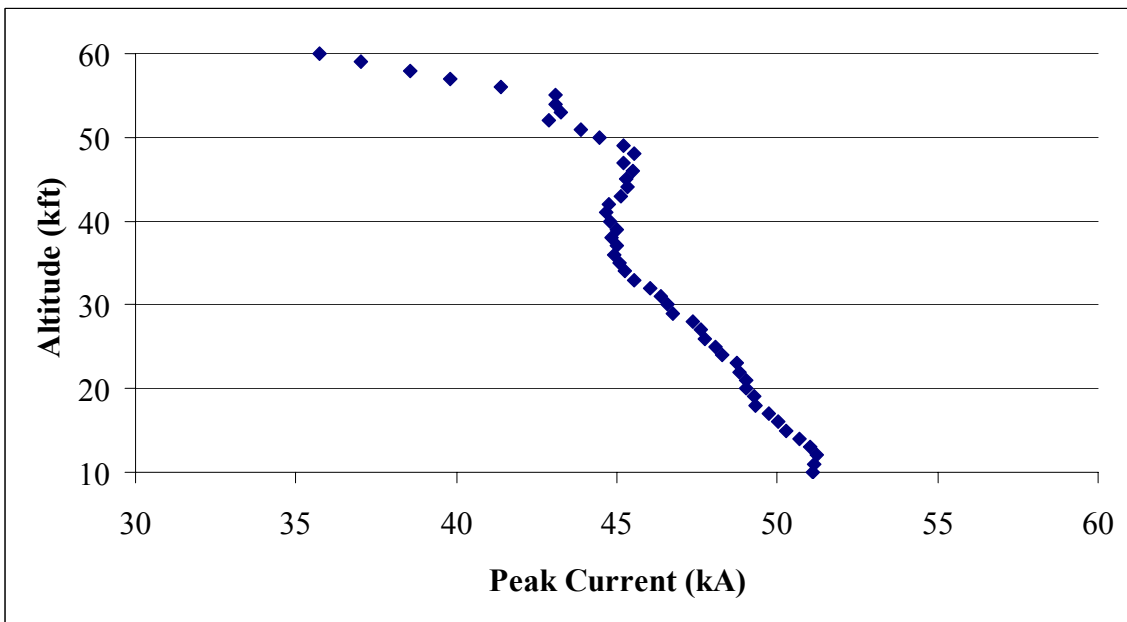


Figure E-9. Negative Peak Current Values as a Function of Altitude for Fall Months. Data points indicate the running average of the 95th percentile negative peak current values.

Winter

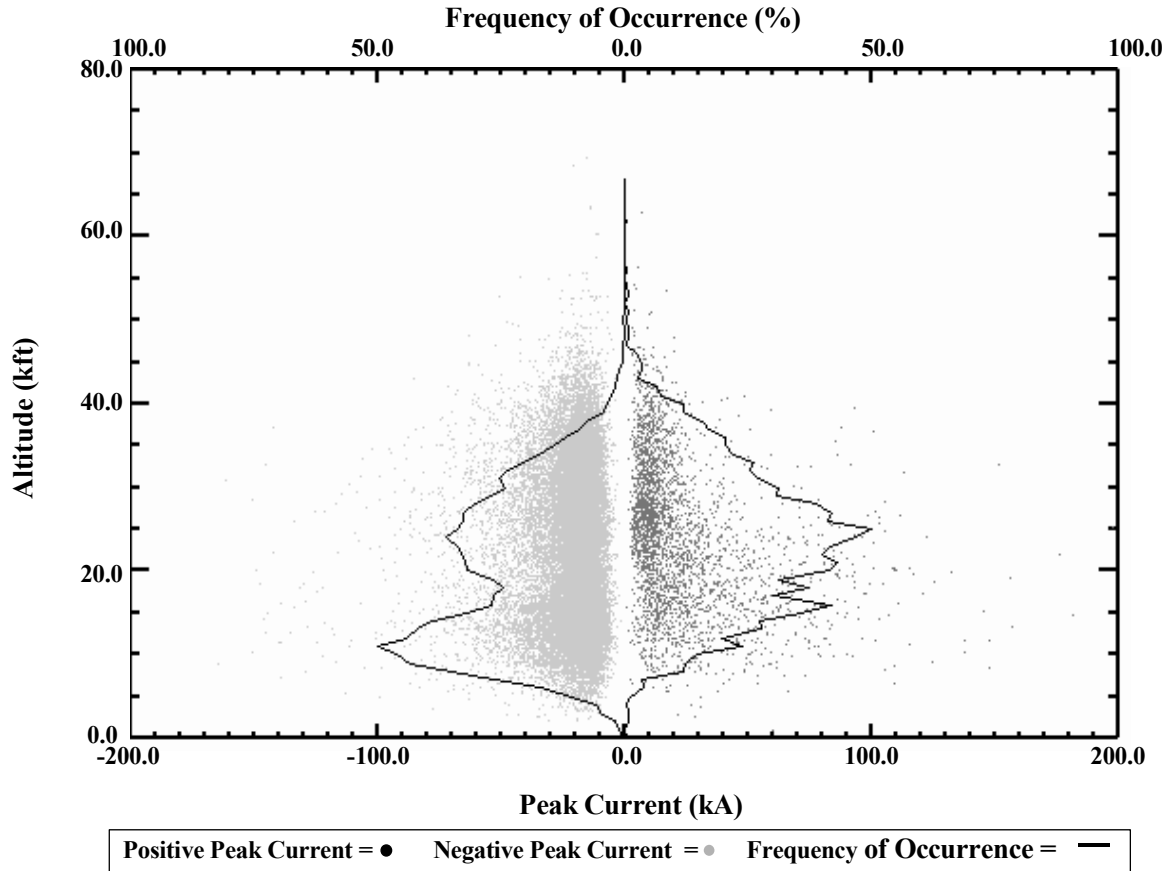


Figure E-10. Winter Scatter Plot of Peak Current Versus Altitude of CG Lightning Stroke Origin Point. Positive peak currents are displayed in black while negative peak currents are in gray. The solid black lines (one for positive and one for negative peak currents) represent the frequency of occurrence for each 1,000 ft height increment.

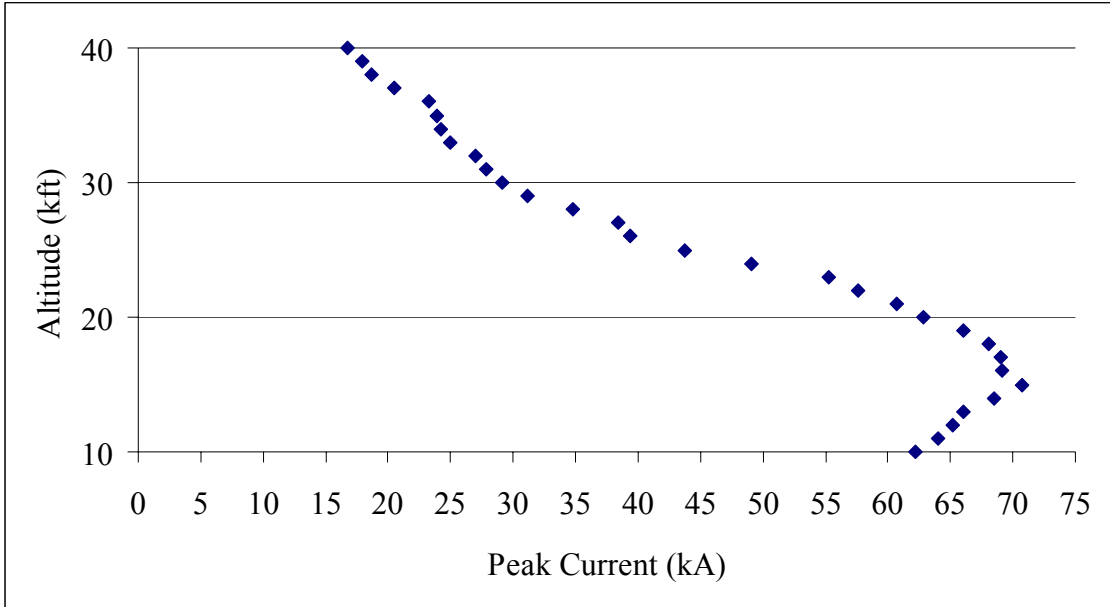


Figure E-11. Positive Peak Current Values as a Function of Altitude for Winter Months. Data points indicate the running average of the 95th percentile positive peak current values.

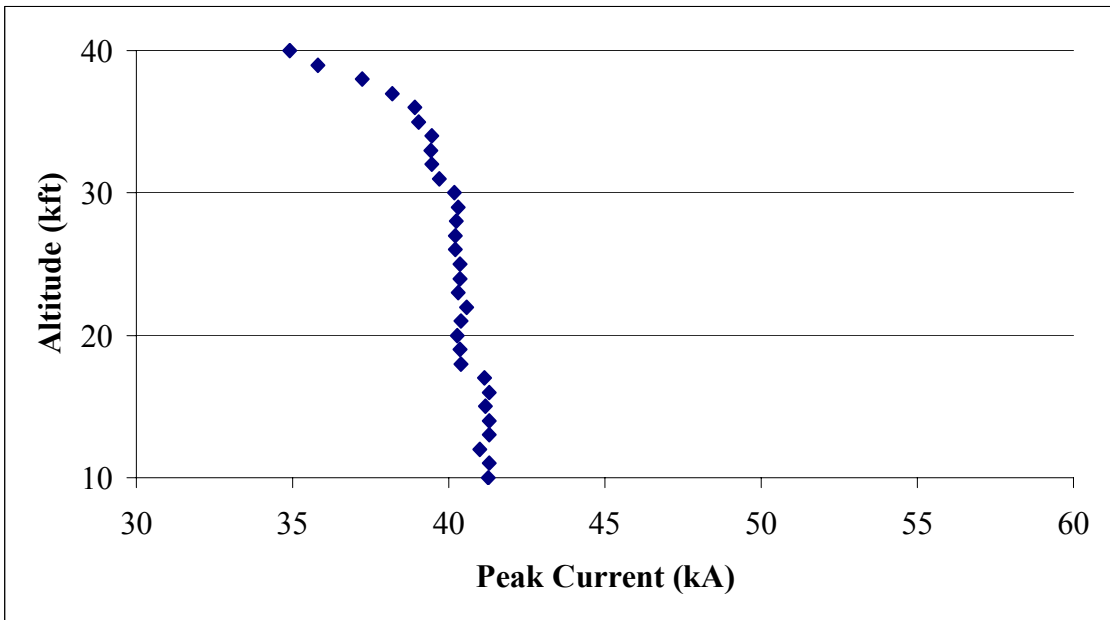


Figure E-12. Negative Peak Current Values as a Function of Altitude for Winter Months. Data points indicate the running average of the 95th percentile negative peak current values.

Appendix F. List of Acronyms

1 st Lt	First Lieutenant
AFIT	Air Force Institute of Technology
AFOSH	Air Force Occupational Safety and Health
CDT	Central Daylight Time
CG	Cloud-to-Ground
DBSF	Distance Between Successive Flash
IDL	Interactive Display Language
IMPACT	IMProved Accuracy from Combined Technology
KSC	Kennedy Space Center
LDAR	Lightning Detection and Ranging
MDF	Magnetic Direction Finder
NASA	National Aeronautics and Space Administration
NLDN	National Lightning Detection Network
NOAA	National Oceanic and Atmospheric Administration
NSSL	National Severe Storms Laboratory
SCIT	Storm Cell Identification and Tracking
STEPS	Severe Thunderstorm Electrification and Precipitation Project
TOA	Time-of-Arrival
UTC	Universal Time Code
WATADS	WSR-88D Algorithm Testing and Display System
WSR-88D	Weather Surveillance Radar – 88 Delta

Bibliography

- Bauman, W. H. 1998: Safety Investigation Board Briefing. Electronic Slide Show 34 Slides, 7 October 1998.
- Beasley, W. H., M. A. Uman, and P. L. Rustan, 1982: *Electric Fields Preceding Cloud-to-Ground Lightning Flashes*. *J. Geophys. Res.*, 87, 4883-4902
- Berger, K., 1977: *The earth flash*. In *Lightning, Volume 1: Physics of Lightning*, R.H. Golde, ed., San Diego: Academic Press, pp. 119-90.
- Boccippio, D. J., S. Heckman, and S. J. Goodman 2000: *A Diagnostic Analysis of the Kennedy Space Center LDAR Network*. *J. Geophys. Res.*, 106, No. D5, 4769-4786.
- Britt, Thomas, O., C. L. Lennon, and L. M. Maier, 1998: *Lightning Detection and Ranging System*. NASA Tech Brief, Vol. 22, Issue 4, 60-61.
- Brook, M., N. Kitagawa, and E. J. Workman, 1962: *Quantitative Study of Strokes and Continuing Currents in Lightning Discharges to Ground*. *J. Geophys. Res.*, 67, 649-659.
- Cox, C. C., 1999: *A Comparison of Horizontal Cloud-To-Ground Lightning Flash Distance Using Weather Surveillance Radar and The Distance Between Successive Flashes Method*. M.S. Thesis, AFIT/GM/ENP/99M-03, Department of Engineering Physics, Air Force Institute of Technology, 130 pp.
- Cummins K. L., E. P. Krider, and M. D. Malone, 1998: The U.S. National Lightning Detection Network and Applications of Cloud-to-Ground Lightning Data by Electric Power Utilities. *IEEE Transactions on Electromagnetic Compatibility*, Vol. 40, No. 4, 465-480.
- Cummins K., M. J. Murphy, I. A. Bardo, W. L. Hiscox, R. B. Pyle, and A. E. Pifer, 1998: A Combined TOA/MDF Technology Upgrade of the U.S. National Lightning Detection Network. *J. Geophys. Res.*, 103, 9035-9044.

Department of the Air Force. *Aircraft Flight Line-Ground Operations and Activities*. AFOSH 91-100. Washington: HQ USAF, 1 May 1998.

Holle, R. L., R. E. Lopez, and E. B. Curran 1999: Demographics of U.S. Lightning Casualties and damages from 1959-1994. *11th International Conference on Atmospheric Electricity*, pp. 200-203.

Huffines, G.R., 1999: *First Stroke Peak Current Characteristics for the United States*. PhD Dissertation, Texas A&M University. (Available from the Texas A&M University Library, College Station, Texas, 77843.)

Idone, V. P., D. Davis, P. Moore, Y. Wang, R. Henderson, M. Ries, and P. Jamason, 1998a: Performance evaluation of U.S. National Lightning Detection Network in Eastern New York, 1. Detection efficiency. *J. Geophys. Res.*, 103, 9045-9055.

_____, 1998b: *Performance evaluation of U.S. National Lightning Detection Network in Eastern New York, 1. Detection efficiency*. *J. Geophys. Res.*, 103, 9057-9069.

Krehbiel, Paul R., M. Brook, and R. A. McCrory 1979: *An Analysis of the Charge Structure of Lightning Discharges to Ground*. *J. Geophys. Res.*, 84, 2432-2456

Krehbiel, Paul R., 1986: *The Electrical Structure of Thunderstorms*. The Earth's Electrical Environment. pp. 90-113.

_____, *Lightning Mapping Observations: What we are Learning*. Address to the American Geophysical Union. San Francisco CA. 11 December 2001.

Kithil, R., 1999: Results of Investigations into Annual USA Lightning Costs and Losses. *11th International Conference on Atmospheric Electricity*, pp. 204-206.

Krider, E. P., 1988: *Spatial Distribution of Lightning Strikes to Ground During Small Thunderstorms in Florida*. Proc. 1988 Int. Aerospace and Ground Conference on Lightning and Static Electricity, Oklahoma City, OK, pp. 318-323.

- Lopez, R. E., and R. L. Holle, 1999: The distance between successive lightning flashes. NOAA Tech. Memo. ERL NSSL-105, National Severe Storms Laboratory, Norman, OK, 29 pp.
- MacGorman, D. R. and W. D. Rust, 1998: *The Electrical Nature of Storms*. Oxford University Press, 422 pp.
- Maier, L, C. Lennon, T. Britt, and S. Schaefer, 1995: Lightning Detection and Ranging (LDAR) System Performance Analysis, *6th International Conference on Weather Systems*, American Meteorological Society Press, pp. 305-309.
- Murphy, Martin J., Kenneth L. Cummins, and Launa M. Maier 2000: *The Analysis and Interpretation of Three-Dimensional Lightning Flash Information*. n. pag. <http://www.Glatmos.com>
- NASA, 2001: *Build_Flash_V6.c*. http://kscdl2.ksc.nasa.gov/public/ldar/build_flash_v6.c.
- Orville, R. E. and V. P. Idone, 1982: *Lightning Leader Characteristics in the Thunderstorm Research International Program (TRIP)*. J. Geophys. Res., 87, 11177-11192.
- Parsons, Tamara, L., 2000: *Determining Horizontal Distance Distribution of Cloud-To-Ground Lightning*. M.S. Thesis, AFIT/GM/ENP/00M-09, Department of Engineering Physics, Air Force Institute of Technology, 88 pp.
- Poehler, Horst, A., 1978: LDAR Observations of a Developing Thunderstorm Correlated With Field Mill, Ground Strike Location, and Weather Radar Data Including the First Report of the Design and Capabilities of a New, Time-of-Arrival Ground-Strike Location System (GSLs). NASA Contract Report CR-154626, 135pp.
- Poehler, H. A. and C. L. Lennon, 1979: *Lightning Detection and Ranging System (LDAR) System Description & Performance Objectives*. NASA Technical Memorandum 74105, 86 pp.

Proctor, D. E., 1983: Lightning and Precipitation in a Small Multicellular Thunderstorm. *J. Geophys. Res.*, 88, 5421-5440.

Renner, S. L., 1998: Analyzing Horizontal Distances Between WSR-88D Thunderstorm Centroids and Cloud-To-Ground Lightning Strikes. M.S. Thesis, AFIT/GM/ENP/98M-09, Department of Engineering Physics, Air Force Institute of Technology, 123 pp.

Stolzenburg, Maribeth, W. David Rust, Bradley F. Smull, and Thomas C. Marshal, 1998: *Electrical Structure in Thunderstorm Convective Regions, I. Mesoscale Convective Systems*. *J. Geophys. Res.*, 103, No. D12, 14059-14078.

Uman, Martin. A., 2000: *The Lightning Discharge*. Orlando: Academic Press, 377 pp.

USAF Fact Sheet: B-2 Spirit, 1999: Excerpt from unpublished article. n. pag.
http://www.af.mil/news/factsheets/B_2_Spirit.html.

Vita

Captain Todd M. McNamara graduated from Wayne Trace High School in Haviland, Ohio in June 1981. He joined the military in 1982 and completed Weather Observer and Weather Forecaster's Courses at Chanute AFB, Illinois. He held positions as Weather Observer at Holloman AFB, New Mexico and Camp Humphries, Korea. In 1985, he was assigned to Scott AFB, Illinois as a Climatologically Information Specialist. As a forecaster, he was assigned to Tropical and Southern Hemisphere Forecast Section at Air Force Global Weather Central, Offutt AFB, Nebraska.

In 1991, Captain McNamara completed his Bachelor of Science degree in Atmospheric Sciences at Creighton University in Omaha, Nebraska. He attended Officer's Training School at Lackland AFB, Texas and was commissioned November 1991.

Captain McNamara's next assignment was to Castle AFB, California as Wing Weather Officer and Flight Chief. In 1994, Captain McNamara was assigned to HQ Air Mobility Command, Scott AFB, Illinois where he was the Assistant Chief, Readiness Section. In 1997, Captain McNamara was assigned to Hickam AFB, Hawaii as the Weather Operations, Flight Commander in support of the 15th Air Base Wing.

Captain McNamara entered the graduate meteorology program in the school of engineering and management, Air Force Institute of Technology at Wright-Patterson AFB, Ohio in August of 2000. Upon graduation, he will be assigned to 335th Training Squadron, Keesler AFB, Mississippi as an instructor.

REPORT DOCUMENTATION PAGE

*Form Approved
OMB No. 0704-0188*

The public reporting burden for this collection of information is estimated to average 1 hour per response, including the time for reviewing instructions, searching existing data sources, gathering and maintaining the data needed, and completing and reviewing the collection of information. Send comments regarding this burden estimate or any other aspect of this collection of information, including suggestions for reducing the burden, to Department of Defense, Washington Headquarters Services, Directorate for Information Operations and Reports (0704-0188), 1215 Jefferson Davis Highway, Suite 1204, Arlington, VA 22202-4302. Respondents should be aware that notwithstanding any other provision of law, no person shall be subject to any penalty for failing to comply with a collection of information if it does not display a currently valid OMB control number.

PLEASE DO NOT RETURN YOUR FORM TO THE ABOVE ADDRESS.

1. REPORT DATE (DD-MM-YYYY) 14-01-2002	2. REPORT TYPE Master's Thesis	3. DATES COVERED (From - To) Jun 2001 - Mar 2002
--------------------------------------------------	------------------------------------------	------------------------------------------------------------

4. TITLE AND SUBTITLE THE HORIZONTAL EXTENT OF CLOUD-TO-GROUND LIGHTNING OVER THE KENNEDY SPACE CENTER	5a. CONTRACT NUMBER
	5b. GRANT NUMBER
	5c. PROGRAM ELEMENT NUMBER

6. AUTHOR(S) McNamara, Todd, M., Captain, USAF	5d. PROJECT NUMBER
	5e. TASK NUMBER
	5f. WORK UNIT NUMBER

7. PERFORMING ORGANIZATION NAME(S) AND ADDRESS(ES) Air Force Institute of Technology Graduate School of Engineering and Management (AFIT/EN) 2950 P Street, Building 640 WPAFB OH 45433-7765	8. PERFORMING ORGANIZATION REPORT NUMBER AFIT/GM/ENP/02M-06
-----------------------------------------------------------------------------------------------------------------------------------------------------------------------------------------------------------------	---------------------------------------------------------------------------

9. SPONSORING/MONITORING AGENCY NAME(S) AND ADDRESS(ES) ASC/YCA ATTN: Lt Col Robert S. Baerst 2590 Loop Road West WPAFB, OH 45433 Phone:986-9419	10. SPONSOR/MONITOR'S ACRONYM(S)
	11. SPONSOR/MONITOR'S REPORT NUMBER(S)

12. DISTRIBUTION/AVAILABILITY STATEMENT

APPROVED FOR PUBLIC RELEASE; DISTRIBUTION UNLIMITED.

13. SUPPLEMENTARY NOTES

14. ABSTRACT
Military base weather stations are required to issue lightning warnings to protect military equipment and personnel. The issuance of warnings is based on a 5 n mi distance criterion. This criterion appears to have evolved over time as a balance between safety and mission impact. This research project had two purposes. First, it determined the distance lightning travels in hopes of aiding decision makers in determining if the current 5 n mi lightning warning criteria is adequate for ensuring the safety of military assets. Second, it examined the characteristics of the peak current of CG lightning strokes to determine if a relationship exists between peak current, the distance a stroke travels, and the altitude of the origin point of the lightning stroke.

This study found that 28.6% of lightning flashes traveled further than 5 n mi from the lightning origin point for approximately four years of data while the spring had the highest seasonal frequency of 38.5%. Peak current analysis indicated that higher peak currents are associated with shorter lightning channel lengths. Higher peak currents were also found to be associated with lightning strokes that originated from lower altitudes.

15. SUBJECT TERMS
Lightning, Cloud-To-Ground Lightning, Lightning Detection and Ranging, LDAR, National Lightning Detection Network, NLDN, Peak Current, Lightning Origin Height

16. SECURITY CLASSIFICATION OF:			17. LIMITATION OF ABSTRACT UU	18. NUMBER OF PAGES 114	19a. NAME OF RESPONSIBLE PERSON Gary R. Huffines, Major, ENP
a. REPORT U	b. ABSTRACT U	c. THIS PAGE U			19b. TELEPHONE NUMBER (Include area code) (937) 255-3636, ext 4511